SANTA LUCIA
NEUROSCIENZE
E RIABILITAZIONE

SAPIENZA
UNIVERSITÀ DI ROMA

Ph.D. Thesis
ABRO Ph.D. Program in Bioengineering - XXXV Cycle

Re-establishing Cortico-Muscular Communication to enhance recovery: development of a hybrid Brain-Computer Interface for post-stroke motor rehabilitation

Valeria de Seta

SAPIENZA
UNIVERSITÀ DI ROMA

Re-establishing Cortico-Muscular Communication to enhance recovery: development of a hybrid Brain-Computer Interface for post-stroke motor rehabilitation

Prof. Giuseppe Oriolo, Ph.D.

Ph.D. Program in Automatic Control, Bioengineering and Operations Research.Curriculum: **BIOENGINEERING** (XXXV cycle)

Valeria de Seta

Advisor
Prof. Febo Cincotti, Ph.D.

Co-Advisors
Prof. Jlenia Toppi, Ph.D.
Dr. Floriana Pichiorri, MD-Ph.D.

External reviewers
Prof. Gernot Müller-Putz, Ph.D.
Prof. Natalie Mrachacz-Kersting Ph.D.

Academic Year 2021/2022

Re-establishing Cortico-Muscular Communication to enhance recovery: development of a hybrid Brain-Computer Interface for post-stroke motor rehabilitation

PhD thesis. Sapienza University of Rome

This thesis has been typeset by LaTeX and the Sapthesis class.

Author's email: deseta@diag.uniroma1.it

"I am among those who think that science has great beauty. A scientist in his laboratory is not only a technician: he is also a child placed before natural phenomena which impress him like a fairy tale."
- Marie Curie

Abstract

Stroke is a leading cause of adult serious and long-term disability. Notably, improving upper limb functioning is the primary therapeutic goal in stroke rehabilitation to maximize patients' functional recovery and reduce long-term disability. Nowadays, Brain-Computer Interfaces (BCIs) can be used as add-on to traditional therapies to activate rehabilitative devices directly decoding the brain activity of the user noninvasively, e.g. by means of electroencephalogram (EEG). However, the consequences of a stroke involve regions apart from the focal lesions due to disruption of connections along neural pathways. Therefore, a BCI system for motor rehabilitation should allow to train both brain and peripheral activity, reinforcing the volition that is brain control over muscular activation together with physiological muscular activation patterns.

In this PhD thesis, Cortico-Muscular Coupling (CMC), which measures the synchronization between central and peripheral activation (recorded respectively through EEG and electromyogram – EMG), was studied as hybrid feature to detect movement attempts and to reinforce the physiological brain control of muscles activity.

The widespread functional brain-muscle connectivity (derived from multiple EEG-EMG pairs) was characterized and compared in healthy subjects and stroke patients by means of indices derived ad-hoc from graph theory. CMC resulted to contain information about the movement type performed as well as the general clinical status of stroke patients in terms of their hand functionality, showing a high potential to be used as input of hybrid BCI (h-BCI) systems.

Thus, a processing pipeline for the translation of CMC computation and the consequent CMC-based movement detection from offline to real-time was defined and optimized. A novel h-BCI prototype aimed to Re-establish Cortico-Muscular communication was developed and its feasibility was validated. Moreover, a study on the feedback delivery strategy (i.e. Functional Electrical Stimulation - FES) was performed with the ultimate aim of tailoring the stimulation to patients' impairment. Such rehabilitative prototype recognizes close-to-normal EEG-EMG coupling during hand movement attempts, taking into account both the CMC features to reinforce during the h-BCI training, and the ones to discourage to avoid the maladaptive movement abnormalities typical of post-stroke recovery. Upon movement detection, it triggers the delivery of FES to the target muscle to support full movement execution. Such system resulted to be reliable and easy-to-use with high accuracy and timing.

The developed hybrid device would allow to follow patients along recovery with a strategy tailored on their rehabilitative stage and hence maximizing the time and amount of functional recovery with potentially high impact on the stroke survivors' quality of life (personalized medicine).

Contents

List of Abbreviations

AH	Affected Hand
ANOVA	ANalysis Of VAriance
Ant_DELT	Anterior deltoid
AP	Abductor pollicis longus
AUC	Area Under the Curve
BCI	Brain-Computer Interface
BIC	Long head of the biceps brachii muscle
CAR	Common Average Reference
CI	Control Interface
CMC	Cortico-Muscular Coupling
CTRL	Control group
DCH	Density of Controlateral Hemisphere
DELT	Lateral deltoid
DIC	Density of Ipsilateral Hemisphere
DIS	Density of Involded Side
DPDR	Distal/Proximal Degree Ratio
DT	Decision tree
DUS	Density of Uninvolved Side
ECG	Electrocardiography
ECU	Extensor carpi ulnaris
ED	Extensor digitorum
EDC	Extensor digitorum communis
EEG	Electroencephalography
EHI	Edinburgh Handedness Inventory
EMG	Electromyography
ERD	Event-Related Desynchronization

EXP	Experimental group
Ext	Extension
FD	Flexor digitorum superficialis
FD	False Detection
FES	Functional Electrical Stimulation
FMA	Fugl-Meyer Assessment scale
FN	False Negative
FNR	False Negative Rate
FP	False Positive
FPR	False Positive Rate
GA	Grand Average
Grasp	Grasping
h-BCI	Hybrid BCI
IMC	Intermuscular coherence
L	Left
Lat_DELT	Lateral deltoid
LDA	Linear Discriminant Analysis
MAS	Modified Ashworth scale
MD	Muscle Degree
MD	Mean Delay
MMT	Manual Muscle Test
MVC	Maximum Voluntary Contraction
ND	Network Density
ND	No Detection
NIHSS	National Institute of Health stroke scale
PEC	Pectoralis major
R	Right
rmANOVA	repeated measures ANOVA
RMS	Root-mean-square
SE	Standard Error
SMR	Sensorimotor rhythms
STICI	STImulation Control Interface
SVM	Support Vector Machine
SVM-RBF	SVM with radial basis kernel
TD	True Detection

TP	True Positive
TPR	True Positive Rate
TRAP	Upper trapezius
TRI	Lateral head of triceps muscle
UH	Unaffacted Hand

General Introduction

Stroke is the leading cause of adult long-term disability in Western countries and the second leading cause of death worldwide [1]. It is no longer a disease of the elderly, indeed the 25% to 30% of patients affected by stroke are younger than 55 years [2].
The overall global burden of stroke, in terms of functional, psychological, social, and also socioeconomic impact, is reaching epidemic proportions in Western industrialized countries [3]. Despite the efforts of traditional rehabilitation approaches, 101 million people are living with stroke aftermath and this number is almost doubled over the last 30 years (data related to 2019 - World Stroke Organization[1]) [4]. The most common and widely recognized impairment caused by stroke is motor impairment contralateral to the affected brain hemisphere (hemiparesis). Notably, the main predictor of an individual resuming a normal professional and personal life is upper limb extremity function [5]. Indeed, improving upper limb functioning is the primary therapeutic goal in stroke rehabilitation to maximize patients' functional recovery and reduce long-term disability [6].

Various innovative neurorehabilitation strategies are emerging in order to enhance beneficial plasticity, which it is known to occur after brain damages, and improve motor recovery after stroke [2], [4]. Among them, Brain-Computer Interfaces (BCIs) have proven their efficacy to enhance upper limb motor recovery exploiting brain signals to control visual or proprioceptive feedbacks/-effectors [2], [7]–[14]. BCI's overall principle is based on the fact that closing the loop between cortical activity (motor intention) and movement — thereby producing afferent feedback activity — might restore functional corticospinal and corticomuscular connections [10]. As for the feedback, it can be delivered in an abstract form (e.g., a moving cursor on a computer screen) or as embodied feedback (e.g., visual representations of the participant's body parts over a virtual avatar on a computer screen, in a VR head-mounted display or directly overlaid on the participant's limbs); or through Functional Electrical Stimulation (FES) which has been employed in stroke rehabilitation for its capability to assist movement and has been shown to induce changes in the brain, bearing witness of brain plasticity modulation [13], [15].

[1] https://www.world-stroke.org

BCIs for post-stroke motor rehabilitation rely on the principle that reinforcement of close-to-normal motor related brain activity (most commonly derived from electroencephalogram - EEG), results in an improvement of motor function [16]. BCI technology allows patients with severe impairment, thus with complete plegia, to exploit motor imagery to elicit changes in EEG sensorimotor power spectra and trigger a contingent sensory feedback (e.g., virtual hand) which drives the brain reorganization toward improved motor function and against maladaptive brain changes [9].
Another BCI paradigm consists of asking patients to attempt the movement with their paretic hand. However, in this case other aspects should be taken into account because the consequences of a stroke involve regions apart from the focal lesion. Indeed, along the process of motor recovery after stroke, several abnormalities in upper limb function have been described such as muscle weakness and spasticity, abnormal muscle co-activation, increased activity of the antagonist muscles [17]–[20]. Electromyography (EMG) can be used to monitor the residual or recovered muscular activity along the rehabilitation processes [21], [22] and EMG-related features can be exploited to avoid the reinforcement of such maladaptive changes in patients with residual or recovered muscle activity who can attempt the movement.
Hybrid BCIs (h-BCIs) include peripheral signals such as EMG, in addition to brain signals, as control feature [23] and they have mostly been developed to improve the classification performance of the system as in assistive BCIs [24]–[27]. Such devices usually combine the EEG and EMG feature in the classification stage, meaning that each feature (brain and muscular) is calculated separately and combined sequentially or simultaneously using a balanced weight or Bayesian fusion approach to better control the assistive device [24], [28]. Nevertheless, there is no consensus on which movement-related features should be encouraged (or discouraged) within a BCI training to pursue physiological muscular activation patterns. Ideally, h-BCI systems specifically developed for hand motor rehabilitation should allow to train both brain and peripheral activity in a top-down framework [29] in which volition, that is brain control over muscular activation, is reinforced together with correct muscular activation patterns [30].

Thus, here a hybrid EEG-EMG feature, Cortico-Muscular coupling (CMC), is proposed as input of a novel h-BCI system aimed at re-establishing the brain-muscles communication after stroke. CMC gives information on how much cortical surface motor potentials are phase-locked to muscular firing during voluntary movement. It can be considered a simple form of hybrid functional connectivity measuring the spectral coherence between EEG and EMG [31]. It has been proposed as a potential biomarker for post-stroke motor deficits [32], indeed its amplitude has been proven to be reduced post-stroke and its increase has been correlated with functional recovery [33]–[36]. Recently, h-BCIs based on CMC have been studied for post-stroke motor rehabilitation testifying the potential role of CMC as control feature in a rehabilitative BCI paradigm [37],

[38].
However, so far most CMC studies in stroke patients have limited the observation to few EEG electrodes in the affected hemisphere and the target muscle [33], [35], [36], [39]. Similarly, the implementation of CMC-based BCIs has been limited to few EEG-EMG couples determined a priori [37], disregarding the comprehensive functional connectivity pattern involving several brain regions and muscles, which participate in the post-lesional re-arrangements [40]–[43].

During the three years of my PhD, I implemented a non-invasive BCI-controlled FES device for upper limb rehabilitation after stroke based on online detection of cortico-muscular activation. The control feature was derived from a combined EEG and EMG connectivity pattern estimated during upper limb movement attempts. In particular, the first year was dedicated to the study of the state of the art and the development of a methodology for the effective extraction of CMC patterns able to characterize physiological movements and to be used for movement classification. Moreover, to analyze the functional connectivity between cortex and muscles after stroke, an ad-hoc protocol was developed for the multimodal acquisition of stroke patients' data during simple and complex tasks and, during the second year the data collected were used to characterize brain-muscles patterns during the movement of the impaired hand. Finally, the CMC computation was translated in real-time and the third year was dedicated to the design and the feasibility testing of a reliable and easy-to-use rehabilitative h-BCI system based on CMC features. Moreover, a study on the strategy of the feedback delivery (i.e. FES) was performed with the ultimate aim of tailoring the stimulation to patients' impairment.

My research activity was carried out in the laboratory on Neuroelectrial Imaging and Brain-Computer Interface Laboratory (NeiLab) at Fondazione Santa Lucia IRCCS (Rome, Italy), run by Dr. Donatella Mattia, where a multidisciplinary team allowed me to have a comprehensive view of the clinical needs for the development of a technology for post-stroke motor rehabilitation. Moreover, thanks to the inpatients and outpatients services of Fondazione Santa Lucia and the availability of patients who believed in our research, the recruitment of participants for the experimental protocol was possible, in accordance with Covid-19 regulations, even during the second phase of the pandemic. Such research was performed within the broader context of the project *RECOMmENceR: RE-establishing COrtico Muscolar COMunication to ENhance Recovery* funded by the Italian Ministry of Health.
Finally, during my last year part of my research was conducted at the Translational Neural Engineering (TNE) Lab of EPFL, run by Prof. Silvestro Micera, where I pursued a secondment as visiting PhD student.

The thesis is divided in two main sections which contain the two main goals achieved in these three years: the first section includes three studies aimed at the characterization of the physiological and pathological cortico-muscular patterns in healthy subjects and stroke patients, whereas the second section

describes in three studies the translation of CMC computational pipeline from offline to online and the design of the BCI prototype.

References

[1] S. S. Virani, A. Alonso, E. J. Benjamin, *et al.*, "Heart Disease and Stroke Statistics-2020 Update: A Report From the American Heart Association," eng, *Circulation*, vol. 141, no. 9, e139–e596, Mar. 2020, ISSN: 1524-4539. DOI: 10.1161/CIR.0000000000000757.

[2] E. Raffin and F. C. Hummel, "Restoring Motor Functions After Stroke: Multiple Approaches and Opportunities," eng, *The Neuroscientist: A Review Journal Bringing Neurobiology, Neurology and Psychiatry*, vol. 24, no. 4, pp. 400–416, Aug. 2018, ISSN: 1089-4098. DOI: 10.1177/1073858417737486.

[3] V. L. Feigin, G. A. Roth, M. Naghavi, *et al.*, "Global burden of stroke and risk factors in 188 countries, during 1990–2013: A systematic analysis for the Global Burden of Disease Study 2013," en, *The Lancet Neurology*, vol. 15, no. 9, pp. 913–924, Aug. 2016, ISSN: 1474-4422. DOI: 10.1016/S1474-4422(16)30073-4. [Online]. Available: http://www.sciencedirect.com/science/article/pii/S1474442216300734 (visited on 09/18/2020).

[4] F. Pichiorri and D. Mattia, "Brain-computer interfaces in neurologic rehabilitation practice," eng, *Handbook of Clinical Neurology*, vol. 168, pp. 101–116, 2020, ISSN: 0072-9752. DOI: 10.1016/B978-0-444-63934-9.00009-3.

[5] S. Micera, M. Caleo, C. Chisari, F. C. Hummel, and A. Pedrocchi, "Advanced Neurotechnologies for the Restoration of Motor Function," en, *Neuron*, vol. 105, no. 4, pp. 604–620, Feb. 2020, ISSN: 0896-6273. DOI: 10.1016/j.neuron.2020.01.039. [Online]. Available: http://www.sciencedirect.com/science/article/pii/S0896627320300660 (visited on 11/17/2020).

[6] M. Coscia, M. J. Wessel, U. Chaudary, *et al.*, "Neurotechnology-aided interventions for upper limb motor rehabilitation in severe chronic stroke," eng, *Brain: A Journal of Neurology*, vol. 142, no. 8, pp. 2182–2197, Aug. 2019, ISSN: 1460-2156. DOI: 10.1093/brain/awz181.

[7] S. Silvoni, A. Ramos-Murguialday, M. Cavinato, *et al.*, "Brain-Computer Interface in Stroke: A Review of Progress," *Clinical EEG and neuroscience : official journal of the EEG and Clinical Neuroscience Society (ENCS)*, vol. 42, pp. 245–52, Oct. 2011. DOI: 10.1177/155005941104200410.

[8] A. Ramos-Murguialday, D. Broetz, M. Rea, *et al.*, "Brain-machine interface in chronic stroke rehabilitation: A controlled study," eng, *Annals of Neurology*, vol. 74, no. 1, pp. 100–108, Jul. 2013, ISSN: 1531-8249. DOI: 10.1002/ana.23879.

[9] F. Pichiorri, G. Morone, M. Petti, *et al.*, "Brain-computer interface boosts motor imagery practice during stroke recovery," eng, *Annals of Neurology*, vol. 77, no. 5, pp. 851–865, May 2015, ISSN: 1531-8249. DOI: 10.1002/ana.24390.

[10] U. Chaudhary, N. Birbaumer, and A. Ramos-Murguialday, "Brain–computer interfaces for communication and rehabilitation," en, *Nature Reviews Neurology*, vol. 12, no. 9, pp. 513–525, Sep. 2016, Number: 9 Publisher: Nature Publishing Group, ISSN: 1759-4766. DOI: 10.1038/nrneurol.2016.113. [Online]. Available: https://www.nature.com/articles/nrneurol.2016.113 (visited on 08/01/2022).

[11] N. Mrachacz-Kersting, N. Jiang, A. J. T. Stevenson, *et al.*, "Efficient neuroplasticity induction in chronic stroke patients by an associative brain-computer interface," eng, *Journal of Neurophysiology*, vol. 115, no. 3, pp. 1410–1421, Mar. 2016, ISSN: 1522-1598. DOI: 10.1152/jn.00918.2015.

[12] E. Monge-Pereira, F. Molina-Rueda, F. M. Rivas-Montero, *et al.*, "Electroencephalography as a post-stroke assessment method: An updated review," eng, spa, *Neurologia (Barcelona, Spain)*, vol. 32, no. 1, pp. 40–49, Feb. 2017, ISSN: 1578-1968. DOI: 10.1016/j.nrl.2014.07.002.

[13] M. A. Cervera, S. R. Soekadar, J. Ushiba, *et al.*, "Brain-computer interfaces for post-stroke motor rehabilitation: A meta-analysis," eng, *Annals of Clinical and Translational Neurology*, vol. 5, no. 5, pp. 651–663, May 2018, ISSN: 2328-9503. DOI: 10.1002/acn3.544.

[14] A. Biasiucci, R. Leeb, I. Iturrate, *et al.*, "Brain-actuated functional electrical stimulation elicits lasting arm motor recovery after stroke," en, *Nature Communications*, vol. 9, no. 1, p. 2421, Jun. 2018, Number: 1 Publisher: Nature Publishing Group, ISSN: 2041-1723. DOI: 10.1038/s41467-018-04673-z. [Online]. Available: https://www.nature.com/articles/s41467-018-04673-z (visited on 08/01/2022).

[15] F. Quandt and F. C. Hummel, "The influence of functional electrical stimulation on hand motor recovery in stroke patients: A review," eng, *Experimental & Translational Stroke Medicine*, vol. 6, p. 9, 2014, ISSN: 2040-7378. DOI: 10.1186/2040-7378-6-9.

[16] J. Wolpaw and E. W. Wolpaw, *Brain-Computer Interfaces: Principles and Practice*. Oxford University Press, Jan. 2012, ISBN: 978-0-19-992148-5.

[17] M. F. Levin, R. W. Selles, M. H. Verheul, and O. G. Meijer, "Deficits in the coordination of agonist and antagonist muscles in stroke patients: Implications for normal motor control," eng, *Brain Research*, vol. 853, no. 2, pp. 352–369, Jan. 2000, ISSN: 0006-8993. DOI: 10.1016/s0006-8993(99)02298-2.

[18] L. C. Miller and J. P. A. Dewald, "Involuntary paretic wrist/finger flexion forces and EMG increase with shoulder abduction load in individuals with chronic stroke," *Clinical Neurophysiology: Official Journal of the International Federation of Clinical Neurophysiology*, vol. 123, no. 6, pp. 1216–1225, Jun. 2012, ISSN: 1872-8952. DOI: 10.1016/j.clinph.2012.01.009.

[19] C. C. Silva, A. Silva, A. Sousa, *et al.*, "Co-activation of upper limb muscles during reaching in post-stroke subjects: An analysis of the contralesional and ipsilesional limbs," *Journal of Electromyography and Kinesiology: Official Journal of the International Society of Electrophysiological Kinesiology*, vol. 24, no. 5, pp. 731–738, Oct. 2014, ISSN: 1873-5711. DOI: 10.1016/j.jelekin.2014.04.011.

[20] Y.-T. Chen, S. Li, E. Magat, P. Zhou, and S. Li, "Motor Overflow and Spasticity in Chronic Stroke Share a Common Pathophysiological Process: Analysis of Within-Limb and Between-Limb EMG-EMG Coherence," *Frontiers in Neurology*, vol. 9, p. 795, 2018, ISSN: 1664-2295. DOI: 10.3389/fneur.2018.00795.

[21] N. Hesam-Shariati, T. Trinh, A. G. Thompson-Butel, C. T. Shiner, and P. A. McNulty, "A Longitudinal Electromyography Study of Complex Movements in Poststroke Therapy. 2: Changes in Coordinated Muscle Activation," *Frontiers in Neurology*, vol. 8, 2017, ISSN: 1664-2295. [Online]. Available: https://www.frontiersin.org/articles/10.3389/fneur.2017.00277 (visited on 08/03/2022).

[22] K. M. Steele, C. Papazian, and H. A. Feldner, "Muscle Activity After Stroke: Perspectives on Deploying Surface Electromyography in Acute Care," *Frontiers in Neurology*, vol. 11, 2020, ISSN: 1664-2295. [Online]. Available: https://www.frontiersin.org/articles/10.3389/fneur.2020.576757 (visited on 08/03/2022).

[23] J. Choi, A. Rajagopal, Y.-F. Xu, J. D. Rabinowitz, and E. K. O'Shea, "A systematic genetic screen for genes involved in sensing inorganic phosphate availability in Saccharomyces cerevisiae," en, *PLOS ONE*, vol. 12, no. 5, e0176085, 2017, Publisher: Public Library of Science, ISSN: 1932-6203. DOI: 10.1371/journal.pone.0176085. [Online]. Available: https://journals.plos.org/plosone/article?id=10.1371/journal.pone.0176085 (visited on 08/01/2022).

[24] R. Leeb, H. Sagha, R. Chavarriaga, and J. d. R. Millán, "A hybrid brain–computer interface based on the fusion of electroencephalographic and electromyographic activities," en, *Journal of Neural Engineering*, vol. 8, no. 2, p. 025 011, Mar. 2011, Publisher: IOP Publishing, ISSN:

1741-2552. DOI: 10.1088/1741-2560/8/2/025011. [Online]. Available: https://doi.org/10.1088/1741-2560/8/2/025011 (visited on 08/01/2022).

[25] G. Müller-Putz, R. Leeb, M. Tangermann, *et al.*, "Towards Noninvasive Hybrid Brain–Computer Interfaces: Framework, Practice, Clinical Application, and Beyond," *Proceedings of the IEEE*, vol. 103, no. 6, pp. 926–943, Jun. 2015, Conference Name: Proceedings of the IEEE, ISSN: 1558-2256. DOI: 10.1109/JPROC.2015.2411333.

[26] A. Riccio, E. M. Holz, P. Aricò, *et al.*, "Hybrid P300-based brain-computer interface to improve usability for people with severe motor disability: Electromyographic signals for error correction during a spelling task," eng, *Archives of Physical Medicine and Rehabilitation*, vol. 96, no. 3 Suppl, S54–61, Mar. 2015, ISSN: 1532-821X. DOI: 10.1016/j.apmr.2014.05.029.

[27] E. López-Larraz, A. Sarasola Sanz, N. Irastorza Landa, N. Birbaumer, and A. Ramos-Murguialday, "Brain-machine interfaces for rehabilitation in stroke: A review," *Neurorehabilitation*, vol. 43, pp. 77–97, Aug. 2018. DOI: 10.3233/NRE-172394.

[28] T. Lalitharatne, K. Teramoto, Y. Hayashi, and K. Kiguchi, "Towards Hybrid EEG-EMG-Based Control Approaches to be Used in Bio-robotics Applications: Current Status, Challenges and Future Directions," *Paladyn, Journal of Behavioral Robotics*, vol. 4, pp. 147–154, Dec. 2013. DOI: 10.2478/pjbr-2013-0009.

[29] G. Morone, G. F. Spitoni, D. De Bartolo, *et al.*, "Rehabilitative devices for a top-down approach," eng, *Expert Review of Medical Devices*, vol. 16, no. 3, pp. 187–195, Mar. 2019, ISSN: 1745-2422. DOI: 10.1080/17434440.2019.1574567.

[30] A. Burns, H. Adeli, and J. A. Buford, "Upper Limb Movement Classification Via Electromyographic Signals and an Enhanced Probabilistic Network," en, *Journal of Medical Systems*, vol. 44, no. 10, p. 176, Aug. 2020, ISSN: 1573-689X. DOI: 10.1007/s10916-020-01639-x. [Online]. Available: https://doi.org/10.1007/s10916-020-01639-x (visited on 06/17/2021).

[31] T. Mima and M. Hallett, "Corticomuscular coherence: A review," *Journal of Clinical Neurophysiology: Official Publication of the American Electroencephalographic Society*, vol. 16, no. 6, pp. 501–511, Nov. 1999, ISSN: 0736-0258.

[32] C. Brambilla, I. Pirovano, R. M. Mira, G. Rizzo, A. Scano, and A. Mastropietro, "Combined Use of EMG and EEG Techniques for Neuromotor Assessment in Rehabilitative Applications: A Systematic Review," eng, *Sensors (Basel, Switzerland)*, vol. 21, no. 21, p. 7014, Oct. 2021, ISSN: 1424-8220. DOI: 10.3390/s21217014.

[33] K. von Carlowitz-Ghori, Z. Bayraktaroglu, F. U. Hohlefeld, F. Losch, G. Curio, and V. V. Nikulin, "Corticomuscular coherence in acute and chronic stroke," *Clinical Neurophysiology: Official Journal of the International Federation of Clinical Neurophysiology*, vol. 125, no. 6, pp. 1182–1191, Jun. 2014, ISSN: 1872-8952. DOI: 10.1016/j.clinph.2013.11.006.

[34] L. H. Larsen, I. C. Zibrandtsen, T. Wienecke, *et al.*, "Corticomuscular coherence in the acute and subacute phase after stroke," en, *Clinical Neurophysiology*, vol. 128, no. 11, pp. 2217–2226, Nov. 2017, ISSN: 1388-2457. DOI: 10.1016/j.clinph.2017.08.033. [Online]. Available: http://www.sciencedirect.com/science/article/pii/S1388245717309604 (visited on 11/08/2019).

[35] R. Krauth, J. Schwertner, S. Vogt, *et al.*, "Cortico-Muscular Coherence Is Reduced Acutely Post-stroke and Increases Bilaterally During Motor Recovery: A Pilot Study," *Frontiers in Neurology*, vol. 10, 2019, ISSN: 1664-2295. [Online]. Available: https://www.frontiersin.org/articles/10.3389/fneur.2019.00126 (visited on 07/20/2022).

[36] Z. Guo, Q. Qian, K. Wong, *et al.*, "Altered Corticomuscular Coherence (CMCoh) Pattern in the Upper Limb During Finger Movements After Stroke," *Frontiers in Neurology*, vol. 11, 2020, ISSN: 1664-2295. [Online]. Available: https://www.frontiersin.org/articles/10.3389/fneur.2020.00410 (visited on 07/20/2022).

[37] A. Chowdhury, H. Raza, Y. K. Meena, A. Dutta, and G. Prasad, "An EEG-EMG correlation-based brain-computer interface for hand orthosis supported neuro-rehabilitation," *Journal of Neuroscience Methods*, vol. 312, pp. 1–11, Jan. 2019, ISSN: 1872-678X. DOI: 10.1016/j.jneumeth.2018.11.010.

[38] Z. Guo, S. Zhou, K. Ji, *et al.*, "Corticomuscular integrated representation of voluntary motor effort in robotic control for wrist-hand rehabilitation after stroke," en, *Journal of Neural Engineering*, vol. 19, no. 2, p. 026 004, Mar. 2022, Publisher: IOP Publishing, ISSN: 1741-2552. DOI: 10.1088/1741-2552/ac5757. [Online]. Available: https://doi.org/10.1088/1741-2552/ac5757 (visited on 07/04/2022).

[39] T. Mima, K. Toma, B. Koshy, and M. Hallett, "Coherence between cortical and muscular activities after subcortical stroke," *Stroke*, vol. 32, no. 11, pp. 2597–2601, Nov. 2001, ISSN: 1524-4628. DOI: 10.1161/hs1101.098764.

[40] G. Silasi and T. H. Murphy, "Stroke and the connectome: How connectivity guides therapeutic intervention," *Neuron*, vol. 83, no. 6, pp. 1354–1368, Sep. 2014, ISSN: 1097-4199. DOI: 10.1016/j.neuron.2014.08.052.

[41] N. Ejaz, J. Xu, M. Branscheidt, *et al.*, "Evidence for a subcortical origin of mirror movements after stroke: A longitudinal study," *Brain: A Journal of Neurology*, vol. 141, no. 3, pp. 837–847, Mar. 2018, ISSN: 1460-2156. DOI: 10.1093/brain/awx384.

[42] J.-H. Park, J.-H. Shin, H. Lee, J. Roh, and H.-S. Park, "Alterations in intermuscular coordination underlying isokinetic exercise after a stroke and their implications on neurorehabilitation," *Journal of NeuroEngineering and Rehabilitation*, vol. 18, no. 1, p. 110, Jul. 2021, ISSN: 1743-0003. DOI: 10.1186/s12984-021-00900-9. [Online]. Available: https://doi.org/10.1186/s12984-021-00900-9 (visited on 07/20/2022).

[43] S. Storch, M. Samantzis, and M. Balbi, "Driving Oscillatory Dynamics: Neuromodulation for Recovery After Stroke," *Frontiers in Systems Neuroscience*, vol. 15, 2021, ISSN: 1662-5137. [Online]. Available: https://www.frontiersin.org/articles/10.3389/fnsys.2021.712664 (visited on 07/20/2022).

Section I

Characterization of cortico-muscular patterns in stroke patients compared to healthy subjects during simple hand movements

Introduction

To address the design of a novel hybrid BCI (h-BCI) for motor rehabilitation, here Cortico-Muscular Coupling (CMC), computed from the EEG and EMG signals, is proposed as control feature. CMC is a measure of synchronization between central and peripheral activation and stroke related CMC studies have shown alterations in both the acute and chronic phases [1]–[4]; furthermore, changes have been correlated with functional recovery [5].
Until recently, most CMC studies in stroke patients have limited the observation to few EEG electrodes in the affected hemisphere and the target muscle [2], [4], [6]. Similarly, the implementation of CMC-based BCIs has been limited to few EEG-EMG couples determined a priori [7]. However, the complexity of post-stroke recovery is such that several brain regions and muscles participate in post-lesional re-arrangements [8]–[11]. Lately, stroke-related CMC studies have broadened the observation to multi-channel recordings to describe complex phenomena such as the contralesional hemisphere contribution [5], [12] or the abnormal recruitment of antagonists and proximal muscles [4], [13], [14]. All this evidence supports the potential role of CMC control feature in a rehabilitative BCI paradigm for its capability to encode both volitional control over movement and possible deviations from the physiological motor system activation, thus well beyond the purpose of increasing system classification performance, usually pursued by h-BCIs [15]–[17].

To characterize the widespread functional brain-muscle connectivity in both physiological and pathological condition, in the first part of this section the cortico-muscular coupling between several EEG-EMG pairs was analyzed as a comprehensive brain-muscles network to characterize simple hand movements (i.e. finger extension and grasping) in healthy subjects (Study 1) [18] and stroke patients (Study 2) [19]. These tasks are the most used in BCI-based rehabilitative context [20]–[22].
In Study 1, the EEG and the EMG data of 20 healthy participants during simple motor task were analyzed, the grand-average cortico-muscular patterns were obtained and compared in different conditions with the aim of identifying their distinctive traits. Moreover, the ability of multi-channels EEG-EMG features in discriminating movements from rest condition and different movements tasks was evaluated with the ultimate aim of addressing the design of a h-BCI able to train both brain and peripheral activity.

Once identified the physiological characteristics of CMC patterns, in Study 2 their alterations were investigated in stoke patients. Thus, high-density CMC networks (derived from multiple EEG and EMG channels) and their relation with upper limb motor deficit were analyzed by comparing data from 12 stroke patients (EXP group) with 12 healthy participants (CTRL group) during simple hand tasks. Network properties were extracted by means of indices derived ad-hoc from graph theory and their ability in quantifying motor impairment was assessed comparing the two groups [19].

Finally, to further investigate the movements specificity of CMC features, their ability to discriminate different types of hand movements was analyzed more in details in Study 3. Different classification approaches were evaluated [23] and performances were compared with the ones obtained by the canonical BCI's classification method based on only brain features. Indeed, going beyond the BCI application for motor rehabilitation, the ability to non-invasively decode different type of movements by exploiting all remaining functionalities is crucial in other BCI applications for motor substitution in which "natural control" (i.e. that resembling physiological control) of prosthetic devices is cutting-edge [24]–[26].

1. Study 1

Cortico-muscular and intermuscular coupling in healthy subjects

1.1 Background and Objectives

Brain activity and connectivity patterns are widely altered after stroke [11] and such changes involve brain areas distant from the lesion, both ipsi and contralateral to the lesion itself. The muscular patterns are also altered after stroke resulting in excess activation of muscles other than the target one (motor overflow, co-activation of agonists and antagonists and even bilateral involvement) [10], [27]. Thus, this study analyzed a combination of cortico-muscular coherence (CMC) and intermuscular coherence (IMC) as control features for a novel hybrid BCI for rehabilitation purposes.
CMC is a measure of brain-muscle interplay during movement, derived from EEG-EMG coupling within motor relevant EEG frequency bands [1], whereas IMC provides information about the common corticospinal drive among different muscles and has been employed to investigate intermuscular coordination during upper limb motor tasks in healthy participants [28], [29]. In stroke subjects, IMC provides information on the pathophysiological basis of altered muscular patterns related e.g. to spasticity [30]. It has been shown that both CMC [31] and IMC [32] can be modulated in a neurofeedback/biofeedback training paradigm.
The combination of information encoded in CMC and IMC would enable a hybrid BCI (h-BCI) to reinforce volitional control of those movement attempts that most resemble physiological muscular activation patterns, thereby lessening the probability to facilitate maladaptive motor re-learning.

Here, both CMC and IMC were explored in healthy participants perform-

ing simple hand movements such as finger extension and grasping. Although some studies in both healthy and stroke participants have employed CMC as a BCI control feature [7], [31], [33] the combined use of CMC-IMC for hybrid rehabilitative BCIs has not been conceived yet.
CMC and IMC values were estimated from multiple EEG and EMG electrodes rather than considering only few pre-determined scalp electrodes and movement target muscles [4], [5], [7], [33]. This multichannel approach returned EEG-EMG and EMG-EMG synchronization pairs as a comprehensive functional connectivity pattern for each tested movement. The performances of CMC and IMC as features to classify simple hand motor tasks versus rest or different tasks against each other were evaluated [18].

This signal processing framework contributed to the design of a novel hybrid BCI system for upper limb motor rehabilitation in stroke subjects (the h-BCI prototype described in Section II-Study 5), providing the necessary knowledge on (i) how multimodal features should be defined for successful detection of correct (i.e. "close-to-normal") movement to be volitionally controlled via BCI, and eventually implemented for the online processing, (ii) the inter-subject and intra-subject variability to be taken into account when approaching the variety of movement impairment in stroke population.

1.2 Materials and Methods

1.2.1 Participants and experimental protocol

Twenty healthy volunteers (9 females/11 males, age 27.8±2.4 yo), all right-handed and with no history of neuromuscular disorders, were enrolled in the study. All participants were informed about the experimental protocol and gave their informed written consent to the study. The study was approved by the ethics board of the IRCCS Fondazione Santa Lucia, Rome, Italy (Prot. CE/PROG. 730).

During the experiment participants were seated in a comfortable chair with their forearms on the armrests. Visual cues were presented on a screen facing them. Participants were instructed to perform four movements: finger extension (Ext) and grasping (Grasp), with either the right (R) and left (L) hand. The experiment was administered in two sessions including 4 blocks (one per movement: ExtR, ExtL, GraspR, GraspL) of 30 trials each. An inter-block break was set to 1 minute and an inter-session break to 10 minutes. The block sequence was randomized inter- and intra-sessions. The total trial duration was 7s with an inter-trial interval of 3.5s. Each trial began with a cursor appearing at the bottom of the screen, moving toward the top at constant velocity on a vertical line, reaching the top of the screen at the end of the trial. The screen was split into two vertically stacked regions with different background colour (black/green for the bottom/top regions, respectively), so that the moving cursor would

cross the boundary between the regions exactly 3s after the trial's start (Figure 1.1). The moving cursor provided the participants with a visual cue of the timing of the tasks: participants were instructed to rest in the first 3s of the trial (cursor in the black region) and to perform the task along the remaining 4s (cursor on the green region). The task consisted of a gradual extension or flexion of their right or left hand fingers, spanning across the final 4s of each trial.

This instruction was given to reduce the inter-subject and intra-subject variability in executing the motor tasks. Furthermore, such gradual/slow execution of finger extension/grasping was chosen as more suitable keeping in mind the target stroke population with different degrees of motor impairment.

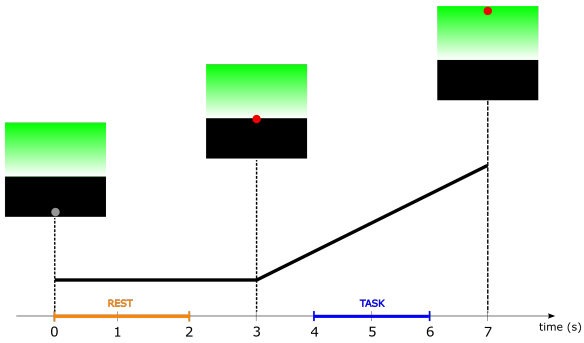

Figure 1.1. Timeline of the experiment with details on the screen shown to the participant. The orange and the blue lines show the time intervals selected for the analysis of rest ([0 2]s) and task ([4 6]s), respectively [18].

1.2.2 EEG and EMG data collection

EEG and EMG signals were simultaneously collected with a sampling frequency of 2400Hz by means of the g.HIamp amplifier (g.tec medical engineering GmbH Austria[1]). Scalp EEG potentials were collected from thirty-one passive electrodes assembled on an electrode cap placed above the sensorimotor area according to an extension of the International 10-20 system (FC5, FC3, FC1, FCz, FC2, FC4, FC6, C5, C3, C1, Cz, C2, C4, C6, CP5, CP3, CP1, CPz, CP2, CP4, CP6, P5, P3, P1, Pz, P2, P4, P6, PO3, POz, PO4). Potentials were referenced to the linked earlobes and grounded to the left mastoid. The contact impedance of each electrode was kept below 5kΩ. The EMG data were collected from 10 muscles of the upper limbs (5 per side) namely: extensor digitorum (ED), flexor digitorum superficialis (FD), triceps (TRI), biceps brachii (BIC) and lateral deltoid (DELT). EMG sensors were placed according to the guidelines reported in Barbero et al. [34]. For each muscle two surface Ag/AgCl

[1] `https://www.gtec.at`

electrodes, 10mm diameter, were placed at 20mm inter-electrode distance on the centre of the muscle belly, in the direction of the muscle fibres, according to the SENIAM recommendations [35]. Crosstalk between forearm muscles during electrode placement was minimized and tested by the execution of specific movements associated with the muscles. The quality of EEG and EMG signals was visually checked prior to beginning the measurements and continuously monitored afterwards. Three maximum voluntary contractions (MVCs) lasting 5s were recorded for each muscle [36], [37] at the beginning of the experiment.

1.2.3 Data Analysis

Figure 1.2 shows the flow chart illustrating the methodological steps of the analyses presented below.

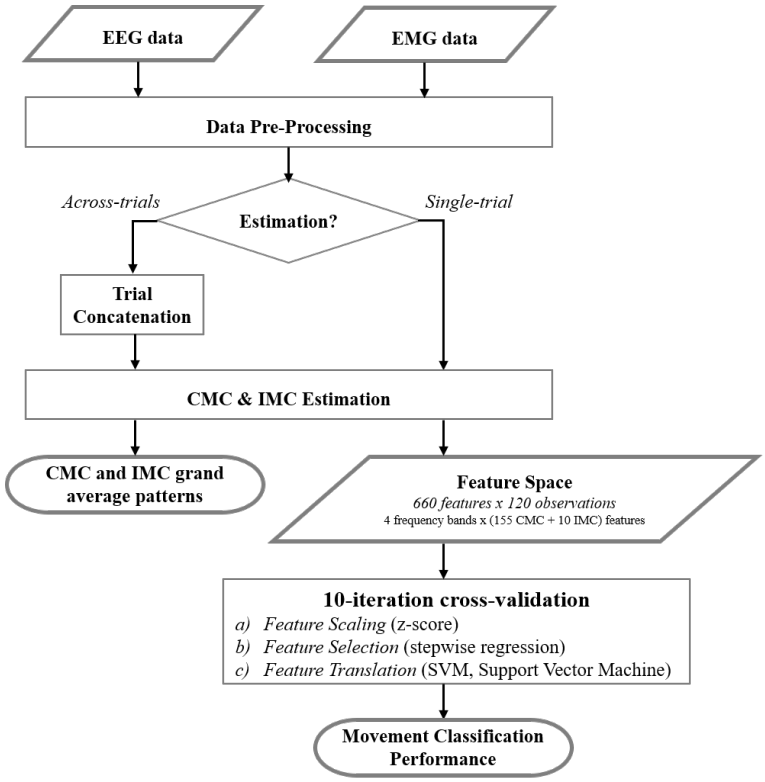

Figure 1.2. Flow chart illustrating the methodological steps of the analyses [18].

EEG and EMG data pre-processing

Vision Analyzer 1.05 software (Brain Products GmbH, Gilching, Germany) was used to pre-process the data. EEG and EMG signals were downsampled to

1000Hz after an appropriate filtering to avoid aliasing. EEG and EMG signals were band-pass filtered with a Butterworth zero-phase filter in the range 3—100 Hz and 3—500 Hz, respectively. A notch filter at 50Hz was applied to remove power-line interference on both signals. Continuous traces were segmented in 7s epochs, comprising the 3s of rest and the 4s of motor execution. Trials with EEG signals exceeding in absolute value the amplitude of 100μV and trials contaminated by muscular artifacts were rejected. All EEG and EMG trials were visually inspected to identify artifacts. Following this assessment, three participants were excluded from further analysis due to artifacts in more than 50% of trials. EEG signals were re-referenced according to the common average reference. The following analyses were performed using custom code developed in Matlab R2019a (The MathWorks, Inc., Natick, Massachusetts, USA).

Assessment of muscle activation

Two time intervals of interest lasting 2s were selected for the CMC and IMC analysis according to the muscle activation level: (i) a rest interval, from 0s to 2s, and (ii) a task interval, from 4s to 6s with respect to the trial start (see Figure 1.1). To verify that participants showed a stable and predictable muscle activation in these windows, the EMG activation was computed as follows. The root-mean-square (RMS) of EMG signal on the target muscle for each trial (FD for grasping movements, ED for finger extension movements) was computed on windows of 0.15s length sliding across the whole trial duration and on the three MVC repetitions of the corresponding muscle. The EMG activation was expressed as percent of the ratio between the RMS in each short window of the trial and the maximum RMS among the three corresponding MVC repetitions (%MVC). The activation level values, expressed as %MVC values were finally averaged across all time points belonging either to the rest or the task intervals, and across trials (EMG activation level).

Coherence estimation

The magnitude squared coherence values between EEG and EMG signals, i.e. CMC, or between EMG signals, i.e. IMC, were computed in the range 8-100 Hz.

Cortico-muscular coherence

The CMC values were computed as

$$CMC_{xy}(f_j) = |S_{xy}(f_j)|^2 \tag{1.1}$$

$$S_{xy}(f_j) = \frac{1}{n}\sum_{i=1}^{n} X_i(f_j) * Y_i(f_j) \tag{1.2}$$

where $S_{xy}(f_j)$ represents the cross-power spectrum between the EEG signal x and the EMG signal y at a given frequency f_j, estimated using the Welch periodogram method with a Hann window. The length and overlap of the

periodogram windows were tailored to the specific aim of the subsequent analysis (see below). EMG signals were rectified before entering in the CMC computation [38].

The absolute square value of the cross-spectrum (as in 1.1) was used as measure of EEG-EMG synchronization, instead of the classical coherence formulation [39]. This approach prevents, in fact, the detection of false positives in CMC when the muscle activation level is around 0, as observed in the rest time interval of the experiment [40]. To be consistent with IMC analysis and previous literature, I will refer to the corticomuscular cross-spectrum by maintaining the designation of coherence.

Intermuscular coherence

Intermuscular coherence was computed between pairs of unrectified EMG signals recorded from muscles of the same side (10 pairs of ipsilateral muscles). The IMC values were computed as [41]

$$IMC_{xy}(f_j) = \frac{|S_{xy}(f_j)|^2}{|S_{xx}(f_j)| * |S_{yy}(f_j)|} \tag{1.3}$$

where $S_{xy}(f_j)$ represents the cross-power spectrum between the EMG signals x and y and $S_{xx}(f_j)$ and $S_{yy}(f_j)$ are the auto-spectra of x and y, respectively. Cross- and auto-spectra were computed according to Welch periodogram with Hann window as described above for the CMC formula.

Across-trials and single-trial estimations

CMC/IMC values were estimated for each participant, movement (ExtR, ExtL, GraspR, or GraspL), and interval of interest (task, rest). Two different procedures were followed for the CMC/IMC estimation (across-trials or single-trial approaches), differing in how the periodogram windows were defined and averaged, serving different purposes in the downstream analysis. In the across-trials approach (periodogram window length of 1s with 0% overlap) a single CMC/IMC spectrum was estimated from all trials in the dataset of a single participant for each EEG-EMG/EMG-EMG pair, in order to have an average CMC/IMC pattern for each participant to be included in the grand average (see paragraph 1.2.4 - CMC and IMC grand average patterns). Before computing the average IMC pattern for each participant, the significance of non-zero IMC values were assessed [41] by comparing them to the chance level defined by the equation [42]

$$CL(\alpha) = 1 - (1 - \alpha)^{\frac{1}{(n-1)}} \tag{1.4}$$

where n is the number of windows of the signals used in the spectra estimation. The significance level was set to α= 0.01 and corrected according to the False Discovery Rate procedure, FDR [43]. Values below $CL(\alpha)$ were set to zero. In the single-trial approach (periodogram window length of 0.125s with 50% overlap), a CMC/IMC spectrum was estimated for each trial in the dataset, in order to have different observations of CMC/IMC patterns for each participant

to be used as features of a classifier discriminating task vs rest or different movements among each other (see paragraph 1.2.3 - Movement classification).

Characteristic frequencies

To select specific frequencies in which CMC and IMC are modulated by a specific task, we divided the frequency spectrum into four bands: alpha (8—12 Hz), beta (13—30 Hz), gamma (31—60 Hz) and high frequencies (HF, 61—100 Hz). In each band we identified a characteristic frequency f_* as the frequency in which $CMC_{xy}(f_j)$ (or $IMC_{xy}(f_j)$) showed the highest value, for all f_j in the band. The characteristic frequency was specific for each pair of signals x and y, thus for each movement type (Ext and Grasp) and in each band we obtained a set of 310 characteristic frequencies for the CMC_{xy} (31 EEG x 5 EMG from muscles ipsilateral to the task side x 2 sides) and a set of 20 characteristic frequencies for the IMC_{xy} (the number of pairs among 5 EMG signals from muscles ipsilateral to the task side x 2 sides). As for "inactive" muscles, characteristic frequencies that were determined when the xy pair included a muscle ipsilateral to the movement (e.g. right DELT during GraspR) were also used for the same xy pair when the movement was contralateral to the muscle (e.g. right DELT during GraspL). Analyses of the rest interval borrowed the characteristic frequencies of the matching task interval. In subsequent analyses, only CMC/IMC values taken at the characteristic frequencies are considered.

Movement classification

A single-subject binary classification model was trained to evaluate the performance of CMC and IMC values to discriminate task vs rest intervals, for each movement. CMC and IMC values from single trials were merged into a feature vector containing, therefore, CMC values from all possible EEG-EMG pairs and IMC values from all possible EMG-EMG pairs, for each frequency band (CMC+IMC approach). Only pairs including muscles ipsilateral to the movement (e.g. the 5 muscles of the right upper limb in ExtR or GraspR) were included in the feature vector. Thus, the feature space was 660-dimensional: 620 CMC features (31 EEG channels x 5 EMG channels x 4 frequency bands) and 40 IMC features (10 pairs among 5 EMG channels x 4 frequency bands). For each movement and participant, the dataset consisted of 120 observations (60 trials x 2 intervals i.e. task and rest).

Feature scaling (z-score standardization) was applied to the dataset to take into account differences among types of features. A feature selection algorithm based on the stepwise regression [44] with an empty initial model was applied to reduce the dimensionality of the feature space before building the classification model. The results of this feature reduction process also served to assess the subset of features most relevant to classification (see below). A support vector machine classifier with linear kernel [45] was used as classification model on the reduced features space. A 10-iteration cross-validation was applied to train the

model and evaluate the classification performances. In each iteration, 70% and 30% of the observations were used as training and testing dataset, respectively.

Two CMC+IMC more models (Ext-Grasp classifiers) were considered to assess whether CMC and IMC features can discriminate different movement types. Only features from task intervals of two ipsilateral movement types were included in each model (one model per side), thus discriminating either GraspR vs ExtR or GraspL vs ExtL classes.

In order to disentangle the role of each feature type (CMC or IMC) in the movement discrimination, the single-subject binary classification Task vs Rest and Ext vs Grasp was repeated considering CMC and IMC values as features separately (CMC and IMC approaches).

Four different metrics were computed to evaluate the performance of all classification models: i) the area under the curve (AUC) of the Receiver Operating Characteristic (ROC) curve [46], ii) the accuracy, iii) the specificity and iv) the sensitivity of the classifier.

The subset of features selected by the stepwise regression were analyzed to identify the most recurrent EEG-EMG and EMG-EMG pairs used in the classification models. The number of times a specific channel pair was selected across participants and cross-validation iteration was counted irrespectively of the frequency band they corresponded to.

1.2.4 Statistical Analysis

CMC and IMC grand average patterns

Each movement was described by a coherence pattern as result of a grand average analysis computed on CMC/IMC values across participants.

For each movement type, frequency band and channel pair a paired sample t-test (across participants, N=17) was applied using as independent variable the interval (task vs rest) and as dependent variable the CMC/IMC values computed in the across-trials procedure. The significance level was set to 0.05. False Discovery Rate (FDR) was used to control family-wise error rate.

Significant differences will be interpreted as a marker of relevance of a specific pair/band in the execution of a specific movement.

Classification performance evaluation

To investigate the effect of the side and type of movement on the performance of task-rest classifiers, a two-way repeated measures analyses of variance (ANOVA) was performed considering as within main factors the MOVEMENT (2 levels:

Ext, Grasp) and the SIDE (2 levels: right, left) and as dependent variable the AUC value.

To evaluate whether the discriminability between grasping and extension movements depends on the side, the resulting AUC values were analysed by means of a paired t-test with significance threshold equal to 0.05.

Performances obtained by the combination of CMC and IMC features and CMC and IMC features alone were statistically compared using a one-way repeated measures ANOVA. AUC values were used as dependent variable and the features type (CMC, IMC, CMC+IMC) as within factor. The same analysis was repeated for each movement and side in the task vs rest classification and for each side in the Ext vs Grasp classification.

The statistical significance level for all tests was set to $p<0.05$ and the Tukey's post-hoc analysis was performed to assess differences among pairs.

1.3 Results

1.3.1 Assessment of muscle activation

The EMG activation levels in the task interval (mean ± standard error across participants, N=17) were 9.5 ± 0.9 %MVC and 9.9 ± 1.0 %MVC for the ED muscle in ExtR and ExtL, respectively and 5.5 ± 0.9 %MVC and 6.3 ± 1.2 %MVC for the FD muscle in GraspR and GraspL, respectively. The activation levels in the rest interval (mean ± standard error across participants, N=17) were 1.3 ± 0.1 %MVC and 1.3 ± 0.2 %MVC for the ED muscle in ExtR and ExtL, respectively and of 1.8 ± 0.3 %MVC and 2.5 ± 0.8 %MVC for the FD muscle in GraspR and GraspL, respectively.

1.3.2 CMC and IMC grand average patterns

Figures 1.3 and 1.4 show the grand average CMC (panels a and c) and IMC (panels b and d) patterns observed for the right and left finger extension and grasping, respectively. As expected for a healthy experimental group, no significant CMC and IMC values were observed for the side contralateral to the movement.

As for right and left Ext movements (Figure 1.3), the highest CMC values were found for connections involving mainly the target muscle (ED) and most of the bilateral sensorimotor EEG electrodes, in alpha and beta bands. At higher frequency bands (gamma and HF), CMC values were lower and less muscle specific. Results also revealed that the left Ext movement (non-dominant hand; left hand, Figure 1.3 c) was characterized by EEG-EMG connections involving

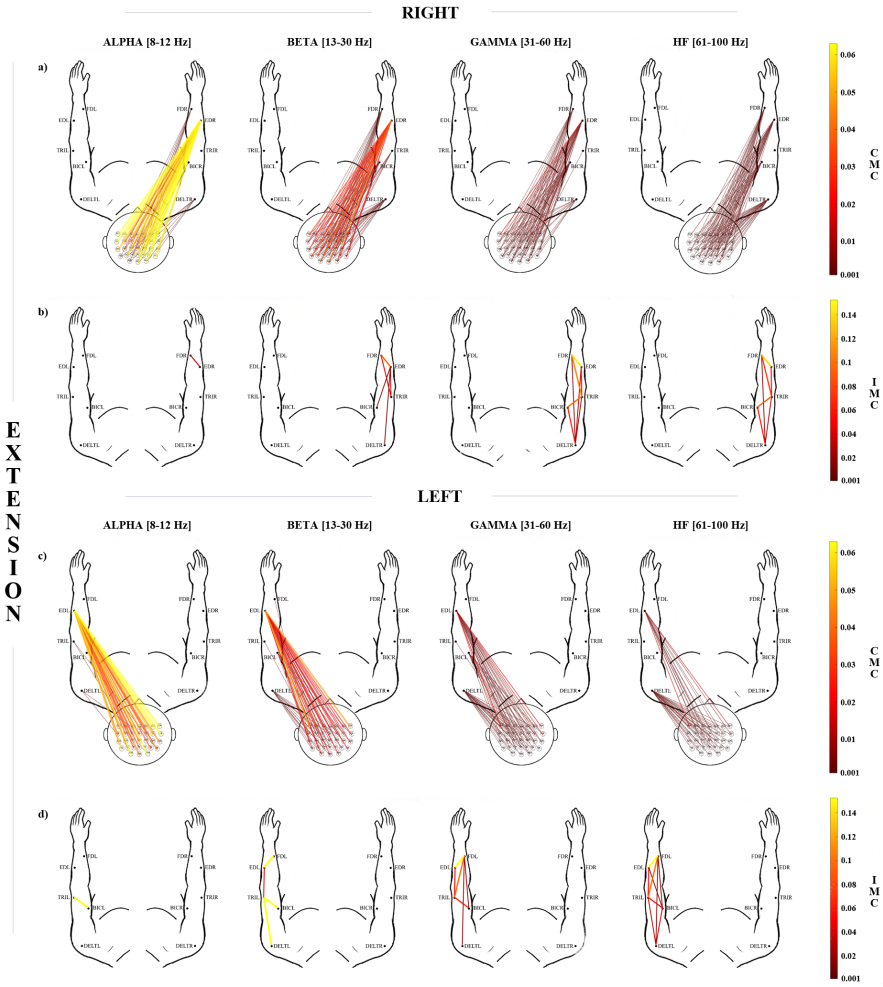

Figure 1.3. Grand average coherence patterns during finger extension. Cortico-muscular (CMC) and Intermuscular (IMC) patterns for the right finger extension movement (Ext) (panels (a) and (b) for CMC and IMC, respectively) and left Ext (panels (c) and (d) for CMC and IMC, respectively) and for each frequency band: alpha (8–12 Hz), beta (13–30 Hz), gamma (31–60 Hz) and high frequency, HF, band (61–100 Hz). The representation is seen from the above: scalp with nose pointing toward the top of the page and arms in front of the participant. Only statistically significant CMC/IMC values are represented (paired t-test between task and rest intervals, $\alpha = 0.05$ FDR correction). The color bar codes for the CMC/IMC average value (across participants, N = 17) in the task interval [18].

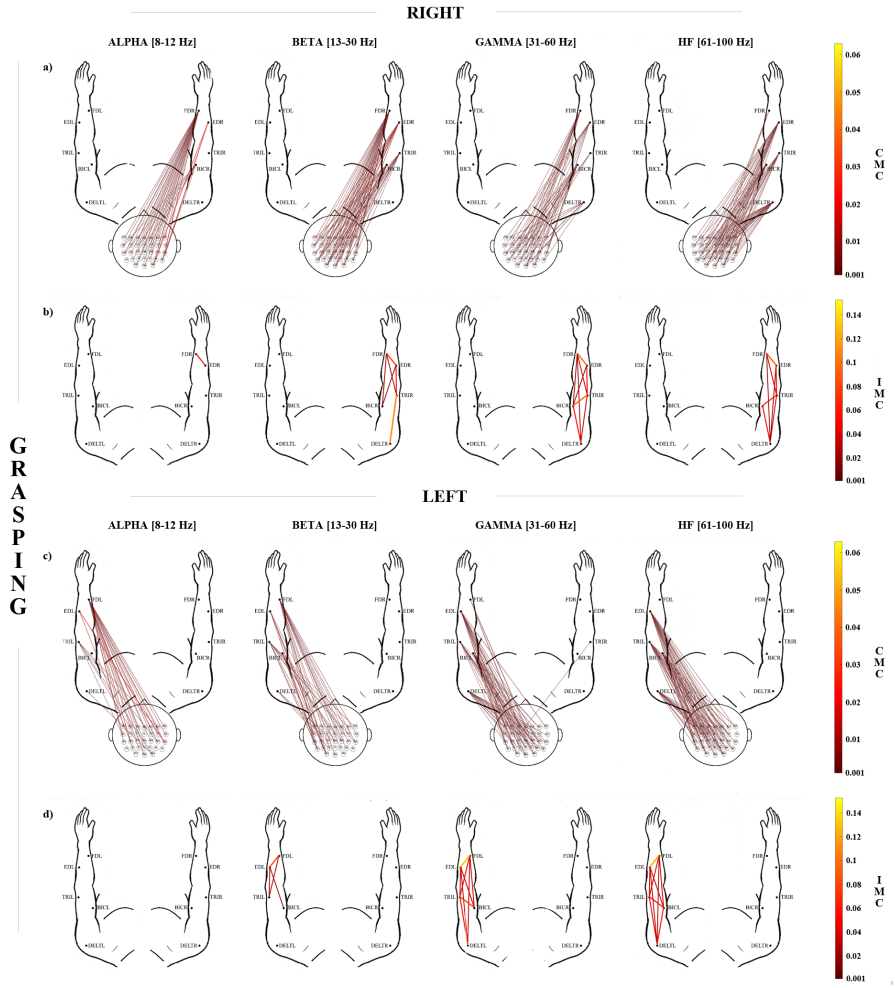

Figure 1.4. Grand average coherence patterns during grasping. Corticomuscular (CMC) and Intermuscular (IMC) patterns for the right finger extension movement (Ext) (panels (a) and (b) for CMC and IMC, respectively) and left Ext (panels (c) and (d) for CMC and IMC, respectively) and for each frequency band: alpha (8–12 Hz), beta (13–30 Hz), gamma (31–60 Hz) and high frequency, HF, band (61–100 Hz). The representation is seen from the above: scalp with nose pointing toward the top of the page and arms in front of the participant. Only statistically significant CMC/IMC values are represented (paired t-test between task and rest intervals, $\alpha = 0.05$ FDR correction). The color bar codes for the CMC/IMC average value (across participants, N = 17) in the task interval [18].

mainly the target ED muscle and other proximal muscles (e.g. deltoid), whereas the same movement executed with the dominant hand (right hand, Figure 1.3 a) showed connections also with the antagonist FD (across all frequency bands). As for the IMC patterns, significant patterns were found for both right and left Ext movement only in beta, gamma and HF bands. None or isolated EMG-EMG connections were found in alpha band. The highest IMC values were observed between target ED and FD for both left and right Ext. For all movements, IMC patterns in HF appeared to be less specific, i.e. involving all muscles.

As for right and left Grasp movements (Figure 1.4), lower CMC values were obtained than in Ext. The EEG-EMG connections mainly involved the target muscle FD in alpha band, whereas ED and proximal muscles were involved in higher frequency bands. Similar to what observed for Ext, the involvement of bilateral sensorimotor areas characterized these CMC patterns. Like the Ext movement, the IMC patterns in both left and right grasping movement showed significant connections in beta, gamma and HF bands, with more muscles progressively involved at higher frequencies. A strong connection between ED and FD across these frequency bands is confirmed for Grasp movement executed with both left and right hand.

1.3.3 Movement Classification

Task-rest classification

The task-rest classification performances expressed as AUC, Accuracy, Specificity and Sensitivity are shown in Table 1.1. Overall, higher classification performances were observed for Ext with respect to Grasp, whereas performances are comparable between left and right movements.

The ANOVA on task-rest classification AUC revealed a significant effect of MOVEMENT ($F(1,16) = 13.16$, $p < 0.01$) and MOVEMENT x SIDE ($F(1,16) = 6.06$, $p = 0.03$) factors. No significant effect of the SIDE factor was observed ($F(1,16) = 0.19$, $p = 0.67$). The Tukey's post-hoc analysis revealed significant differences ($p < 0.01$) between movements (Ext and Grasp) for both the right and the left side, as already suggested from the mean values in Table 1.1 (see Figure 1.5).

Table 1.1. Classification performances (AUC, Accuracy, Specificity and Sensitivity) of the CMC + IMC approach, reported as mean (standard error) across 17 participants, of the task-rest classifier. ExtR: finger extension with the right hand; ExtL: finger extension with the left hand; GraspR: grasping with the right hand; GraspL: grasping with the left hand.

Task vs Rest				
Movement	**AUC**	**Accuracy**	**Specificity**	**Sensitivity**
ExtR	0.95(0.01)	0.90(0.02)	0.95(0.01)	0.85(0.02)
ExtL	0.98(0.01)	0.94(0.01)	0.98(0.01)	0.90(0.01)
GraspR	0.89(0.03)	0.82(0.03)	0.86(0.03)	0.79(0.02)
ExtR	0.87(0.02)	0.80(0.02)	0.85(0.01)	0.76(0.02)

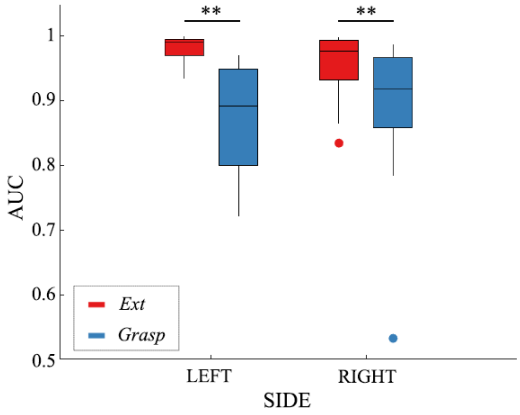

Figure 1.5. Distribution of task-rest classification performance. Boxplot of the distributions (N = 17 participants) of the AUC values for each movement (Ext, finger extension, and Grasp, grasping) executed with either hand (right and left). Markers (**) indicate significant differences ($p < 0.01$) between groups resulting from the Tukey's post-hoc test on the significant factor MOVEMENT X SIDE. Significant differences were observed between movements, with higher performance in Ext movement classification.The intra-group variability, expressed as interquartile range of each AUC distribution, is higher for the grasping (0.14 and 0.11 for left and right grasping, respectively) than for extension (0.02 and 0.07 for left and right finger extension, respectively). Differences between sides were not significant [18].

The analysis on selected features revealed that about 60 features were selected by the stepwise regression for each iteration and participant: 62 ± 3 ExtR, 64 ± 3 ExtL, 57 ± 3 GraspR, 52 ± 5 GraspL, presented as mean $\pm$ standard error. Figure 1.6 illustrates the most recurrent features across participants (N = 17) and cross-validation iterations (IT = 10). For Ext movements, the IMC feature between the extensor digitorum muscle and the flexor digitorum

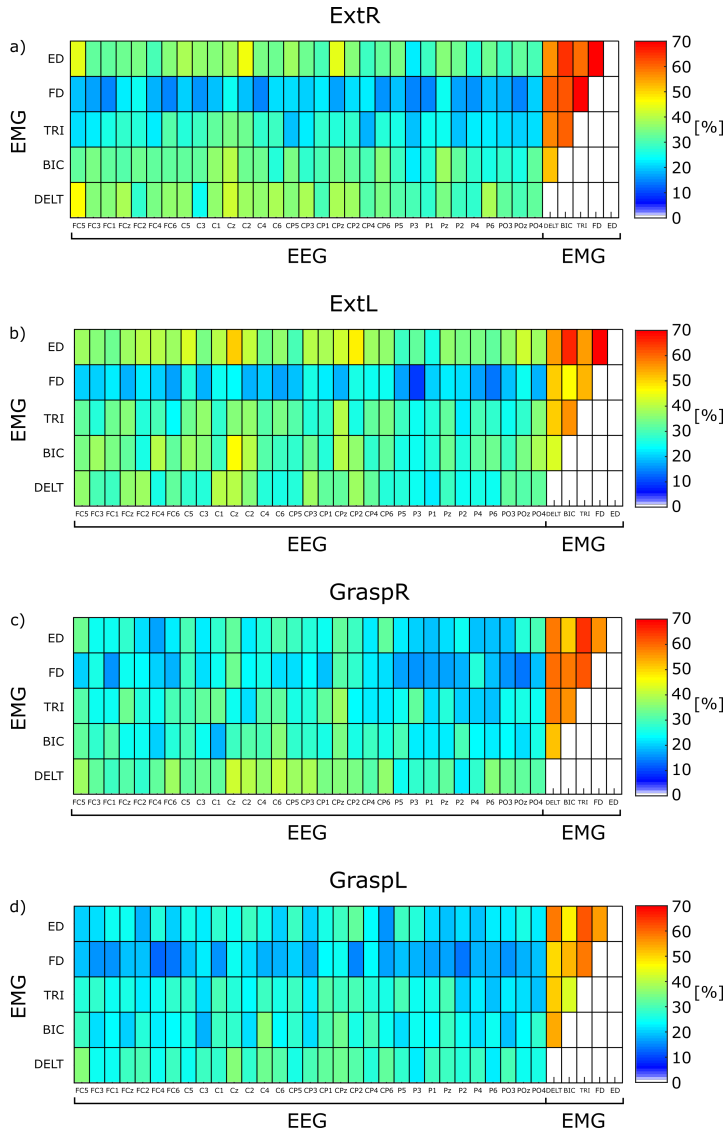

Figure 1.6. Features selected in task versus rest classification. Most recurrent EEG-EMG pairs and EMG-EMG pairs selected by the stepwise regression across participants (N = 17) and cross-validation iterations (IT = 10) in the classification of each movement versus rest. The matrix shows for each EEG-EMG pair and EMG-EMG pair the number of times, expressed as percentage, each pair was selected over all participants and all iterations of the cross-validation. EEG-EMG pairs are identified by boxes from the intersection of EEG channels on the x-axis and EMG channels on the y-axis. EMG-EMG pairs are identified by boxes from the intersection of EMG channels on the x-axis and EMG channels on the y-axis. Panels (a) ExtR: finger extension with right hand, (b) ExtL: finger extension with left hand, (c) GraspR: grasping with right hand, (d) GraspL: grasping with left hand [18].

muscle resulted the most recurrent (∼70%). As for the type of movements, CMC features involving the extensor digitorum muscle were recurrent in Ext movement. The CMC features involving distal (extensor and flexor digitorum muscles) as well as proximal muscles were selected in the Grasp movement, thus indicating a less "muscle-specific" selection for Grasp with respect to Ext movement. The CMC features mostly involved the central and centro-parietal EEG channels strips bilaterally, including the midline electrodes. No clear lateralization of CMC patterns (i.e. involvement of EEG electrode position contralateral to the movement) was found, except for ExtL (CP2 with the extensor digitorum muscle).

The same classification approach was applied separately for CMC and IMC features. The one-way repeated measures ANOVA on AUC, applied to test differences among types of features (CMC + IMC, CMC, IMC), revealed significant lower performance for IMC features in each of the four movements, as shown in Table 1.2. No significant differences were observed between CMC and CMC + IMC features. The following classification performances for the three types of features were achieved: 0.92 (0.01) for CMC + IMC, 0.92 (0.01) for CMC and 0.74 (0.02) for IMC, presented as mean AUC (standard error) across movements.

Table 1.2. Results of the one-way repeated measure ANOVA on AUC considering as independent variables the type of features (CMC + IMC, CMC and IMC) for each movement. The last three columns show the results of the Tuckey post-hoc analysis, — no significant differences, ** significance differences ($p < 0.01$).

Movement	F(p)	CMC+IMC versus CMC	CMC+IMC versus IMC	CMC versus IMC
ExtR (df=2,32)	28.86 (<0.01)	—	**	**
ExtL (df=2,32)	22.37 (<0.01)	—	**	**
GraspR (df=2,32)	43.59 (<0.01)	—	**	**
GraspL (df=2,32)	57.29 (<0.01)	—	**	**

Ext-Grasp classification

The ability of CMC and IMC features to discriminate between Ext and Grasp movements was tested with the same approach used to classify each movement versus rest. The Ext-Grasp classification performances expressed as AUC,

Accuracy, Specificity and Sensitivity are shown in Table 1.3.

Table 1.3. Classification performances (AUC, Accuracy, Specificity and Sensitivity), reported as mean (standard error) across 17 participants, Ext-Grasp classifier.

Ext versus Grasp				
Side	**AUC**	**Accuracy**	**Specificity**	**Sensitivity**
Right Hand	0.98 (<0.01)	0.95 (0.01)	0.95 (0.01)	0.95 (0.01)
Left hand	0.99 (<0.01)	0.95 (0.01)	0.96 (0.01)	0.95 (0.01)

The paired t-test on Ext-Grasp classification AUC values did not reveal any significant effect of the SIDE ($t = 0.77$, $p = 0.45$). The analysis on selected features revealed that about 60 features were selected by the stepwise regression for each iteration and participant: 64 ± 3 ExtR-GraspR, 55 ± 5 ExtL-GraspL, presented as mean $\pm$ standard error. Figure 1.7 illustrates the most recurrent features across participants ($N = 17$) and cross-validation iterations ($IT = 10$). The CMC features mostly involved the central and centro-parietal EEG channels strips bilaterally, including the midline electrodes. No clear lateralization of CMC patterns (i.e. involvement of EEG electrode position contralateral to the movement) was found.

The same classification approach was applied separately for CMC and IMC features. The one-way repeated measures ANOVA on AUC, applied to test differences among types of features (CMC + IMC, CMC, IMC), revealed significant lower performance in Ext versus Grasp classification for IMC features when movements were executed with both the right and the left side, as shown in Table 1.4. No significant differences were observed between CMC and CMC + IMC features. The following classification performances for the three types of features were achieved: 0.98 (<0.01) for CMC + IMC, 0.98 (<0.01) for CMC and 0.85 (0.02) for IMC, presented as mean AUC (standard error) across sides.

Table 1.4. Results of the one-way repeated measure ANOVA on AUC considering as independent variables the type of features (CMC + IMC, CMC and IMC) for each side. The last three columns show the results of the Tuckey post-hoc analysis,— no significant differences, ** significance differences ($p < 0.01$).

Side	**F(p)**	**CMC+IMC versus CMC**	**CMC+IMC versus IMC**	**CMC versus IMC**
Right hand (df = 2,32)	16.91 (<0.01)	—	**	**
Left hand (df = 2,32)	22.04 (<0.01)	—	**	**

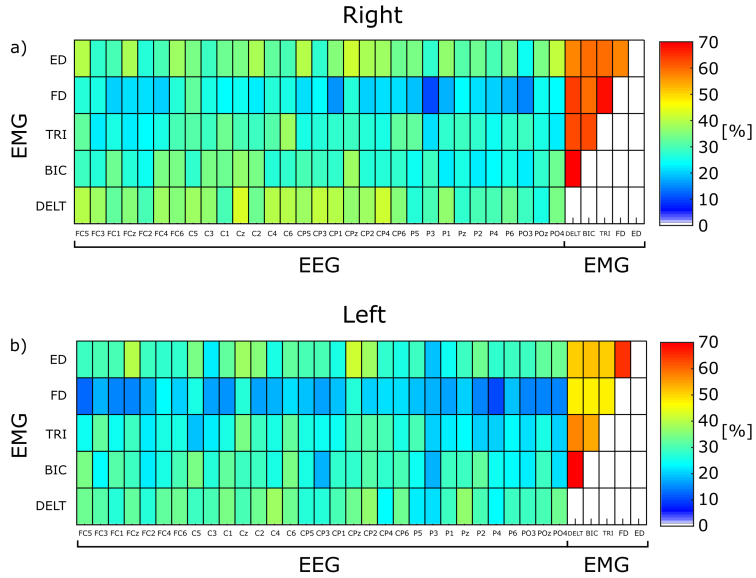

Figure 1.7. Features selected in Ext versus Grasp classification. Most recurrent EEG-EMG pairs and EMG-EMG pairs selected by the stepwise regression across participants (N = 17) and cross-validation iterations (IT = 10) in the classification of finger extension versus grasping for each side. The matrix shows for each EEG-EMG pair and EMG-EMG pair the number of times, expressed as percentage, each pair was selected over all participants and all iterations of the cross-validation. EEG-EMG pairs are identified by boxes from the intersection of EEG channels on the x-axis and EMG channels on the y-axis. EMG-EMG pairs are identified by boxes from the intersection of EMG channels on the x-axis and EMG channels on the y-axis. Panels: (a) Right hand movements, (b) Left hand movements [18].

1.4 Discussion

This study identified the corticomuscular and intermuscular synchronization patterns (CMC and IMC) derived from EEG/EMG multichannel recording performed during the execution of simple hand movements (Ext and Grasp) in a sample of healthy participants. The finger extension and grasping movements could be distinguished by using the combination of CMC and IMC with better (offline) classification performances for the Ext with respect to Grasp movement. Furthermore, such combined CMC + IMC features allowed for successful classification of Ext versus Grasp. All in all, these findings represent a first step in designing novel hybrid BCI systems which better cope with central and peripheral drive of functional motor recovery after stroke.

1.4.1 CMC patterns characterization

The CMC grand average patterns showed significant connections between the whole sensorimotor areas and the muscles of the limb involved in the movement in the entire frequency range from alpha to gamma bands. This is in line with previous studies identifying beta as the typical band for CMC and alpha and gamma bands as reflecting feedback and feed-forward EEG-EMG interaction, respectively [47].

Focusing on the distribution of those connections on the scalp, it can be noticed that the sensorimotor areas bilaterally concurred to the pattern regardless of the side and type of movement performed. Indeed, a prevalent activation of the contralateral sensorimotor cortex during upper limb movements would be expected according to common anatomical and physiological knowledge [48]. This lateralized cortical activation has been widely described in several EEG [24], [49], [50] and CMC studies [3], [6], [51]. Nevertheless, the active contribution of the ipsilateral motor cortex was described to have a facilitatory role in the control of the moving limb [52].

It is well-known that movement preparation and execution is associated to an event-related desynchronization (ERD) which is an oscillatory phenomenon occurring within motor-related EEG frequency bands [53]. While ERD is highly lateralized (i.e. occurs mainly on the sensorimotor areas contralateral to the movement) at movement onset, it has been described to evolve bilaterally on the scalp as movement progresses [54], [55]. In the paradigm analyzed here, participants were explicitly asked to perform Ext and Grasp movement slowly (for 4 s) and the time window for coherence analysis was defined as to start one second after the actual movement onset (see Figure 1.1). It could be hypothesized that the bilateral involvement of the scalp sensorimotor areas in CMC patterns observed in this experimental condition would reflect the progression in time of the execution of the movements. It remains to be elucidated whether such bilateral scalp involvement are confirmed in stroke subjects [5] and how this impacts on appropriate CMC features selection in a rehabilitative hybrid BCI setting.

Regarding the muscle-specificity of the observed CMC patterns, a central role of the agonist muscle (ED) was found during Ext movement, especially with the non-dominant hand. This observation was consistent with the task versus rest classification finding wherein the ED connections were the most recurrently selected among EEG-EMG pairs (see Figure 1.6). The observed difference between dominant and non-dominant hand patterns did not affect task versus rest classification performances, which achieved around 90% for both ExtR and ExtL.

Grand average CMC patterns during Grasp movement showed lower CMC values than those obtained for Ext. This finding could reflect a certain degree of

the inter-individual variability in performing the grasping movement that could be attributed to the wide spectrum of functional and behavioral correlates of the grasping movement [56]. A previous study on healthy participants showed how motor imagery of grasping movement was characterized by behavioral differences among individuals which significantly impacted on EEG sensorimotor reactivity [57]. The CMC patterns of Grasp showed less muscle-specificity (with respect to Ext). This finding is consistent with that observed for task versus rest classification where no muscle among the EEG-EMG pairs appeared more frequently selected than others (see Figure 1.6).

1.4.2 IMC patterns characterization

As for IMC pattern representation, results showed significant differences across frequency bands. Specifically, IMC patterns appeared to be more movement-specific in beta and gamma bands whereas unconnected and fully connected IMC patterns were observed in the alpha and HF band, respectively. Overall, these findings are in line with previous evidence [29] showing that IMC in alpha encodes for postural and subcortical control whose relevance is likely marginal in the paradigm used here (simple hand movements executed by healthy participants), while beta and gamma bands reflect cortical control on movement execution [28], [41], [58], [59].

Among EMG-EMG pairs, the connection between ED and FD muscles (i.e. the agonist/antagonist and antagonist/agonist for the Ext and Grasp movements, respectively), resulted to be the strongest in IMC patterns found in this analysis, confirming findings of Kamper and colleagues [41]. The occurrence of spasticity and pathological co-contraction after stroke results in weakening of the agonist–antagonist coupling [41]. For this reason, the ED-FD synchronization would likely be a crucial feature for the implementation of the proposed hybrid BCI paradigm for stroke subjects' rehabilitation. Nevertheless, the analysis of the features selected by the offline classification model to recognize each movement showed that connections involving the muscles other than ED and FD were also recurrent among healthy participants (e.g. biceps brachii in Grasp). This finding supports the methodological approach used overall throughout this thesis of acquiring information from multiple muscles (i.e. not limited to the forearm muscles) as necessary for the accurate classification of different hand movements. This will be especially true in the case of stroke subjects, where movement is often characterized by abnormal muscular activations (motor overflow, agonist–antagonist co-contractions) whose occurrence should be capable of being monitored and discouraged.

1.4.3 Movement Classification

Classification results revealed high performance of CMC/IMC features in discriminating each task against rest. Lower classification performances were,

however, observed for the Grasp movement with respect to Ext. This finding is consistent with higher intra-individual variability for the Grasp already highlighted by the observation of CMC and IMC patterns. Again, a possible explanation for this could be found in the complexity of behavioral and functional implications of the grasping movement with respect to finger extension [56], [57]. Overall, our classification performances are higher than those reported in similar studies [60], and this is especially true for the Ext movement. Of note, finger extension, and more generally extension movements are commonly employed in the rehabilitation of stroke subjects, especially when effectors such as robots or functional electrical stimulation are employed [21], [61], [62], to contrast the common pathological flexion synergy of the upper limb [63].

To further evaluate the movement specificity of CMC and IMC features, here their ability to classify Ext versus Grasp in the dominant and non-dominant upper limb was tested. Performances were again very high for both sides. The ability to non-invasively decode different types of movement is potentially interesting to achieve the so-called "natural control" of neuroprostheses [64], which is an emerging issue in the field of BCIs for clinical applications beyond stroke (e.g. control of hand neuroprostheses after spinal cord injury [25]).

In all conditions (task versus rest and Ext versus Grasp), the hybrid approach presented here did not outperform the classification results obtained by CMC alone, while both CMC and hybrid were significantly better than IMC. Thus, further studies focused only on CMC features and its ability to monitor the quality of movement was evaluated more in details.

1.4.4 Conclusions, limitations and feature steps

Results obtained on CMC and IMC from healthy participants support the validity of the elements of novelty proposed in this paradigm. First, the conception of a h-BCI which includes EEG and EMG derived features encoding for physiological movement patterns (beyond the mere pursue of higher classification rates, yet showing satisfying performances). Second, the use of multiple EEG electrodes and EMG from several muscles bilaterally to compute CMC, in compliance with the literature showing that post-stroke changes may involve brain areas distant from the lesion and muscles other than the target ones. The characterization of CMC patterns in a population of stroke subjects will be discussed in the next study of this section aiming at (i) defining how interactions between central and peripheral nervous systems are altered after stroke and (ii) providing new potential neurophysiological markers for post-stroke motor impairment and recovery along the rehabilitative process.

Despite the promising findings reported in this study, further investigations are needed to evaluate the feasibility of real-time extraction of CMC-based features suitable to control a hybrid BCI system and are addressed in Section II. The proposed multi-channel approach including signals from the whole sensori-

motor areas and both upper limb muscles has been useful to comprehensively describe each simple movement by means of a CMC pattern highly discriminable against rest. However, this approach could hardly be translated as it is in an online BCI paradigm. To cope with this computational issue, the complexity of such multi-channel analysis were reduced in the subsequent analyses on the real-time control of a hybrid BCI by selecting the best individual hybrid features for each task (e.g. few EEG-EMG channels pairs in specific frequency bands).

The study just presented was published in the International Journal of Neural Systems as part of the Special Issue: "Brain/Neural Assistive Technologies" [18].

2. Study 2

High-density cortico-muscular networks in stroke patients

2.1 Background and Objectives

The potential of CMC patterns derived from high-density EEG/EMG as a feature for a rehabilitative hybrid BCI (h-BCI) in healthy subjects performing simple hand movements (most commonly employed in BCI paradigms) was explored in Study 1, obtaining high classification performances with the most discriminant EEG-EMG features [18]. With respect to currently available h-BCI systems which combine different signals at the classification stage, CMC can be conceived as an intrinsically hybrid feature *per se* allowing simultaneous monitoring of the interaction between brain (EEG) and muscular (EMG) activity. A successful introduction of CMC control feature in rehabilitative BCIs requires to first identify which properties of the widespread corticomuscular network (namely which EEG-EMG features) would best outline the complexity of post-stroke motor deficit to ensure that such h-BCI will favor functional motor recovery and eventually discourage maladaptive changes.

In the present study, CMC patterns were estimated by means of high-density recordings to best capture the widespread corticomuscular network properties in stroke patients during the execution of simple hand movements such as grasping and finger extension. With this aim, the network's properties were then characterized by means of ad-hoc indices derived from a graph theoretical approach [65]. Statistical analysis was performed to outline differences between healthy subjects and patients, performing the movements both with the affected and unaffected hand (AH, UH), and to seek correlation with upper limb motor impairment as assessed by clinical scales.

2.2 Materials and Methods

2.2.1 Participants

Thirteen stroke participants (6 females/7 males, age 52.7±17.7 yo) were enrolled in the study according to the following inclusion criteria: (1) first-ever unilateral, cortical, subcortical, or mixed stroke, caused by ischemia or hemorrhage (confirmed by magnetic resonance imaging), that occurred 3 to 12 months prior to study inclusion; (2) upper limb hemiparesis that was caused by the stroke; and (3) age between 18 and 80 years. The exclusion criteria were the presence of: i) neuropsychological deficits preventing the ability to understand the instructions related to the experiment; ii) concomitant diseases affecting the upper limb motor function (i.e. orthopedic injuries or other neurologic diseases affecting reaching or grasping); iii) spasticity of each segment of the upper limb scored higher than 4 on the Modified Ashworth Scale (MAS [66]). All stroke participants were recruited within the inpatients and outpatients services of Fondazione Santa Lucia, IRCCS, Rome, Italy and were undergoing a rehabilitative treatment (usual care).
Fifteen right-handed healthy participants (10 females/5 males, age 48.7±17.9 yo) were involved in the experimental protocol. Subjects did not present any evidence/known history of neurologic or neuromuscular disorders, nor any permanent/transient condition that could affect upper limb motor function. The study was approved by the local ethics board at Fondazione Santa Lucia, IRCCS, Rome, Italy (CE PROG.752/2019) and all the participants signed an informed consent.
Twelve of the thirteen stroke participants were selected as experimental group for this study (EXP group: 6 females/6 males age 52.5±18.5 yo), one stroke patient was excluded due to too many artifacts after the pre-processing in the data analyzed here. Whereas, twelve of the of fifteen healthy participants (CTRL group: 9 females/3 males, age 43.6 ± 15.3 yo), matched in age and gender with the EXP group (see Results paragraph 2.3.1), were analyzed in the study as a control group.
Clinical and functional evaluation was performed by expert physiotherapists before data acquisition (same day) by means of the following scales: i) the National Institute of Health Stroke Scale (NIHSS) to assess general impairment derived from stroke [67]; ii) the Manual Muscle Test (MMT) to assess strength in the paretic upper limb testing shoulder abduction, elbow flexion/extension and wrist flexion/extension [68]; iii) the MAS scale to assess spasticity of shoulder, elbow and wrist muscles. The upper extremity section of the Fugl-Meyer Assessment scale (FMA), comprising the four sub-scales “Upper Limb”, “Wrist”, “Hand”, “Coordination and Velocity” was performed to extensively describe the paretic upper limb residual function [69]. Handedness was assessed in all participants by means of the short form of the Edinburgh Handedness Inventory (EHI [70]).

2.2.2 Experimental Design and Data Acquisition

The EEG and EMG signals were acquired simultaneously and sampled at 1 and 2 KHz, respectively. 61-channel EEG was recorded from the scalp by means of active electrodes (Brain Products GmbH, Germany[1]) arranged according to an extension of 10-20 International System (reference on left mastoid and ground on right mastoid). Surface bipolar EMG signals were recorded by means of Pico EMG sensors (Cometa S.r.l., Italy[2]) from the following 16 muscles: extensor digitorum (ED), flexor digitorum superficialis (FD), lateral head of the triceps muscle (TRI), long head of the biceps brachii muscle (BIC), pectoralis major (PEC), lateral deltoid (Lat_DELT), anterior deltoid (Ant_DELT) and upper trapezius (TRAP) of both sides (L: left, R: right for healthy subjects, AH: affected hand, UH: unaffected hand for stroke participants). EEG and EMG signals were amplified by means of BrainAmp (Brain Products GmbH, Germany) and Wave plus 16 channels (Cometa S.r.l., Italy) amplifiers, respectively. A TriggerBox (Brain Products GmbH, Germany) was adopted to synchronize the EEG and EMG acquisition.

The experimental setting is illustrated in Figure 2.1. All participants were seated in a comfortable chair or wheelchair if needed, with their forearms resting on a pillow placed over a table (Figure 2.1a). Participants were presented with visual cues displayed on a screen (1m distance). The experimental session consisted of 4 runs (intermingled with breaks adapted to the patients' necessities) during which the participant was asked to perform finger extension (Ext) and grasping (Grasp) with the right and the left hand separately (UH, AH for stroke participants). Each run comprised 40 trials (20 "task" trials of 8s each and 20 "rest" trials of 4s each in random order). The inter-trial-interval lasted 3s during which participants were required to fixate a cross in the middle of the screen. "Task" trials started with 4s of preparation ("get ready" instruction) afterward a go stimulus appeared ("task" instruction) and the participant had to perform the task for 4s (Figure 2.1b). In "rest" trials participants had to relax for 4s ("relax" instruction – Figure 2.1c). The Maximum Voluntary Contraction (MVC) was recorded for each muscle at the beginning of the experiment for 5s and the MVC values of the target muscles (ED and FD of both sides) were computed right after. Participants were instructed to perform the movement as fast as they could and hold it at approximately 15% of the MVC of the target muscle until the end of the trial. Before starting the experiment, participants were asked to perform some repetitions guided by the experimenter, to understand how to perform the task at the desired activation level of 15% with respect to MVC of the target muscle. Subjects' EMG level of activation of the target muscle normalized by its MVC was monitored by the experimenter via the EMG acquisition software (EMG and Motion Tools, Cometa S.r.l., Italy) during the entire experiment and indications on the muscular performance were given to the participants at each trial, when different from those requested. Stroke

[1] https://www.brainproducts.com
[2] https://www.cometasystems.com

participants attempted the movement with their paretic hand to the best of their own residual ability.

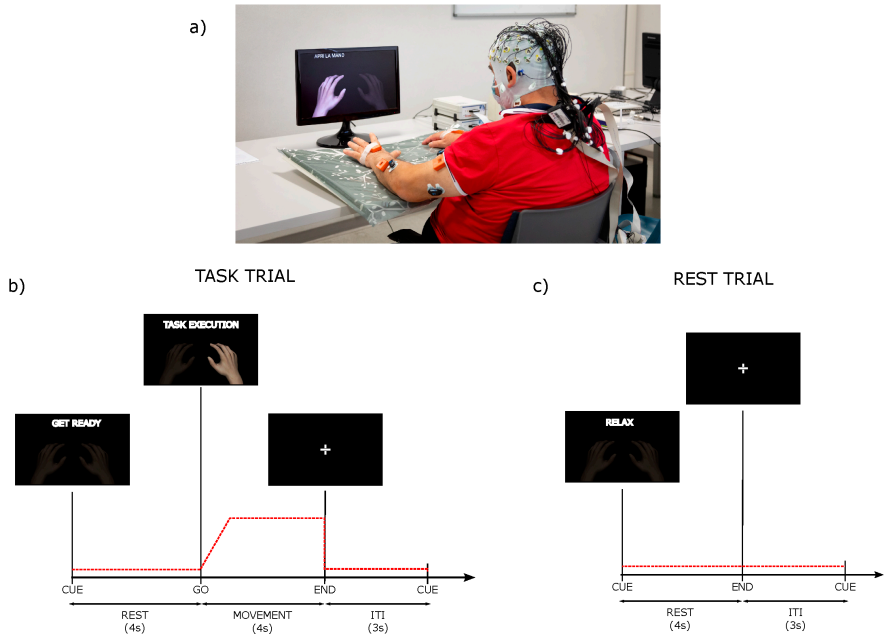

Figure 2.1. Experimental setting. a) participant setting; b and c) experiment timeline for Task (movement) and rest trials. The red dotted line represents the activation profile required to correctly complete the task as for the target muscle (ED for Ext and FD for Grasp) and Rest. In addition to EEG and EMG data, the recording included also kinematic data. They were collected at 100 Hz by means of 8 IMUs (MTw Awinda, Xsens Technologies, The Netherlands). The IMUs were placed by a double-sided medical tape on the following anatomical points: hand, mid forearm, mid arm of both upper limbs, over the clavicular notch and at the lumbar vertebrae level. Such data were not included in this study.

2.2.3 Data Analysis

EEG-EMG Data Pre-processing

EEG data were band-pass filtered [3-60]Hz and Independent Component Analysis was used to remove ocular artifacts (Vision Analyzer 1.05 software, Brain Products GmbH, Gilching, Germany). EMG signals were downsampled to 1000Hz, band-pass filtered [3-500]Hz and the electrocardiographic (ECG) component was rejected through template matching approach [71]. A notch filter at 50Hz was applied to remove power-line artifacts on both EEG and EMG signals. Task trials were segmented in 8s epochs while Rest trials were segmented in

4s epochs, both from the cue onset. To obtain EEG and EMG artifact-free trials, a semi-automatic procedure was applied. Specifically, for the EEG trials a voltage threshold ($\pm 100\mu$V) was defined and all trials in which 5 channels exceeded the threshold were rejected, otherwise a spherical interpolation was performed to replace noisy channels and the trial was saved. As for the EMG trials, a statistical criterion based on the comparison between the EMG characteristics of each trial and the median EMG characteristics of all trials (reference characteristic) [72] was applied then the selected trials were visually inspected and validated.

As for the EXP group, the EEG time series recorded over different scalp positions from patients with right-sided lesions were flipped along the midsagittal plane so that the ipsilesional side was common to all patients. Similar procedure was also applied to EMG data in all the patients with left affected hand (right hemisphere lesion). Both flipping procedures thus ensured to label the left hemisphere and contralateral right hand as "affected" in all the stroke participants, independently from their actual lesion side.

Corticomuscular coupling (CMC) pattern computation

The EEG signals were re-referenced according to the common average reference (CAR) to correctly localize CMC peaks over sensorimotor areas in agreement with physiology of movement, as it has been demonstrated in [38]. The EEG edge electrodes (Fpz, Fp2, AF8, F8, FT8, T8, TP8, P8, PO8, O2, Oz, O1, PO7, P7, TP7, T7, FT7, F7, AF7, Fp1) were excluded from the analysis due to the possible presence of artifacts related to facial movements, thus only 41 EEG electrodes were included in the analysis. EMG signals were rectified before entering the CMC computation.

The CMC was computed in a 2s-window which were selected differently for Task and Rest condition. As for "task" trials, the interval of [5-7]s from cue onset was selected whereas the first artifact-free interval of 2s length in "rest" trials was selected.
CMC values were estimated in the range [1-60]Hz for each participant, movement (ExtR/AH, ExtL/UH, GraspR/AH, or GraspL/UH) and interval of interest (Task, Rest) as in Study 1 paragraph 1.2.3. Two different procedures were followed for the CMC estimation: across-trials and single-trials for Group Analysis and Single Subject Analysis, respectively. As for the across-trials approach (periodogram window length of 1s with 0% overlap), a single CMC pattern was estimated from all trials in the dataset of a single participant, in order to have an average of CMC pattern for each single participant to enter in the grand average (see paragraph 2.2.4 – GA patterns). As for the single-trial approach (periodogram window length of 0.250s with 50% overlap), a CMC spectrum was estimated for each trial in the dataset, to obtain different observations of CMC patterns for each single participant. The CMC values were then extracted for the 3 considered frequency bands defined as alpha

[8-12]Hz, beta [13-30]Hz and gamma [31-60]Hz. For each of these bands, the characteristic frequency was identified as the frequency in which CMC showed the highest value for each pair of signals. The characteristic frequency was specific for each pair of signals, it was computed in the Task condition and used also for the Rest in order to compare patterns at the same frequency (see Study 1 paragraph 1.2.3 for further details).

Analysis of CMC patterns properties by graph theory indices

CMC networks estimated at single-subject level were assessed against chance level and thus transformed into weighted CMC adjacency matrices. The single-subject CMC adjacency matrices were built as follows: for each EEG-EMG pair an unpaired t-test was applied between task and rest conditions on CMC values estimated by means of the single-trial procedure. The significance level was set to 0.05. False Discovery Rate (FDR) was used to control family-wise error rate [43]. Such statistical comparison was used to assess CMC values obtained during movement execution/attempt against chance level using as null-case statistical threshold the corresponding CMC values in rest condition. The application of this test allowed to obtain for each subject and each movement a CMC adjacency matrix where null-values correspond to EEG-EMG connections not significantly different from rest while non-null values correspond to connections where CMC values were significantly higher during movement than rest condition. The comparison between task and rest conditions allowed also to reduce the presence of spurious connections in CMC networks due to volume conduction which is an intrinsic phenomenon of the EEG signals.

The Graph Theory was applied to the obtained CMC adjaceny matrices to extract a set of ad-hoc indices which synthetically described the main properties of the CMC patterns. This procedure aimed at reducing the CMC matrix complexity and thus allowing its interpretation. Such computation was repeated for each subject, movement, and band.
Global network properties:

- *CMC Weight* is defined as the average of CMC values of the existing connections in the network. It is a measure of the strength of the EEG-EMG connections which is well-known to be reduced in stroke patients [5].
- *Network Density (ND)* computed as the total number of existing connections in the pattern normalized for the possible number of connections.

Network density was also calculated for each of the identified 4 sub-networks as follows (local networks properties):

- *Density (of) Contralateral Hemisphere (DCH)* calculated as the total number of existing connections that link the target muscle (FD in Grasp and ED in Ext) with EEG electrodes in contralateral hemisphere (normalized for the possible number of connections in this sub-network).

- *Density (of) Ipsilateral Hemisphere (DIH)* calculated as the total number of existing connections that link the target muscle (FD in Grasp and ED in Ext) with EEG electrodes in ipsilateral hemisphere (normalized for the possible number of connections in this sub-network).

- *Density (of) Involved Side (DIS)* calculated as the total number of existing connections entailing muscles in the side involved in a given motor task – target muscles (normalized for the possible number of connections in this sub-network).

- *Density (of) Uninvolved Side (DUS)* calculated as the total number of existing connections entailing muscles in the side which is not involved in a given motor task – non-target muscles (normalized for the possible number of connections in this sub-network).

To further investigate the selective engagement of muscles, the following indices were computed:

- *Muscle Degree (MD)* defined as the total number of connections that each muscle establishes with EEG channels normalized for the maximum number of possible connections involving it. This index allowed us to measure the involvement of each muscle in the pattern and to identify the muscles with a dominant role (higher degree) with respect to others. It was calculated for each of the recorded 16 muscles both during Ext and Grasp, and then a qualitative comparison was performed between the muscle degree values relative to the movement involved and uninvolved side.

- *Distal/Proximal Degree Ratio (DPDR)* was computed considering the degree of the muscles of the movement involved side, that were labeled as distal (FD and ED) and proximal (BIC, TRI, Ant_DELT, Lat_DELT, PEC, TRAP). It was defined as the ratio between the degree of distal muscles and the sum of degrees in distal and proximal muscles. DPDR value was set as equal to: 1 if the activation regarded only distal muscles; 0 for the activation of only proximal muscles; 0.5 in the case of both proximal and distal muscle activation with the same weight.

2.2.4 Statistical Analysis

Grand Average (GA) CMC patterns

Each movement was described by a coherence pattern as a result of a GA analysis computed for the CMC values across participants (see Figure 2.2 and 2.3). A paired sample t-test with the interval (Task vs Rest) as independent variable and the CMC values computed in the across-trials procedure as dependent variable was applied to each movement type, frequency band and channel pair. The significance level was set to 0.05. FDR was used to control family-wise error rate.

Between-groups differences in CMC pattern properties
A Kruskal-Wallis test was applied on each graph theory derived index considering as factor the three groups: CTRL - control group executing the task with the right hand; EXP_UH - stroke group executing the task with the unaffected hand; EXP_AH - stroke group executing the task with the affected hand. A Tukey's post hoc test was applied to assess between groups differences. The right hand for CTRL group was selected since no significant differences were observed in the graph indices between left and right hand.

Correlation between network indices and functional/clinical scales
Network indices that significantly described the CMC patterns of stroke patients performing movements with the affected arm were correlated with the scores obtained from the following clinical scales: FMA total, FMA sub-scales and MMT. The Spearman's correlation test was applied with the indices values as the dependent variable and the clinical scales' scores as the independent variable.

2.3 Results

2.3.1 Participants

No significant between group (EXP and CTRL groups) differences were found in age (t-test p=0.22) and number of subjects per gender (Chi-square test p=0.08). All subjects in the CTRL group were right-handed according to the EHI. Ten patients in the EXP group were also right-handed while 2 were ambidextrous. Stroke severity was mild according to NIHSS which was lower or equal to 4 in all EXP participants [73]). Upper limb deficit as classified with FMA was mild to moderate, ranging from 23/66 to 63/66 [74]. See Table 2.1 for further details about participants.

2.3.2 CMC Grand Average (GA) patterns

Figure 2.2 illustrates the GA CMC patterns obtained for the Ext (left panel) and Grasp (right panel) executed with left (panel a, c) and right (panel b, d) hand in CTRL group. As expected, these results confirmed what obtained in Study 1 [18]. In Ext condition (Figure 2.2, Ext, panel a-b), the highest CMC values were found for connections involving mainly the target muscle (ED) and most of the bilateral sensorimotor EEG electrodes, in alpha and beta bands. In gamma band, CMC patterns were more diffuse involving almost all the muscle of the relative side and showed lower values of coherence with respect to those in the alpha and beta band. The Grasp condition (Figure 2.2, Grasp, panel c-d) showed CMC values lower than those obtained in Ext. The target muscle FD was connected with almost all the electrodes over the bilateral sensorimotor areas in alpha band, whereas ED and proximal muscles were more involved in higher frequency bands (beta, gamma).

Table 2.1. Demographic and clinical characteristics of the patients expressed in means (± standard deviation). C=Chronic; FMA=Fugl-Meyer Assessment scale, upper limb section, ranging from 0 (most affected) to 66 (least affected); H=Hemorrhagic; I=Ischemic; L=left; LH=left-handed; MH=mixed-handed; MAS=Modified Ashworth Scale; NIHSS=National Institute of Health Stroke Scale; R=right; RH=right-handed S=Subacute.

GROUP	EXP (N=12)	CTRL (N=12)
AGE (YR)	52.2 (±18.5)	43.6 (±15.3)
HANDEDNESS	10RH + 2MH	12RH
TIME FROM EVENT (MO)	5.5 (±3.3)	–
TYPE (S/C)	6S + 6C	–
ETIOLOGY (I/H)	6I + 6H	–
SIDE OF LESION (R/L)	7L + 5R	–
FMA	49.4 (±13.7)	–
NIHSS	2.42 (±1.3)	–
MAS	0.9 (±1.4)	–
MMT	20.3 (±4.8)	

Different CMC patterns were observed in the stroke group (EXP) as illustrated in Figure 2.3. First, the GA CMC patterns obtained in all experimental conditions showed a lower number of connections and lower CMC values with respect to the CTRL group (Figure 2.3, both Ext and Grasp), being the CMC lowest values observed in the AH condition (attempted movements; Figure 2.3 b-d). The UH condition (Figure 2.3 a-c) revealed CMC patterns that mainly linked the bilateral sensorimotor areas with ED in Ext and FD in Grasp, respectively. Similar to what observed for the CTRL group, both tasks were characterized by a reduction of CMC values and a less specificity of the muscles involved in the task as the frequency increased. The GA CMC patterns were poor of significant connections when Ext and Grasp were executed with the affected hand (Figure 2.3 b-d). Very few connections were found between ED and bilateral sensorimotor areas during Ext. The CMC patterns were denser in Grasp condition with respect to Ext but they show less muscle selectivity, involving muscles other than the target ones even in alpha band.

2.3.3 Analysis of CMC patterns by graph theory indices

Table 2.2 reports the results of the between-group (CTRL, EXP-UH, EXP-AH) analysis on graph theory derived indices which characterized the CMC patterns in the different frequency bands and movements. The trends relative to these statistical differences are reported in Figure 2.4 for beta band during Ext movement. A similar behavior was observed in the other two frequency bands (data not shown).

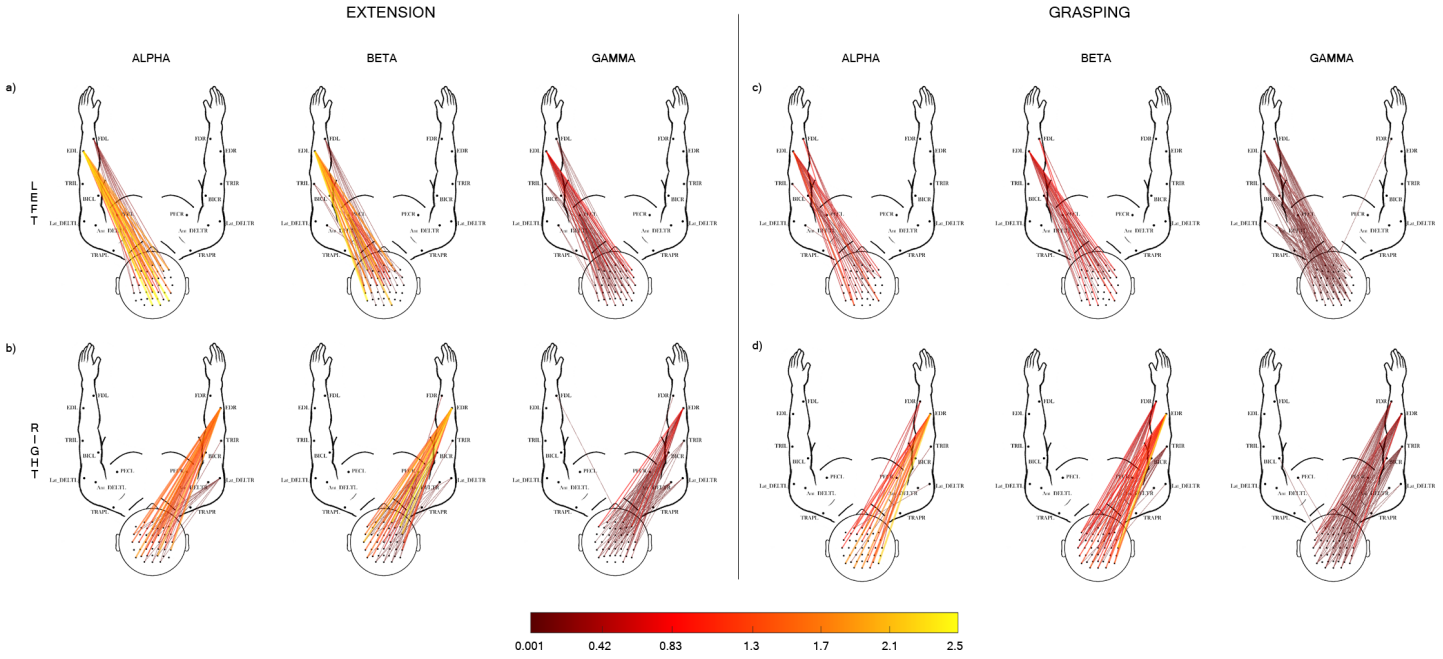

Figure 2.2. Grand average corticomuscular coupling patterns in CTRL group estimated for each of the 3 frequency bands, alpha (8–12)Hz, beta (13–30)Hz, gamma (31–60)Hz. Ext: CMC patterns obtained for the extension movement executed with left (panel a) and right (panel b) hand. Grasp: CMC patterns obtained for the grasping movement, executed with left (panel c) and right (panel d) hand. The 2D body model is seen from the above: scalp with nose pointing up the top and arms in front of the participant. Only statistically significant CMC values are represented (paired t-test between task and rest trials, $\alpha = 0.05$ FDR correction). The color bar codes for the CMC average value (across participants, N=12) in the task trial.

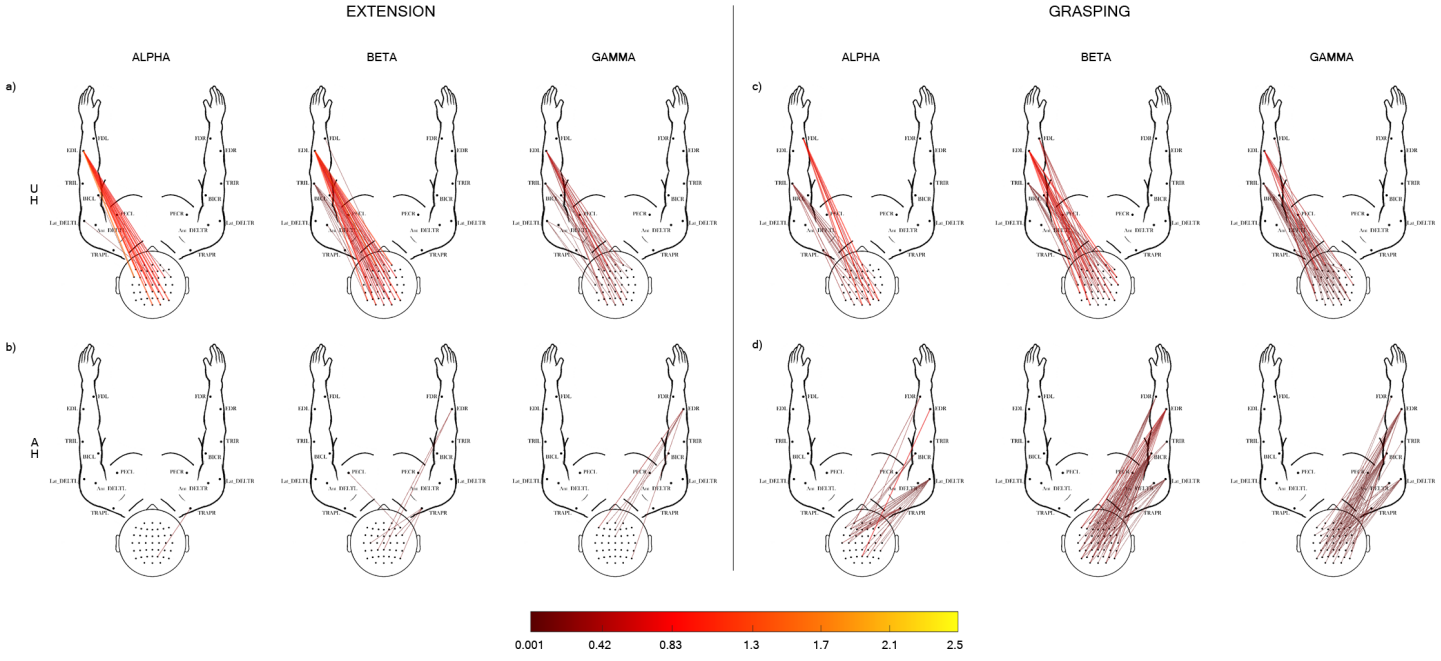

Figure 2.3. Grand average corticomuscular coupling patterns in EXP (stroke) group estimated for each of the 3 frequency bands, alpha (8–12)Hz, beta (13–30)Hz, gamma (31–60)Hz. Ext: CMC patterns obtained for the extension movement executed with UH and (panel a) and AH (panel b). Grasp: CMC patterns obtained for the grasping movement executed with UH (panel c) and AH (panel d). The 2D body model is seen from the above: scalp with nose pointing up the top and arms in front of the participant. Only statistically significant CMC values are represented (paired t-test between task and rest intervals, $\alpha = 0.05$ FDR correction). The color bar codes for the CMC average value (across participants, N = 12) in the task trial.

Table 2.2. Results of the Kruskal-Wallis test (p-values) obtained considering as dependent variables the different graph theory indices separately and as between factor the group (CTRL, EXP-UH, EXP-AH). Tests were repeated for each frequency band (alpha, beta, gamma) and each movement (Ext, Grasp). ND – network density; DIS – density involved side; DUS – density uninvolved side; DCH – density contralateral hemisphere; DIH – density ipsilateral hemisphere; DPDR - distal/proximal degree ratio.

	EXTENSION			GRASPING		
	ALPHA	**BETA**	**GAMMA**	**ALPHA**	**BETA**	**GAMMA**
CMC weight	0.113	**0.009***	**0.014***	0.068	**0.003***	**0.006***
ND	**0.033***	**0.005***	**0.001***	0.84	0.719	0.831
DCH	0.55	0.31	0.73	0.62	0.89	0.46
DIH	0.28	0.87	0.7	0.45	0.32	0.77
DIS	0.344	0.133	**0.029***	0.934	0.776	0.384
DUS	**0.012***	**0.0001***	**0.011***	0.125	0.337	0.299
DPDR	**0.071***	**0.004***	**0.014***	0.503	0.551	0.982

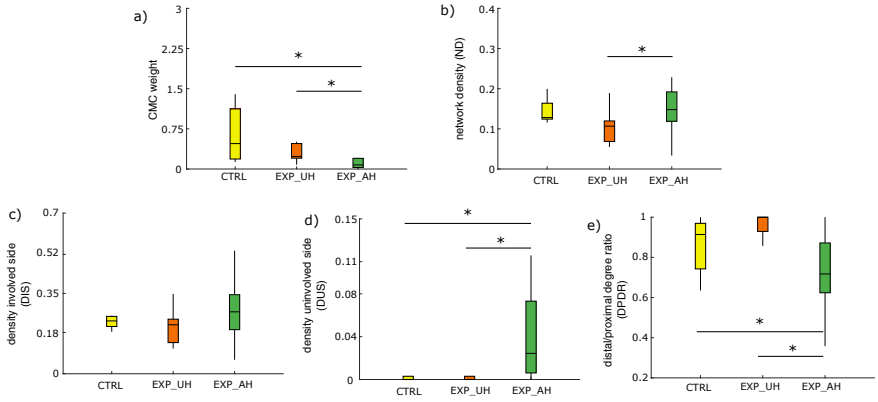

Figure 2.4. Boxplot diagrams reporting the distribution of graph theory derived indices characterizing CMC patterns in beta band during extension movement for the three different groups (CTRL, EXP-UH, EXP-AH). Each panel refers to a specific index: a) CMC weigth, b) network density, c) density (of) involved side d) density (of) uninvolved side, e) degree ratio of distal/proximal muscle. The symbol * indicates a statistical difference as revealed by the post-hoc test.

The CMC weight index estimated in beta and gamma bands was significantly different between the EXP and CTRL group in both Ext and Grasp conditions, showing lower weight when the EXP group performed Ext with AH with respect to UH and to the CTRL group (Figure 2.4 a).
A significant effect of the group factor was found for ND only for the Ext movement in all the frequency bands: higher connection density was observed for AH with respect to the UH in the EXP group (Figure 2.4 b). As for the sub-network density analysis, no between-group differences were found for densities

in both ipsi- and contra-lateral hemispheres. On the other hand, significantly higher density of connections with muscles of the uninvolved side (DUS) were observed in all frequency bands (Table 2.2) when the movement was performed by the EXP group with AH (Figure 2.4 d) with respect to UH and to the CTRL group. A similar trend was observed for density in the involved side (Figure 2.4 c), reaching statistical significance only in gamma band (Table 2.2).

Significant between-group differences were observed for DPDR index for Ext movement in all frequency bands (Table 2.2). The EXP group showed a significantly lower DPDR when the movement was performed with AH with respect to UH and to the CTRL group (Fig. 2.4e). The DPDR is almost 1 in CTRL and in EXP-UH, reflecting the exclusive engagement of distal muscles in movement execution. Such ratio decreased to a median of 0.7 in the EXP group when the movement was attempted with AH, revealing a contribution of proximal muscles.

Figure 2.5 illustrates the degree distribution for each of the 8 considered muscle in both arms for the 3 frequency bands during extension movement performed by CTRL and EXP group (similar results were observed for grasping). As for the CTRL group (Figure 2.5 a), maximum degree was observed for ED and FD in the involved side in all the frequency bands. The median was around 90% with a very short inter-quartile range, indicating a high reproducibility of this result across healthy participants. Degree close to zero was obtained for all the other muscles both in involved and uninvolved side in alpha and beta bands. Small degree (around 10%) was found only in gamma band for all the muscles in the involved side other than FD and ED reflecting the more diffuse CMC patterns at high frequencies.
As for the EXP group, a different behavior was found when the Ext was executed with unaffected (Figure 2.5 b) and affected (Figure 2.5 c) hand. Under the UH condition, the maximum degree was found for ED muscle (median around 95%) in almost all the patients (short inter-quartile range). Degree distribution for FD muscle showed a median around 60% with a high inter-quartile range, reflecting the variability among patients in the engagement of the FD during Ext task. The degree distribution of all the other muscles was similar to that described in CTRL group: zero degree of the uninvolved side in all the frequency bands; zero degree of all the muscles in the involved side other than ED and FD in alpha and beta bands; small degree (around 10%) for all the non-target muscles in the involved side in gamma band.
The observation of muscle degree distribution during movement attempt with AH showed a degree different from zero for most of the non-target muscles (both proximal and distal) in the involved side with a high variance across the patients in all the frequency bands. Furthermore, a non-null degree was observed in muscles in the side not involved in the task (the unaffected side), especially of ED and FD in alpha and beta bands and of all other muscles in gamma band.

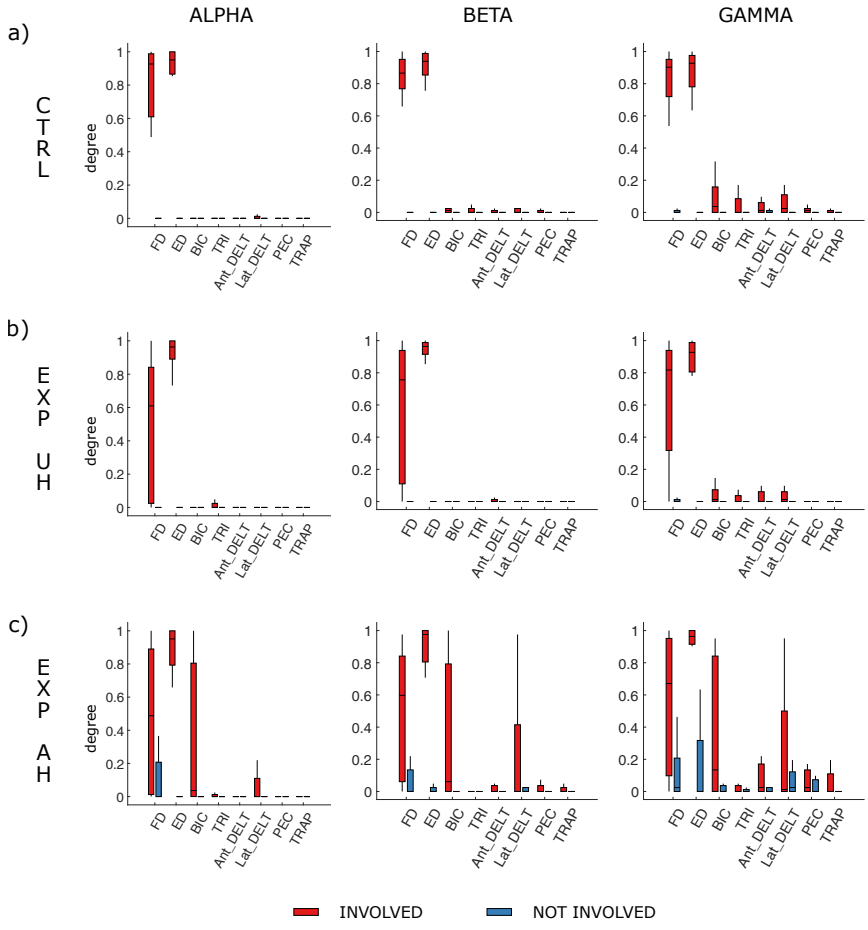

Figure 2.5. Degree distribution for each muscle in both involved and uninvolved sides for the 3 frequency bands during extension movement. Panels refer to the CTRL group executing movement with right side (panel a) and the EXP group when the movement was executed with unaffected (UH, panel b) and affected (AH, panel c) side.

2.3.4 Correlation of CMC patterns properties with clinical scales

The Table 2.3 reports the results of the correlation analysis conducted between graph theory derived indices which significantly characterized the CMC patterns in Ext and Grasp movements, and the clinical scale scores describing upper limb motor function and strength (FMA total and subsections and MMT). Positive correlation was found between CMC weight and FMA-"Hand" subsection scores for Ext and between CMC weight and MMT for Grasp, in all the frequency bands. The DPDR index positively correlated with MMT for Grasp only in beta band. Negative correlation was observed between DIS index and FMA-"Hand" scores in alpha and beta bands for Ext and in gamma band for Grasp.

Table 2.3. Results of the correlation between the scores obtained for the two clinical scales, FMA-Hand subsection and MMT, and each of the graph theory derived indices which significantly characterized the CMC patterns in stroke patients during AH condition. The analysis was repeated for each frequency band (alpha, beta and gamma) and each movement (Ext, Grasp). ND – network density; DIS – density involved side; DUS – density uninvolved side; DPDR - distal/proximal degree ratio.

	FMA HAND					
	EXTENSION			**GRASPING**		
	ALPHA	**BETA**	**GAMMA**	**ALPHA**	**BETA**	**GAMMA**
CMC weight	**0.75**	**0.72**	**0.59**	0.36	0.46	0.44
ND	-0.55	-0.55	-0.52	-0.54	-0.53	**-0.58**
DIS	**-0.59**	**-0.59**	-0.41	-0.52	-0.5	**-0.59**
DUS	-0.53	-0.3	-0.44	-0.35	-0.2	-0.17
DPDR	0.48	0.14	0.16	0.55	0.39	0.55
	MMT					
	EXTENSION			**GRASPING**		
	ALPHA	**BETA**	**GAMMA**	**ALPHA**	**BETA**	**GAMMA**
CMC weight	0.57	0.53	0.49	**0.62**	**0.62**	**0.58**
ND	-0.25	-0.25	-0.23	-0.28	-0.27	-0.33
DIS	-0.24	-0.28	-0.12	-0.27	-0.26	-0.31
DUS	-0.3	-0.12	-0.3	-0.06	-0.002	0.08
DPDR	0.2	-0.15	-0.18	0.46	**0.59**	0.48

2.4 Discussion

The main objective of this study was to identify corticomuscular network properties which would describe the upper limb motor impairment in stroke patients, to ultimately guide the design of a novel hybrid BCI for motor recovery. To this aim, CMC networks related to simple hand movements attempted with the affected hand and executed with the unaffected hand in stroke patients were analyzed and compared with those obtained from a sample of age-matched healthy participants performing the same movements with right and left hand.

As for healthy participants, results retrace those obtained in the Study 1 [18]. This analysis confirmed that CMC patterns observed during simple hand movements (Figure 2.2) are widely distributed over the sensorimotor scalp areas, muscle involvement is more selective to the target muscle during extension than grasping, and less specific in higher bands for both movements. Furthermore, CMC values are lower for the grasping movement with respect to extension.

Grand average patterns obtained from stroke patients (Figure 2.3) show much less connections with lower CMC values, both in the UH and AH conditions, probably due to a higher inter-subject variability as well as to the expected reduction in CMC weight. Indeed CMC weight had significantly lower values in patients for both movements, under UH and AH conditions in beta and gamma bands (Table 2.2), already identified as most significant to highlight brain-muscle communication disorders [30].

As evident in Figure 2.3, grand average patterns in patients during AH are almost devoid of connection, especially for extension movement. As mentioned, this shortage of connections in the grand average pattern can be imputed to a high inter-subject variability among patients, that was possibly higher in the extension task with respect to grasping. Indeed, it might be argued that the extension task resulted more challenging to our patients and thus lead to individually distinct compensation strategies. The pattern for grasping with AH is slightly richer, possibly due to the fact that grasping holds a high behavioral and functional complexity and that the patients involved in the study were all undergoing a standard rehabilitative program likely including upper limb functional exercises when the experiments were performed. Nevertheless, with respect to grasping patterns from healthy subjects, patients showed lower muscle specificity in all bands. This result is largely expected from a revision of CMC literature in stroke patients, showing involvement of proximal muscles to compensate for distal impairment [13] or higher contribution of antagonist muscles with respect to healthy subjects [4], [14]. More generally, alterations of muscular involvement in post-stroke patients have largely been described through the phenomena of motor-overflow, co-activation of agonists and antagonists, spasticity and appearance of mirror movements [30].

To characterize these alterations through CMC pattern evaluation in a quantifiable and objective manner, indices derived from graph theory were defined and applied to single-subject networks. Overall network density was higher in the patient group for the AH condition (Ext movement only), suggesting that a higher number of connections in the network is required to accomplish the task. In classical graph theory, indeed, an increase in overall network density is described as a deterioration of such an optimal criterion according to which physiological networks are organized (well-known as small-world networks) [75]. This increase in overall density could be ascribed to compensatory strategies which were more relevant in the extension task. To further interpret this result and thus, to characterize deviations from the physiological condition, the index

was split considering four sub-networks relative to the hemispheres contra- or ipsi- lateral to the hand task, and to the muscles on the side involved and uninvolved (contralateral) in the task.

As for the distribution of connections on the scalp, no statistical differences were observed in indices describing scalp lateralization of CMC patterns. Such bilateral distribution of connections was already observed in healthy subjects and discussed in Study 1. The current findings on patients demonstrate that the presence of a unilateral stroke lesion does not affect this pattern distribution that remains balanced between the ipsilateral and contralateral hemisphere during movement with the healthy or paretic hand. This is not entirely expected according to the widely described interhemispheric unbalance of electrical activity after stroke [76]. However, patients involved in this study were all in subacute to chronic phase, with low level of impairment and undergoing a standard rehabilitative treatment when the experiments were performed. A lack of interhemispheric unbalance has already been associated with good recovery [77], thus it could be that more severe patients recorded closely to the stroke event might still show the differences in CMC pattern distribution between the affected and unaffected hemisphere that were not seen in the analyzed sample.

As for sub-networks related to muscles of the involved and uninvolved task side, while density values were higher in both the involved and uninvolved side (Figure 2.4 panels c and d), the uninvolved side density only was significantly higher in patients for AH condition, demonstrating an abnormal recruitment of healthy side muscles during the extension task with the paretic side. Visible mirror movements were not present in our sample during AH tasks (except for two patients), however the occurrence of non-paretic upper limb movements during paretic motor attempts in stroke is largely described [10], [27]. Thus, it can be speculated that this analysis on CMC network properties might reveal subclinical alterations.
Muscle degree, i.e. the number of connections involving each recorded muscle was employed in order to quantify muscle specificity for each task. As expected, the target muscle of the involved side holds the highest degree in both groups and conditions (in Figure 2.5, red ED bars). However, in the CTRL group and only in UH condition for EXP group all other muscles have very low degrees (except for low values appearing mainly in gamma band), whereas in the AH conditions several muscles are represented from the involved and contralateral side. Among those, the highest values are observed in the ipsilateral BIC muscle. The bicep is crucial for post stroke upper limb flexion spasticity [78] as testified by clinical studies [79], [80]. Despite the low or absent clinical spasticity in our patients (as assessed by MAS), it can be argued that this finding may represent a subclinical substrate for elbow flexion spasticity; future studies involving stroke patients showing higher level of spasticity are needed to definitely corroborate this argumentation.

As for the distal/proximal degree ratio, results show that during AH in

the EXP group, proximal muscles were involved confirming a compensatory proximal activity during hand motor tasks in paretic patients [4].

Altogether these findings confirm that CMC is a promising metric to analyze post-stroke changes in upper limb motor activity as it allows to quantify commonly reported alterations (co-activation of proximal and contralateral muscles as possible substrates for spasticity and for mirror movements). To further evaluate the solidity of such a method to describe post-stroke upper limb motor impairment, the correlation of CMC indices with clinical/functional scales of the upper limb was tested. Significant results were found for the FMA "Hand" subscale (mainly for the extension movement) and for MMT (grasping only). In particular, CMC weight was lower in more impaired patients. Similarly, the distal/proximal muscle degree ratio was lower in more impaired patients, proving the higher need of proximal compensation. Conversely, density and involved side muscle density were negatively correlated, showing a network organization that was more similar to healthy subjects in less impaired patients (lower density as a possible indicator of a higher network efficiency). With the caution required by the relatively small sample in this study, these results could be interpreted taking into account the differences between the two clinical scales. Indeed, FMA is a fairly complex scale which entails several aspects such as reflex activity, different functional movements and synergies, coordination, and speed; on the other hand, MMT is merely a measure of residual strength in different upper limb segments. It might be speculated that grasping being less challenging for stroke patients as compared to extension could be responsive to a grosser evaluation such as MMT, while correlations with FMA are observed for extension task as the scale reflects motor functional improvement in a more complex fashion.

To my knowledge, the present work is among the first to analyze CMC in stroke patients in terms of a widely distributed network (i.e., considering several EEG scalp positions and muscles) [4], [12]–[14], and the first to apply a graph theoretical approach to such networks. In a recent study [81], Xi et al. applied graph theory to CMC networks in healthy subjects. The present work moves a step forward by defining specific indices apt to describe post-stroke movement alterations in a quantifiable and objective manner.

The results obtained in this study grounded the design and the implementation of the novel hybrid BCI system described in Section II-Study 5 which reinforces only those CMC network features that most resemble normal activation with the aim of subsiding favorable motor outcome. The findings of the present work indeed confirmed that the reinforcement of CMC throughout a BCI paradigm is desirable, as a reduction of its weight is correlated with upper limb motor impairment. Moreover, the identified CMC features that describe derangements from physiological motor system activation will be discouraged along the BCI training protocol to counteract maladaptive changes (see Study 5). A major limitation of the present study is that the small number

of patients included resulted in a consequent low variability in the degree of impairment. Indeed, most enrolled patients were mildly impaired and with little or no spasticity. This was mainly due to the complex experimental setup and relatively long experiment that could result too tiring (if at all doable) for more severe patients. Future steps will require an optimization of the setup and experimental protocol (even according to the results presented here) to be able to include more patients with different levels of impairment.

This study showed that analysis of high-density CMC networks by means of graph theory indices can describe motor abnormalities in stroke patients during simple hand movements, which are the most commonly employed motor tasks in rehabilitative BCI paradigms. Such results have driven the implementation of a novel hybrid BCI system (the h-BCI prototype-Study 5) able to reinforce those CMC network features that most resemble normal activation and thus, subside favorable motor outcome. Indeed, correlations of graph theory indices with upper limb motor impairment support their use in wider clinical and rehabilitative applications. As an example, correlations between CMC network properties and clinical scales are promising for the application of such measurements as rehabilitation outcome metrics, in line with the constant need for evidence-based and personalized rehabilitation approaches [82], [83].

The analysis presented here was published in the Journal of NeuroEngineering and Rehabilitation [19].

3. Study 3

Cortico-muscular coupling to discriminate different types of hand movements

3.1 Background and Objectives

CMC was assessed to be a valuable feature to discriminate movement from rest condition and different movement types (see Study 1) [18]. Thus, a CMC-based paradigm might be useful not only for motor rehabilitation but also for BCI applications aimed to replace or restore lost motor functions [84].
Indeed, an emerging issue in the field of assistive BCIs for spinal cord injuries is to achieve the so-called natural control of external devices that assist movements (e.g., functional electrical stimulation or robots) [64]. In this context the ability to non-invasively decode different type of movements by exploiting all remaining functionalities is crucial [24], [25].
EEG-based BCIs for neuroprostheses control rely typically on changes of oscillations originating from sensorimotor areas [53], [85], [86]. The analysis proposed in this study has the main aim to evaluate the ability of hybrid features, such as CMC, with respect to existing methods based on only brain features, such as sensorimotor rhythms (SMR), in discriminating different hand movements in 15 healthy subjects. In particular, I i) identified the best classification algorithm in discriminating between hand grasping and extension and ii) explored how the variation in the dimensionality of the feature domain would influence the different classifier performances for each type of feature (CMC/SMR).

Although many classification approaches have already been investigated for EEG-based features [87], classification algorithms able to discriminate different tasks through CMC features has never been investigated before. To identify the best classification approach, four classification methods were compared: support

vector machine with linear kernel (SVM) and with radial basis or gaussian kernel (SVM-RBF), linear discriminant analysis (LDA) and decision tree (DT) [23]. Since the number of features used for the classification directly impacts on the number of physical electrodes required to collect data, the performances of the different classification approaches were evaluated on varying of the feature space size (two, four or ten features). The performances obtained using the best combination of classifier-number of features were compared between the two feature types (hybrid and only EEG-based).

3.2 Materials and Methods

3.2.1 Participants and experimental protocol

The fifteen right-handed healthy participants (10 females/5 males, age 48.7±17.9 yo) enrolled in the experimental protocol described in Study 2 were analyzed in this study.
The experimental paradigm used to collect the data is reported in details in Study 2 paragraph 2.2.2 and summarized here. EEG and EMG data were acquired simultaneously and sampled respectively at 1000Hz and 2000Hz. EEG signals were recorded from the scalp with 61 active electrodes arranged according to an extension of 10-20 system (reference on left mastoid and ground on right mastoid) by means of BrainAmp amplifiers (Brain Products GmbH, Germany); surface EMG data were recorded through Pico EMG sensors (Cometa S.r.l., Italy) from 16 muscles of the arm and the forearm collected in bipolar fashion. The experiment consisted of 4 runs, with a break among them, in which the participants was asked to perform finger extension (Ext) and grasping (Grasp) with the right (R) and the left (L) hand separately. Each run comprised 40 trials, half labelled as "task" and half as "rest" condition. Task and rest trials lasted respectively 8s and 4s. The inter-trial-interval, consisting in a fixation cross in the middle of the screen, was set to 3s. Task trials started with 4s of preparatory period, after which a go stimulus occurred and the participant had to perform the task for 4s (see Figure 2.1).

3.2.2 EEG and EMG data pre-processing

EEG signals were band-pass filtered [3-60]Hz and Independent Component Analysis was used to remove ocular artifacts. EMG signals were downsampled to 1000Hz, band-pass filtered [3-500]Hz and the ECG component was rejected through template matching [71]. A notch filter at 50Hz was applied to remove power-line artifacts on both signals and data were segmented in 8s epochs for task trials and 4s epochs for rest trials from the cue onset.

A subset of EEG channels over the sensorimotor area (FC5, FC3, FC1, FCz, FC2, FC4, FC6, C5, C3, C1, Cz, C2, C4, C6, CP5, CP3, CP1, CPz, CP2,

CP4, CP6, P5, P3, P1, Pz, P2, P4, P6) were selected and analyzed in the next steps. The same procedure used in Study 2 paragraph 2.2.3-EEG-EMG Data Pre-processing was applied to reject trials with EEG and EMG artifacts. After artifact rejection, 19.8 ± 0.11 and 19.7 ± 0.2 artifact-free task trials were obtained respectively for Ext and Grasp movements of the left hand, whereas 19.5 ± 0.3 and 19.1 ± 0.4 for Ext and Grasp movements of the right hand.

3.2.3 Feature Extraction

CMC and SMR features were extracted in the time interval [5-6]s with respect to the cue onset in task trials of both Ext an Grasp conditions.

Cortico-Muscular Coupling

Only the 8 EMG channels over the muscles ipsilateral to the movement (e.g. the 8 muscles of the right upper limb in ExtR and GraspR) were selected for CMC features extraction. EMG signals were rectified [38] and the cortico-muscular coupling between each EEG-EMG pair was computed as in Study 1 paragraph 1.2.3 (Welch periodogram method, 250ms-Hann windows and 50% of overlap). For each movement type, the characteristic frequency of each EEG-EMG pair was extracted in three frequency bands of interest showed to be most informative for CMC features according to the results obtained in Study 1: alpha (8-12)Hz, beta (13-30)Hz and gamma (31-60)Hz. The single-trial CMC values at the characteristic frequencies of each EEG-EMG pair were then used as feature space of dimension 672 (28 EEG channels x 8 EMG channels x 3 frequency bands).

Sensorimotor rhythms

To extract SMR features, Welch periodogram was used to compute the power spectrum of each EEG channel dividing the selected 1s-window in 7 segments (250ms-Hann windows with 50% of overlap), as for CMC features. Two frequency bands of interest, normally associated to brain correlates of voluntary movements, were considered: alpha and beta bands. SMR features were extracted as the mean value in each frequency band of interest of the power spectrum in dB. Thus, SMR feature space was 56 dimensional (28 EEG channels x 2 frequency bands).
To visualize SMR features during finger extension and grasping, SMR values were extracted also in rest condition (time interval [2-3]s of rest trials) and the mean SMR values across trials of the 15 healthy subjects were compared for all the 61 EEG channels in task and rest condition by means of a paired t-test (α = 0.05, False Discovery Rate correction). Scalp maps with the topographical distribution of SMR features were then visualize.

3.2.4 Movement Classification

Only task trials were considered in both Ext an Grasp condition for the movements classification. CMC and SMR features were used separately as features to classify finger extension from grasping in each limb by means of a single-subject 10-iteration cross-validation. In each iteration, the 80% of Ext an Grasp observations were used as training set, whereas the remaining 20% were used as testing set. Feature scaling (z-score standardization) was applied to the dataset to avoid numerical difficulties during the calculation [88]. Four classifiers were compared in terms of classification performances for each type of feature (CMC and SMR): SVM, SVM-RBF, LDA and DT.
Support vector machine algorithm uses a discriminant hyperplane to identify classes. The selected hyperplane is the one that maximizes the distance (margin) from the nearest data points (support vectors) of each class and it can apply different kernel functions to define the hyperplane decision boundary between the classes. Two types of kernel were tested: SVM with linear kernel, most basic type of kernel usually faster than other kernel; and the SVM-RBF that non-linearly maps samples into a higher dimensional space. Thus, unlike the linear kernel, it can handle the case when the relation between class labels and attributes is nonlinear [88].
For the LDA classifier, a regularized LDA classifier was used which include a regularization term for which the two classes have the same covariance matrix. Regularized classifier has been demonstrated to be more effective and more robust for small dataset than LDA [87].
DT is a classifier which partitions the feature space until terminal nodes, each one assigned to a predicted value. DTs are very easy to use for no-statisticians, they work for non-linear functions and the treatment of missing values is more satisfactory than most other model classes. However, the best model might not be able to be found at all and results can be quite variable: small changes in the data can potentially lead to completely different splits (i.e. trees) [89].

All classifiers were tested, even on varying of the input number of features N: two, four and ten features were considered. To select the best N features, a feature selection algorithm based on the stepwise regression [44] with an empty initial model was applied.

The following metrics were computed to evaluate the performance of all classification models: i) the area under the curve (AUC) of the Receiver Operating Characteristic (ROC) curve [46], ii) the accuracy, iii) the specificity and iv) the sensitivity of the classifier.

3.2.5 Statistical Analysis

To investigate the effect on the performances of the classification approach and number of features used in the model, a two-way repeated measures ANOVA (rmANOVA) was performed for each type of feature and side separately, consid-

ering as within main factors the CLASSIFIER (4 levels: SVM, SVM-RBF, LDA, DT) and the NUMBER OF FEATURES (3 levels: 10, 4, 2) and as dependent variable the AUC value. The statistical significance level for all tests was set to $p < 0.05$ and the Duncan post-hoc analysis was performed to assess differences among pairs.

To evaluate the ability of CMC and SMR features to discriminate finger extension from grasping, the best combination of classifier-number of features was identified by the rmANOVA for each type of feature and the performances obtained with the two approaches were compared (paired t-test, $\alpha = 0.05$).

3.2.6 Analysis of Ext vs Grasp feature space

For the best combination of classifier-number of features obtained in the CMC-based classification, the same feature analysis performed in the Study 1 paragraph 1.2.3-Movement classification for CMC and IMC features was applied here to evaluate the most recurrent EEG-EMG pairs selected by the stepwise. Thus, the number of times a specific channel pair was selected across participants and cross-validation iteration was counted irrespectively of the frequency band they corresponded to. Moreover, to characterize the physiological process that allows to discriminate the two movement types, the same procedure was applied to evaluate the most recurrent frequency band selected by the stepwise.

The same approach performed for CMC features was used to evaluate the most recurrent EEG channels and frequency bands selected by the stepwise when using SMR features as inputs of the best classifier type revealed by the statistical analysis for the SMR-based classification.

3.3 Results

3.3.1 Feature extraction

To better understand how each type of feature behaves during Ext and Grasp movements, the grand-average CMC patterns and the grand-average SMR scalp maps were reported.

Cortico-Muscular Coupling

CMC grand-average patterns in healthy participants can be visualize in the Study 2 paragraph 2.3.2-Figure 2.2 for each movement type in the three frequency bands of interest. CMC values during finger extension movements resulted to be higher than in Grasp movement and CMC patterns more muscle-specific. Moreover, increasing the frequency band led to more connections in the patterns with the involvement of also the proximal muscles, in particular during Grasp movements.

Sensorimotor rhythms

Figure 3.1 shows the topographical distribution of significant SMR values in task condition with respect to rest for each movement type and frequency band of interest. Similar desynchronizations (SMR Task < SMR Rest) were obtained for Ext (panel a and b) and Grasp (panel c and d) movements in both sides. A prevalent activation of the contralateral sensorimotor cortex over the hand motor area [48] is obtained for both movement types in particular in beta band (13-30)Hz, whereas alpha band (8-12)Hz is characterized by a more widespread distribution over the scalp.

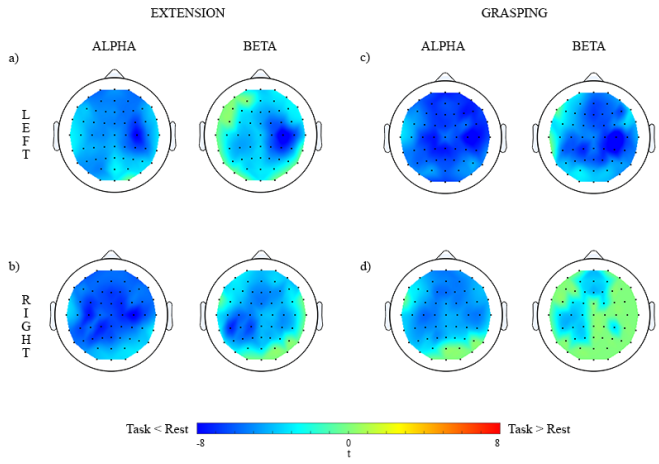

Figure 3.1. Grand average SMR scalp map estimated for each of the 2 frequency bands of interest: alpha (8-12)Hz and beta (13-30)Hz bands. Ext: SMR scalp map obtained for the extension movement executed with left (panel a) and right (panel b) hand. Grasp: SMR scalp map obtained for the grasping movement executed with left (panel c) and right (panel d) hand. Scalp maps were obtained comparing (paired t-test, $\alpha = 0.05$, False Discovery Rate correction) the mean SMR values of the 15 healthy participants in task and rest condition for all the 61 EEG channels. Hot colours codes for t-values when Task>Rest, blue colours code for t-values when Task<Rest.

3.3.2 Movement Classification

Figure 3.2 shows the distribution of AUC values obtained for each combination of classifier-number of features tested when using CMC (Figure 3.2 a and b) and SMR (Figure 3.2 c and d) features to discriminate finger extension from grasping. Overall, CMC-based classification showed higher performances than SMR-based classification for both sides. Indeed, regardless of the classification model the AUC distributions when using CMC features resulted to overcome more considerably the chance level (AUC on average higher than 0.79, chance level = 0.5) than when using SMR features (AUC on average higher than 0.67).

High inter-subject variability resulted in the distributions of the Ext-vs-Grasp performances obtained with the SMR-based classification approach, whereas tight distributions were obtained in the CMC-based classification with lower variability for the classification movements of the dominant side (right side).

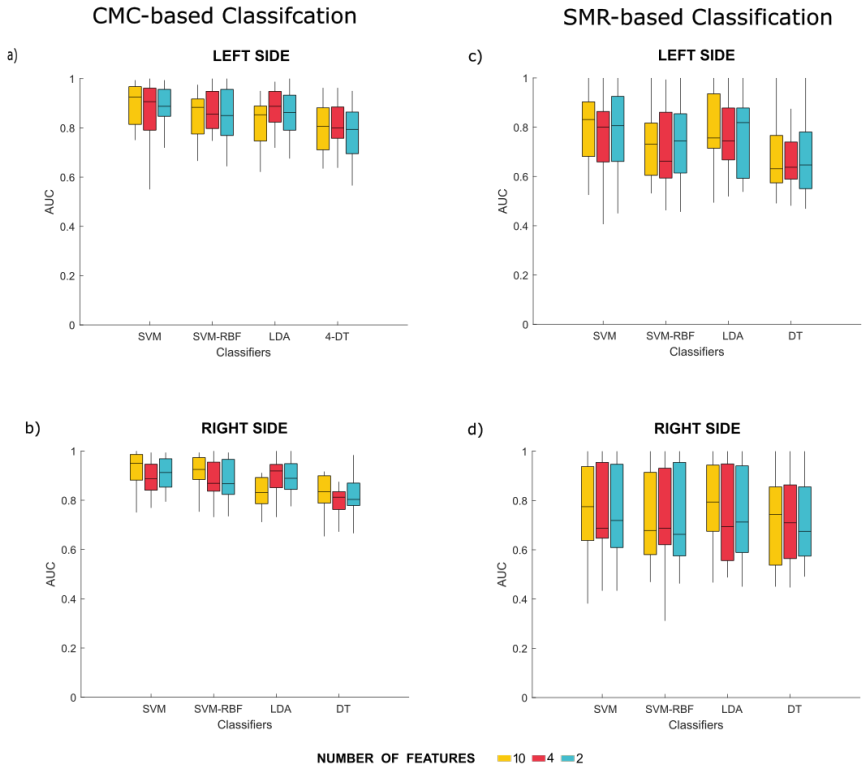

Figure 3.2. Distribution (boxplots) of the Ext-vs-Grasp classification performances expressed as AUC achieved when using CMC (panel a and b) and SMR (panel c and d) features, for each combination of classifier and number of features tested in both left (panel a and c) and right (panel b and d) side.

The two-way rmANOVA performed on the AUC values obtained with the CMC-based classification for the two sides separately revealed a significant effect of CLASSIFIER ($F(3,42)=15.61$, $p<0.01$ for left side and $F(3,42)=29.35$, $p<0.01$ for right side) and CLASSIFIER x NUMBER OF FEATURES ($F(6,84)=5.32$, $p<0.01$ for left side and $F(6,84)=4.25$, $p<0.01$) factors. No significant differences were found for the number of features used. The Duncan post-hoc test on CLASSIFIER factor showed that SVM had highest performances compared to the other classifier types, whereas DT had the lowest ones, with the only exception for SVM and SVM-RBF during right hand movements between which no significant differences were found. The post-hoc test on CLASSIER x NUMBER OF

FEATURES factor revealed that even the best combination of classifier-number of features for the SVM-RBF, LDA and DT approaches did not significantly differ from the SVM with linear kernel based on 2 features, for both right and left hand movements. Such combination resulted to achieve on average the highest performance with the lowest number of features and thus to be the best classification approach for the CMC-based Ext-Grasp classification [23].

As for SMR-based classification, the two-way rmANOVA showed a significant effect in both sides only for the CLASSIFIER factor ($F(3,42)=16.4$, $p<0.01$ for left side and $F(3,42)=7.6$, $p<0.01$ for right side). From the post-hoc test, the two linear models SVM and LDA resulted to achieve higher performances with respect to the other classification models, no significant differences were obtained between the two classifier types. Thus, LDA with 2 input features was selected for the comparison with the CMC-based SVM classification approach. As suggested by Figure 3.2, the paired t-test revealed the superiority of the CMC-based approach in discriminating finger extension from grasping of both hands ($p<0.01$ for both sides).

Tables 3.1 and 3.2 report the metrics of the best combination of classifier-number of features identified by the statistical analysis for the CMC and SMR-based classification respectively. The superiority of CMC features in discriminating Ext and Grasp movements is consistent for all the metrics.

Table 3.1. Classification performances (AUC, Accuracy, Specificity and Sensitivity), reported as mean (standard error) across 15 participants, obtained using the CMC-based SVM classifier with 2 features.

Side	AUC	Accuracy	Specificity	Sensitivity
Left Hand	0.88 (0.02)	0.78 (0.02)	0.78 (0.03)	0.79 (0.04)
Right hand	0.91 (0.02)	0.82 (0.02)	0.78 (0.03)	0.85 (0.03)

Table 3.2. Classification performances (AUC, Accuracy, Specificity and Sensitivity), reported as mean (standard error) across 15 participants, obtained using the SMR-based LDA classifier with 2 features.

Side	AUC	Accuracy	Specificity	Sensitivity
Left Hand	0.76 (0.04)	0.72 (0.04)	0.71 (0.04)	0.73 (0.04)
Right hand	0.76 (0.05)	0.72 (0.04)	0.69 (0.05)	0.74 (0.04)

3.3.3 Analysis of Ext vs Grasp feature space

To investigate the neurophysiological processes involved in Ext-Grasp classification based on both hybrid (CMC) and cortical (SMR) features, Figures 3.3 and 3.4 show the most frequently selected features for the CMC-based and SMR-based classification when only 2 features were selected by the stepwise. The most recurrent EEG-EMG pairs (Figure 3.3 left) and EEG channels (Figure 3.4 left) selected by the stepwise regression regardless of the frequency band were flanked by pie-charts (3.3 and 3.4 right) reporting the number of times (in percentage) each frequency band is selected irrespective of the EEG-EMG pair or EEG channel, respectively for CMC and SMR features.

Overall, the same CMC feature was selected no more than 7% of times. However, the agonists/antagonist muscles (extensor digitorum - ED and flexor digitorum superficialis - FD) resulted to be involved in the selected pair respectively 64.7% and 33.3% of times for left hand movements and 52.7% and 25.3% of times for right hand movements. Moreover, more than 30% of the selected CMC features involved the Lateral deltoid muscle (Lat_DELT), for both left and right side. No clear lateralization of selected CMC features (i.e. involvement of EEG electrode position contralateral to the movement) was found. With regards to frequency bands, beta and gamma bands resulted to be the most recurrent frequency bands in both sides (Figure 3.3).

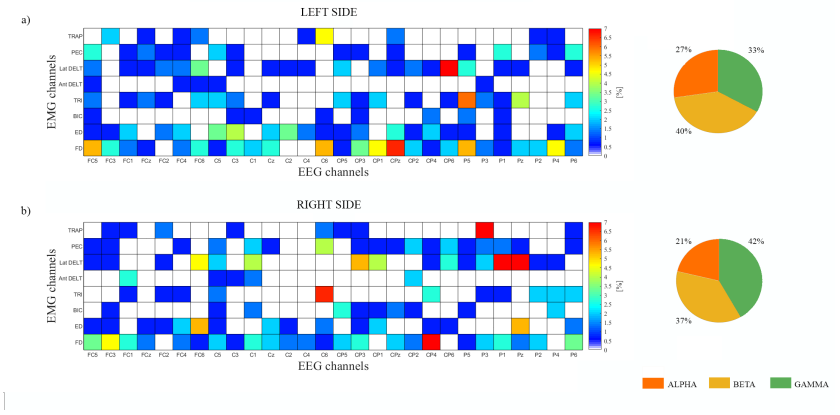

Figure 3.3. Features selected in CMC-based Ext vs Grasp classification. Most recurrent EEG-EMG pairs selected by the stepwise regression across participants (N = 15) and cross-validation iterations (IT=10) when using as classification approach a SVM classifier based on two features. The matrix shows for each EEG-EMG pair the number of times, expressed as percentage, each pair was selected over all participants and all iterations of the cross-validation. EEG-EMG pairs are identified by boxes from the intersection of the 28 EEG channels on the x-axis and the 8 EMG channels on the y-axis. Pie charts report the percentage each frequency band of interest was selected under the same condition. Panels: (a) Left hand movements, (b) Right hand movements.

As for SMR features, the same EEG channels was selected up to 20% of times and the most recurrent features resulted to be placed over the hemisphere contralateral to the involved side. Pie charts show how beta band was slightly more frequent than alpha band in both sides (Figure 3.4).

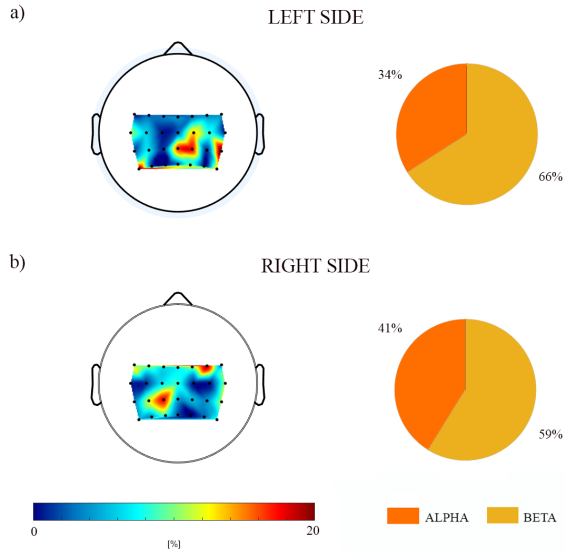

Figure 3.4. Features selected in SMR-based Ext vs Grasp classification. Most recurrent EEG channels selected by the stepwise regression across participants (N = 15) and cross-validation iterations (IT=10) when using as classification approach a LDA classifier based on two features. The scalp map shows the topographical distribution of the number of times each of the 28 EEG channels was selected. Pie charts report the percentage each frequency band of interest was selected under the same condition. Panels: (a) Left hand movements, (b) Right hand movements.

3.4 Discussion

This study had the aim to analyze cortico-muscular coupling as feature to discriminate different types of hand movements, and thus its potentiality to be used as input of a hybrid BCI. Data of 15 healthy subjects were analyzed during finger extension and grasping to identify the best classification approach to use when using CMC features, taking into account also the usability of a future BCI system (i.e. number of features required), and compared the performances obtained with existing BCI paradigms, such as those based on sensorimotor rhythms.

Overall, Figure 2.2 shows how CMC patterns derived from multiple EEG and EMG channels are able to characterize the execution of simple hand move-

ments such as finger extension and grasping. Whereas, considering only the brain correlates, similar desynchronizations of the EEG power spectrum occur during the two movements execution (Figure 3.1).
Indeed, CMC features extracted from multiple EEG-EMG pairs within 3 frequency bands of interest, allow for a successful classification of two different movements types, confirming results obtained in Study 1 even with a much smaller number of features (up to 10). Whereas, lower performances were obtained using SMR-based classification regardless on the classification algorithm used.

Furthermore, identifying the best classification approach according to the BCI application is one of the main challenges faced by BCI technology [87]. This study showed that a CMC-based SVM classifier with linear kernel achieved higher performance with respect to the other classification approaches based on the same feature. A linear classifier is fast and powerful in interpretative terms. As in rehabilitation contexts the reinforcement of physiological brain-muscles patterns is the main aim, such a classifier can optimize timing and consistency of feedback to patients favoring effective motor re-learning. Moreover, the high performances achieved by the SVM classifier with linear kernel based on only 2 features are promising in term of system usability and patient's set-up time, matching the use of BCI technology in clinical context or home environment.

As for SMR features, linear classifiers achieved the highest performances, indeed they are generally the first choice for EEG signal classification due to their simplicity, stability and insensitivity to overfitting [90].

Comparing the two types of features, higher performances and less inter-subject variability were obtained using cortico-muscular features to discriminate the two tasks than using only brain features. Previous studies demonstrated that exploiting also peripheral signals in addition to brain ones allows to increase BCI's movement detection from rest condition [15], [91], this study showed how using a hybrid feature potentially manages to better distinguish also different hand movements. Indeed, CMC features provide a wider feature space with the respect to only brain features and thus more information to discriminate the two movements. Moreover, it worthy of note that the proposed approach consists of exploiting the interplay between the cerebral and residual or recovered muscular activity involved in a given movement, rather than simply combining EEG and EMG features.

CMC features selected by the stepwise regression reflect the CMC grand average patterns (Figure 2.2): involvement of agonist muscle for Ext and agonist and antagonist muscles for Grasp, bilateral EEG connections, involvement of proximal muscles at higher frequency bands in particular for Grasp movements. The features selected with this classification approach belonged mainly to frequency bands in which EEG and EMG spectral contributions overlap [18], [19]. Despite of the similar activation during Ext and Grasp movements for EEG fea-

tures (Figure 3.1), the most recurrent features during SMR-based classification are distributed over the hand motor area [48]. The difference in occurrences between the most recurrent features across participants (N=15) and cross-validation iteration (IT=10) between the two approaches could be attributed to the higher dimensionality of the CMC features space.

Results achieved here show how CMC based-classification resulted to outperform SMR-based classification in the discrimination of finger extension from grasping. However, further analysis on other types of EEG correlates, such as movement related cortical potentials (MRCP) [49], are currently ongoing. MRCP occurs naturally right before movements attempt, reaching the maximum negativity near the onset [49], [92]–[94], it was shown to be able to decode movement intention [95], [96] and to discriminate different upper-limb movements [25], [97], thus comparison between the approach proposed here and an approach based on such features would be of utmost interest.

Moreover, such results were obtained considering earlobe referenced EEG data given that the employment of a spatial filter requires to increase the computational time of the BCI and implies the use of more EEG electrodes, increasing the set-up time needed to kept the impedance under a satisfactory level, as well as worsening the user's comfort. However, EEG spatial filtering is used to deblur the recorded signals so as to derive a more faithful representation of the sources within the brain, and/or to remove the influence of the reference electrode from the signal. It resulted to affect the extraction of both brain [54], [98]–[100] and CMC features [38], [51]. Thus, the effects of EEG spatial filtering such as Laplacian spatial filter, commonly used in EEG-based BCIs [101], are currently under analysis.

In conclusion, the possibility to achieve high classification performances with few features, in addition to the linearity and the interpretability of the model yielded SVM with linear kernel to be considered the best classification approach for a CMC-based h-BCI aimed at discriminating two simple hand movements. The higher classification performances obtained with respect to a classification approach based on only brain features showed the potentiality of a hybrid approach, that take into account the interconnection between brain and muscles during motor tasks, with respect to a canonical one. As such, this system could be relevant for motor rehabilitation but also for technological applications for motor substitution. Further investigations are needed to evaluate the feasibility of real-time extraction of CMC features and the classification performances in people with disability.

Conclusion

The analyses performed in this section report how cortico-muscular patterns show movement-specific characteristics and are able to quantify stroke-related alterations in brain-muscle communications (see Studies 1 and 2) [18], [19]. The analysis of the widespread brain-muscles connectivity patterns underlined the potentiality of the CMC as tool to characterize motor abnormalities after stroke during different motor tasks and provide a global picture of patient clinical status. Such multimodal features could be used as objective biomarkers to quantify motor impairment in stroke patients and could be valuable to assess the recovery induced by a motor rehabilitation treatment.
Moreover, CMC features resulted to be able to discriminate movement from rest condition and different movement tasks, showing a high potential to be used as inputs of hybrid BCI systems. Indeed, CMC could provide a comprehensive framework of the physiological and pathological patterns during simple hand movements to be employed in a h-BCI system for post-stroke motor rehabilitation. Such BCI could be able to encourage physiological movements and discourage pathological ones providing a rehabilitative instrument congruent to neurophysiological principles.

In the next section, the real-time extraction of CMC features and the translation in an online BCI paradigm is addressed.

References

[1] Mima Tatsuya, Toma Keiichiro, Koshy Benjamin, and Hallett Mark, "Coherence Between Cortical and Muscular Activities After Subcortical Stroke," *Stroke*, vol. 32, no. 11, pp. 2597–2601, Nov. 2001. DOI: 10.1161/hs1101.098764. [Online]. Available: https://www.ahajournals.org/doi/full/10.1161/hs1101.098764 (visited on 11/10/2019).

[2] K. von Carlowitz-Ghori, Z. Bayraktaroglu, F. U. Hohlefeld, F. Losch, G. Curio, and V. V. Nikulin, "Corticomuscular coherence in acute and chronic stroke," *Clinical Neurophysiology: Official Journal of the International Federation of Clinical Neurophysiology*, vol. 125, no. 6, pp. 1182–1191, Jun. 2014, ISSN: 1872-8952. DOI: 10.1016/j.clinph.2013.11.006.

[3] L. H. Larsen, I. C. Zibrandtsen, T. Wienecke, *et al.*, "Corticomuscular coherence in the acute and subacute phase after stroke," en, *Clinical Neurophysiology*, vol. 128, no. 11, pp. 2217–2226, Nov. 2017, ISSN: 1388-2457. DOI: 10.1016/j.clinph.2017.08.033. [Online]. Available: http://www.sciencedirect.com/science/article/pii/S1388245717309604 (visited on 11/08/2019).

[4] Z. Guo, Q. Qian, K. Wong, *et al.*, "Altered Corticomuscular Coherence (CMCoh) Pattern in the Upper Limb During Finger Movements After Stroke," *Frontiers in Neurology*, vol. 11, 2020, ISSN: 1664-2295. [Online]. Available: https://www.frontiersin.org/articles/10.3389/fneur.2020.00410 (visited on 07/20/2022).

[5] R. Krauth, J. Schwertner, S. Vogt, *et al.*, "Cortico-Muscular Coherence Is Reduced Acutely Post-stroke and Increases Bilaterally During Motor Recovery: A Pilot Study," *Frontiers in Neurology*, vol. 10, 2019, ISSN: 1664-2295. [Online]. Available: https://www.frontiersin.org/articles/10.3389/fneur.2019.00126 (visited on 07/20/2022).

[6] T. Mima, K. Toma, B. Koshy, and M. Hallett, "Coherence between cortical and muscular activities after subcortical stroke," *Stroke*, vol. 32, no. 11, pp. 2597–2601, Nov. 2001, ISSN: 1524-4628. DOI: 10.1161/hs1101.098764.

[7] A. Chowdhury, H. Raza, Y. K. Meena, A. Dutta, and G. Prasad, "An EEG-EMG correlation-based brain-computer interface for hand orthosis supported neuro-rehabilitation," *Journal of Neuroscience Methods*, vol. 312, pp. 1–11, Jan. 2019, ISSN: 1872-678X. DOI: 10.1016/j.jneumeth.2018.11.010.

[8] J.-H. Park, J.-H. Shin, H. Lee, J. Roh, and H.-S. Park, "Alterations in intermuscular coordination underlying isokinetic exercise after a stroke and their implications on neurorehabilitation," *Journal of NeuroEngineering and Rehabilitation*, vol. 18, no. 1, p. 110, Jul. 2021, ISSN: 1743-0003. DOI: 10.1186/s12984-021-00900-9. [Online]. Available: https://doi.org/10.1186/s12984-021-00900-9 (visited on 07/20/2022).

[9] S. Storch, M. Samantzis, and M. Balbi, "Driving Oscillatory Dynamics: Neuromodulation for Recovery After Stroke," *Frontiers in Systems Neuroscience*, vol. 15, 2021, ISSN: 1662-5137. [Online]. Available: https://www.frontiersin.org/articles/10.3389/fnsys.2021.712664 (visited on 07/20/2022).

[10] N. Ejaz, J. Xu, M. Branscheidt, *et al.*, "Evidence for a subcortical origin of mirror movements after stroke: A longitudinal study," *Brain: A Journal of Neurology*, vol. 141, no. 3, pp. 837–847, Mar. 2018, ISSN: 1460-2156. DOI: 10.1093/brain/awx384.

[11] G. Silasi and T. H. Murphy, "Stroke and the connectome: How connectivity guides therapeutic intervention," *Neuron*, vol. 83, no. 6, pp. 1354–1368, Sep. 2014, ISSN: 1097-4199. DOI: 10.1016/j.neuron.2014.08.052.

[12] R. Tian, J. P. A. Dewald, and Y. Yang, "Assessing the Usage of Indirect Motor Pathways Following a Hemiparetic Stroke," *IEEE transactions on neural systems and rehabilitation engineering: a publication of the IEEE Engineering in Medicine and Biology Society*, vol. 29, pp. 1568–1572, 2021, ISSN: 1558-0210. DOI: 10.1109/TNSRE.2021.3102493.

[13] M. Fauvet, D. Gasq, A. Chalard, J. Tisseyre, and D. Amarantini, "Temporal Dynamics of Corticomuscular Coherence Reflects Alteration of the Central Mechanisms of Neural Motor Control in Post-Stroke Patients," *Frontiers in Human Neuroscience*, vol. 15, 2021, ISSN: 1662-5161. [Online]. Available: https://www.frontiersin.org/articles/10.3389/fnhum.2021.682080 (visited on 07/20/2022).

[14] S. Zhou, Z. Guo, K. Wong, *et al.*, "Pathway-specific cortico-muscular coherence in proximal-to-distal compensation during fine motor control of finger extension after stroke," *Journal of Neural Engineering*, vol. 18, no. 5, Sep. 2021, ISSN: 1741-2552. DOI: 10.1088/1741-2552/ac20bc.

[15] G. Müller-Putz, R. Leeb, M. Tangermann, *et al.*, "Towards Noninvasive Hybrid Brain–Computer Interfaces: Framework, Practice, Clinical Application, and Beyond," *Proceedings of the IEEE*, vol. 103, no. 6, pp. 926–943, Jun. 2015, Conference Name: Proceedings of the IEEE, ISSN: 1558-2256. DOI: 10.1109/JPROC.2015.2411333.

[16] A. Riccio, F. Pichiorri, F. Schettini, *et al.*, "Chapter 12 - Interfacing brain with computer to improve communication and rehabilitation after brain damage," en, in *Progress in Brain Research*, ser. Brain-Computer Interfaces: Lab Experiments to Real-World Applications, D. Coyle, Ed., vol. 228, Elsevier, Jan. 2016, pp. 357–387. DOI: 10.1016/bs.pbr.2016.04.018. [Online]. Available: https://www.sciencedirect.com/science/article/pii/S0079612316300449 (visited on 04/11/2021).

[17] I. Choi, K. Bond, and C. S. Nam, "A hybrid BCI-controlled FES system for hand-wrist motor function," in *2016 IEEE International Conference on Systems, Man, and Cybernetics (SMC)*, Oct. 2016, pp. 002 324–002 328. DOI: 10.1109/SMC.2016.7844585.

[18] E. Colamarino, V. de Seta, M. Masciullo, *et al.*, "Corticomuscular and Intermuscular Coupling in Simple Hand Movements to Enable a Hybrid Brain-Computer Interface," eng, *International Journal of Neural Systems*, vol. 31, no. 11, p. 2 150 052, Nov. 2021, ISSN: 1793-6462. DOI: 10.1142/S0129065721500520.

[19] F. Pichiorri, J. Toppi, V. de Seta, *et al.*, "Exploring high-density corticomuscular networks after stroke to enable a hybrid Brain-Computer Interface for hand motor rehabilitation," *Journal of NeuroEngineering and Rehabilitation*, accepted, Jan. 2023.

[20] F. Pichiorri, G. Morone, M. Petti, *et al.*, "Brain-computer interface boosts motor imagery practice during stroke recovery," eng, *Annals of Neurology*, vol. 77, no. 5, pp. 851–865, May 2015, ISSN: 1531-8249. DOI: 10.1002/ana.24390.

[21] A. Biasiucci, R. Leeb, I. Iturrate, *et al.*, "Brain-actuated functional electrical stimulation elicits lasting arm motor recovery after stroke," en, *Nature Communications*, vol. 9, no. 1, p. 2421, Jun. 2018, Number: 1 Publisher: Nature Publishing Group, ISSN: 2041-1723. DOI: 10.1038/s41467-018-04673-z. [Online]. Available: https://www.nature.com/articles/s41467-018-04673-z (visited on 08/01/2022).

[22] A. Ramos-Murguialday, D. Broetz, M. Rea, *et al.*, "Brain-machine interface in chronic stroke rehabilitation: A controlled study," eng, *Annals of Neurology*, vol. 74, no. 1, pp. 100–108, Jul. 2013, ISSN: 1531-8249. DOI: 10.1002/ana.23879.

[23] V. de Seta, J. Toppi, E. Colamarino, *et al.*, "Cortico-Muscular Coupling to control a hybrid Brain-Computer Interface for upper limb motor rehabilitation: A pseudo-online study on stroke patients," *Frontiers in Human Neuroscience*, accepted, Oct. 2022. DOI: 10.3389/fnhum.2022.1016862.

[24] P. Ofner, A. Schwarz, J. Pereira, and G. R. Müller-Putz, "Upper limb movements can be decoded from the time-domain of low-frequency EEG," eng, *PloS One*, vol. 12, no. 8, e0182578, 2017, ISSN: 1932-6203. DOI: 10.1371/journal.pone.0182578.

[25] P. Ofner, A. Schwarz, J. Pereira, D. Wyss, R. Wildburger, and G. R. Müller-Putz, "Attempted Arm and Hand Movements can be Decoded from Low-Frequency EEG from Persons with Spinal Cord Injury," eng, *Scientific Reports*, vol. 9, no. 1, p. 7134, May 2019, ISSN: 2045-2322. DOI: 10.1038/s41598-019-43594-9.

[26] G. R. Müller-Putz, R. J. Kobler, J. Pereira, *et al.*, "Feel Your Reach: An EEG-Based Framework to Continuously Detect Goal-Directed Movements and Error Processing to Gate Kinesthetic Feedback Informed Artificial Arm Control," *Frontiers in Human Neuroscience*, vol. 16, 2022, ISSN: 1662-5161. [Online]. Available: https://www.frontiersin.org/articles/10.3389/fnhum.2022.841312.

[27] J. Tisseyre, D. Amarantini, A. Chalard, P. Marque, D. Gasq, and J. Tallet, "Mirror Movements are Linked to Executive Control in Healthy and Brain-injured Adults," *Neuroscience*, vol. 379, pp. 246–256, May 2018, ISSN: 1873-7544. DOI: 10.1016/j.neuroscience.2018.03.027.

[28] S. W. Lee, K. Landers, and M. L. Harris-Love, "Activation and intermuscular coherence of distal arm muscles during proximal muscle contraction," eng, *Experimental Brain Research*, vol. 232, no. 3, pp. 739–752, Mar. 2014, ISSN: 1432-1106. DOI: 10.1007/s00221-013-3784-x.

[29] C. Charissou, D. Amarantini, R. Baurès, E. Berton, and L. Vigouroux, "Effects of hand configuration on muscle force coordination, co-contraction and concomitant intermuscular coupling during maximal isometric flexion of the fingers," eng, *European Journal of Applied Physiology*, vol. 117, no. 11, pp. 2309–2320, Nov. 2017, ISSN: 1439-6327. DOI: 10.1007/s00421-017-3718-6.

[30] Y.-T. Chen, S. Li, E. Magat, P. Zhou, and S. Li, "Motor Overflow and Spasticity in Chronic Stroke Share a Common Pathophysiological Process: Analysis of Within-Limb and Between-Limb EMG-EMG Coherence," *Frontiers in Neurology*, vol. 9, p. 795, 2018, ISSN: 1664-2295. DOI: 10.3389/fneur.2018.00795.

[31] K. von Carlowitz-Ghori, Z. Bayraktaroglu, G. Waterstraat, G. Curio, and V. V. Nikulin, "Voluntary control of corticomuscular coherence through neurofeedback: A proof-of-principle study in healthy subjects," eng, *Neuroscience*, vol. 290, pp. 243–254, Apr. 2015, ISSN: 1873-7544. DOI: 10.1016/j.neuroscience.2015.01.013.

[32] D. C. Marquez, V. v. Tscharner, K. Murari, and B. M. Nigg, "Development of a multichannel current-EMG system for coherence modulation with visual biofeedback," en, *PLOS ONE*, vol. 13, no. 11, e0206871, Nov. 2018, Publisher: Public Library of Science, ISSN: 1932-6203. DOI: 10.1371/journal.pone.0206871. [Online]. Available: https://journals.plos.org/plosone/article?id=10.1371/journal.pone.0206871 (visited on 08/02/2021).

[33] Z. Guo, S. Zhou, K. Ji, *et al.*, "Corticomuscular integrated representation of voluntary motor effort in robotic control for wrist-hand rehabilitation after stroke," en, *Journal of Neural Engineering*, vol. 19, no. 2, p. 026 004, Mar. 2022, Publisher: IOP Publishing, ISSN: 1741-2552. DOI: 10.1088/1741-2552/ac5757. [Online]. Available: https://doi.org/10.1088/1741-2552/ac5757 (visited on 07/04/2022).

[34] M. Barbero, R. Merletti, and A. Rainoldi, *Atlas of Muscle Innervation Zones: Understanding Surface Electromyography and Its Applications*, en. Mailand: Springer-Verlag, 2012, ISBN: 978-88-470-2462-5. DOI: 10.1007/978-88-470-2463-2. [Online]. Available: https://www.springer.com/gp/book/9788847024625 (visited on 03/11/2021).

[35] D. Stegeman and H. Hermens, "Standards for suface electromyography: The European project Surface EMG for non-invasive assessment of muscles (SENIAM)," vol. 1, Jan. 2007.

[36] A. Rainoldi, G. Galardi, L. Maderna, G. Comi, L. Lo Conte, and R. Merletti, "Repeatability of surface EMG variables during voluntary isometric contractions of the biceps brachii muscle," eng, *Journal of Electromyography and Kinesiology: Official Journal of the International Society of Electrophysiological Kinesiology*, vol. 9, no. 2, pp. 105–119, Apr. 1999, ISSN: 1050-6411. DOI: 10.1016/s1050-6411(98)00042-x.

[37] S. Rota, I. Rogowski, S. Champely, and C. Hautier, "Reliability of EMG normalisation methods for upper-limb muscles," eng, *Journal of Sports Sciences*, vol. 31, no. 15, pp. 1696–1704, 2013, ISSN: 1466-447X. DOI: 10.1080/02640414.2013.796063.

[38] V. de Seta, J. Toppi, F. Pichiorri, *et al.*, "Towards a hybrid EEG-EMG feature for the classification of upper limb movements: Comparison of different processing pipelines," in *2021 10th International IEEE/EMBS Conference on Neural Engineering (NER)*, ISSN: 1948-3554, May 2021, pp. 355–358. DOI: 10.1109/NER49283.2021.9441390.

[39] T. Mima and M. Hallett, "Corticomuscular coherence: A review," *Journal of Clinical Neurophysiology: Official Publication of the American Electroencephalographic Society*, vol. 16, no. 6, pp. 501–511, Nov. 1999, ISSN: 0736-0258.

[40] J. Bigot, M. Longcamp, F. Dal Maso, and D. Amarantini, "A new statistical test based on the wavelet cross-spectrum to detect time-frequency dependence between non-stationary signals: Application to the analysis of cortico-muscular interactions," *NeuroImage*, vol. 55, no. 4, pp. 1504–1518, Apr. 2011, ISSN: 1095-9572. DOI: 10.1016/j.neuroimage.2011.01.033.

[41] D. G. Kamper, H. C. Fischer, M. O. Conrad, J. D. Towles, W. Z. Rymer, and K. M. Triandafilou, "Finger-thumb coupling contributes to exaggerated thumb flexion in stroke survivors," eng, *Journal of Neurophysiology*, vol. 111, no. 12, pp. 2665–2674, Jun. 2014, ISSN: 1522-1598. DOI: 10.1152/jn.00413.2013.

[42] J. R. Rosenberg, A. M. Amjad, P. Breeze, D. R. Brillinger, and D. M. Halliday, "The Fourier approach to the identification of functional coupling between neuronal spike trains," eng, *Progress in Biophysics and Molecular Biology*, vol. 53, no. 1, pp. 1–31, 1989, ISSN: 0079-6107. DOI: 10.1016/0079-6107(89)90004-7.

[43] Y. Benjamini and D. Yekutieli, "The Control of the False Discovery Rate in Multiple Testing under Dependency," *The Annals of Statistics*, vol. 29, no. 4, pp. 1165–1188, Aug. 2001, ISSN: 00905364. [Online]. Available: http://www.jstor.org/stable/2674075 (visited on 10/12/2010).

[44] J. O. Rawlings, S. G. Pantula, and D. A. Dickey, *Applied Regression Analysis: A Research Tool* (Springer Texts in Statistics), en, 2nd ed. New York: Springer-Verlag, 1998, ISBN: 978-0-387-98454-4. DOI: 10.1007/b98890. [Online]. Available: https://www.springer.com/gp/book/9780387984544 (visited on 03/11/2021).

[45] A. Chowdhury, H. Raza, Y. K. Meena, A. Dutta, and G. Prasad, "An EEG-EMG correlation-based brain-computer interface for hand orthosis supported neuro-rehabilitation," en, *Journal of Neuroscience Methods*, vol. 312, pp. 1–11, Jan. 2019, ISSN: 0165-0270. DOI: 10.1016/j.jneumeth.2018.11.010. [Online]. Available: https://www.sciencedirect.com/science/article/pii/S0165027018303790 (visited on 07/22/2021).

[46] T. Fawcett, "An introduction to ROC analysis," en, *Pattern Recognition Letters*, ROC Analysis in Pattern Recognition, vol. 27, no. 8, pp. 861–874, Jun. 2006, ISSN: 0167-8655. DOI: 10.1016/j.patrec.2005.10.010. [Online]. Available: https://www.sciencedirect.com/science/article/pii/S016786550500303X (visited on 08/02/2022).

[47] J. Liu, Y. Sheng, and H. Liu, "Corticomuscular Coherence and Its Applications: A Review," *Frontiers in Human Neuroscience*, vol. 13, 2019, ISSN: 1662-5161. [Online]. Available: https://www.frontiersin.org/articles/10.3389/fnhum.2019.00100 (visited on 08/02/2022).

[48] A. Nakamura, T. Yamada, A. Goto, *et al.*, "Somatosensory Homunculus as Drawn by MEG," en, *NeuroImage*, vol. 7, no. 4, pp. 377–386, May 1998, ISSN: 1053-8119. DOI: 10.1006/nimg.1998.0332. [Online]. Available: http://www.sciencedirect.com/science/article/pii/S1053811998903329 (visited on 11/18/2020).

[49] C. Toro, G. Deuschl, R. Thatcher, S. Sato, C. Kufta, and M. Hallett, "Event-related desynchronization and movement-related cortical potentials on the ECoG and EEG," eng, *Electroencephalography and Clinical Neurophysiology*, vol. 93, no. 5, pp. 380–389, Oct. 1994, ISSN: 0013-4694. DOI: 10.1016/0168-5597(94)90126-0.

[50] A. Schwarz, M. K. Höller, J. Pereira, P. Ofner, and G. R. Müller-Putz, "Decoding hand movements from human EEG to control a robotic arm in a simulation environment," eng, *Journal of Neural Engineering*, vol. 17, no. 3, p. 036 010, May 2020, ISSN: 1741-2552. DOI: 10.1088/1741-2552/ab882e.

[51] T. Mima and M. Hallett, "Electroencephalographic analysis of corticomuscular coherence: Reference effect, volume conduction and generator mechanism," en, *Clinical Neurophysiology*, vol. 110, no. 11, pp. 1892–1899, Nov. 1999, ISSN: 1388-2457. DOI: 10.1016/S1388-2457(99)00238-2. [Online]. Available: http://www.sciencedirect.com/science/article/pii/S1388245799002382 (visited on 11/05/2019).

[52] C. Rau, C. Plewnia, F. Hummel, and C. Gerloff, "Event-related desynchronization and excitability of the ipsilateral motor cortex during simple self-paced finger movements," eng, *Clinical Neurophysiology: Official Journal of the International Federation of Clinical Neurophysiology*, vol. 114, no. 10, pp. 1819–1826, Oct. 2003, ISSN: 1388-2457. DOI: 10.1016/s1388-2457(03)00174-3.

[53] G. Pfurtscheller and F. H. Lopes da Silva, "Event-related EEG/MEG synchronization and desynchronization: Basic principles," eng, *Clinical Neurophysiology: Official Journal of the International Federation of Clinical Neurophysiology*, vol. 110, no. 11, pp. 1842–1857, Nov. 1999, ISSN: 1388-2457. DOI: 10.1016/s1388-2457(99)00141-8.

[54] C. Babiloni, F. Carducci, F. Cincotti, *et al.*, "Human movement-related potentials vs desynchronization of EEG alpha rhythm: A high-resolution EEG study," English, *NeuroImage*, vol. 10, no. 6, pp. 658–665, Dec. 1999, Publisher: Academic Press Inc., ISSN: 1053-8119. DOI: 10.1006/nimg.1999.0504.

[55] C. Neuper and G. Pfurtscheller, "Event-related dynamics of cortical rhythms: Frequency-specific features and functional correlates," eng, *International Journal of Psychophysiology: Official Journal of the International Organization of Psychophysiology*, vol. 43, no. 1, pp. 41–58, Dec. 2001, ISSN: 0167-8760. DOI: 10.1016/s0167-8760(01)00178-7.

[56] A. I. Sburlea and G. R. Müller-Putz, "Exploring representations of human grasping in neural, muscle and kinematic signals," en, *Scientific Reports*, vol. 8, no. 1, p. 16 669, Nov. 2018, Number: 1 Publisher: Nature Publishing Group, ISSN: 2045-2322. DOI: 10.1038/s41598-018-35018-x. [Online]. Available: https://www.nature.com/articles/s41598-018-35018-x (visited on 03/11/2021).

[57] F. Pichiorri, F. D. V. Fallani, F. Cincotti, *et al.*, "Sensorimotor rhythm-based brain–computer interface training: The impact on motor cortical responsiveness," en, *Journal of Neural Engineering*, vol. 8, no. 2, p. 025 020, Mar. 2011, Publisher: IOP Publishing, ISSN: 1741-2552. DOI: 10.1088/1741-2560/8/2/025020. [Online]. Available: https://doi.org/10.1088/1741-2560/8/2/025020 (visited on 03/05/2021).

[58] P. Brown and J. F. Marsden, "Cortical network resonance and motor activity in humans," eng, *The Neuroscientist: A Review Journal Bringing Neurobiology, Neurology and Psychiatry*, vol. 7, no. 6, pp. 518–527, Dec. 2001, ISSN: 1073-8584. DOI: 10.1177/107385840100700608.

[59] J. A. Norton and M. A. Gorassini, "Changes in cortically related intermuscular coherence accompanying improvements in locomotor skills in incomplete spinal cord injury," eng, *Journal of Neurophysiology*, vol. 95, no. 4, pp. 2580–2589, Apr. 2006, ISSN: 0022-3077. DOI: 10.1152/jn.01289.2005.

[60] X. Lou, S. Xiao, Y. Qi, X. Hu, Y. Wang, and X. Zheng, *Corticomuscular Coherence Analysis on Hand Movement Distinction for Active Rehabilitation*, en, Research Article, ISSN: 1748-670X Pages: e908591 Publisher: Hindawi Volume: 2013, Apr. 2013. DOI: https://doi.org/10.1155/2013/908591. [Online]. Available: https://www.hindawi.com/journals/cmmm/2013/908591/ (visited on 12/04/2020).

[61] F. Quandt and F. C. Hummel, "The influence of functional electrical stimulation on hand motor recovery in stroke patients: A review," eng, *Experimental & Translational Stroke Medicine*, vol. 6, p. 9, 2014, ISSN: 2040-7378. DOI: 10.1186/2040-7378-6-9.

[62] M. Gandolfi, N. Valè, E. K. Dimitrova, *et al.*, "Effectiveness of Robot-Assisted Upper Limb Training on Spasticity, Function and Muscle Activity in Chronic Stroke Patients Treated With Botulinum Toxin: A Randomized Single-Blinded Controlled Trial," English, *Frontiers in Neurology*, vol. 10, 2019, Publisher: Frontiers, ISSN: 1664-2295. DOI: 10.3389/fneur.2019.00041. [Online]. Available: https://www.frontiersin.org/articles/10.3389/fneur.2019.00041/full (visited on 03/10/2021).

[63] K. S. Sunnerhagen, A. Opheim, and M. Alt Murphy, "Onset, time course and prediction of spasticity after stroke or traumatic brain injury," eng, *Annals of Physical and Rehabilitation Medicine*, vol. 62, no. 6, pp. 431–434, Nov. 2019, ISSN: 1877-0665. DOI: 10.1016/j.rehab.2018.04.004.

[64] V. Mondini, R. J. Kobler, A. I. Sburlea, and G. R. Müller-Putz, "Continuous low-frequency EEG decoding of arm movement for closed-loop, natural control of a robotic arm," eng, *Journal of Neural Engineering*, vol. 17, no. 4, p. 046 031, Aug. 2020, ISSN: 1741-2552. DOI: 10.1088/1741-2552/aba6f7.

[65] M. Rubinov and O. Sporns, "Complex network measures of brain connectivity: Uses and interpretations," *Neuroimage*, vol. 52, no. 3, pp. 1059–1069, Sep. 2010, ISSN: 1095-9572. DOI: 10.1016/j.neuroimage.2009.10.003. [Online]. Available: http://www.ncbi.nlm.nih.gov/pubmed/19819337 (visited on 04/03/2012).

[66] A.-B. Meseguer-Henarejos, J. Sánchez-Meca, J.-A. López-Pina, and R. Carles-Hernández, "Inter- and intra-rater reliability of the Modified Ashworth Scale: A systematic review and meta-analysis," *European Journal of Physical and Rehabilitation Medicine*, vol. 54, no. 4, pp. 576–590, Aug. 2018, ISSN: 1973-9095. DOI: 10.23736/S1973-9087.17.04796-7.

[67] L. B. Goldstein, C. Bertels, and J. N. Davis, "Interrater reliability of the NIH stroke scale," *Archives of Neurology*, vol. 46, no. 6, pp. 660–662, Jun. 1989, ISSN: 0003-9942. DOI: 10.1001/archneur.1989.00520420080026.

[68] E. Fan, N. D. Ciesla, A. D. Truong, V. Bhoopathi, S. L. Zeger, and D. M. Needham, "Inter-rater reliability of manual muscle strength testing in ICU survivors and simulated patients," *Intensive care medicine*, vol. 36, no. 6, pp. 1038–1043, Jun. 2010, ISSN: 0342-4642. DOI: 10.1007/s00134-010-1796-6. [Online]. Available: https://www.ncbi.nlm.nih.gov/pmc/articles/PMC2891143/ (visited on 07/20/2022).

[69] A. R. Fugl-Meyer, L. Jääskö, I. Leyman, S. Olsson, and S. Steglind, "The post-stroke hemiplegic patient. 1. a method for evaluation of physical performance," *Scandinavian Journal of Rehabilitation Medicine*, vol. 7, no. 1, pp. 13–31, 1975, ISSN: 0036-5505.

[70] R. C. Oldfield, "The assessment and analysis of handedness: The Edinburgh inventory," *Neuropsychologia*, vol. 9, no. 1, pp. 97–113, Mar. 1971, ISSN: 0028-3932. DOI: 10.1016/0028-3932(71)90067-4. [Online]. Available: https://www.sciencedirect.com/science/article/pii/0028393271900674 (visited on 07/20/2022).

[71] S. Abbaspour and A. Fallah, "Removing ECG Artifact from the Surface EMG Signal Using Adaptive Subtraction Technique," *Journal of biomedical physics & engineering*, 2014.

[72] T. Roland, "Motion Artifact Suppression for Insulated EMG to Control Myoelectric Prostheses," *Sensors*, vol. 20, no. 4, p. 1031, Jan. 2020, ISSN: 1424-8220. DOI: 10.3390/s20041031. [Online]. Available: https://www.mdpi.com/1424-8220/20/4/1031 (visited on 07/20/2022).

[73] J. Yu, S. Park, H. Lee, C.-S. Pyo, and Y. S. Lee, "An Elderly Health Monitoring System Using Machine Learning and In-Depth Analysis Techniques on the NIH Stroke Scale," *Mathematics*, vol. 8, no. 7, p. 1115, Jul. 2020, ISSN: 2227-7390. DOI: 10.3390/math8071115. [Online]. Available: https://www.mdpi.com/2227-7390/8/7/1115 (visited on 07/20/2022).

[74] M. L. Woodbury, C. A. Velozo, L. G. Richards, and P. W. Duncan, "Rasch analysis staging methodology to classify upper extremity movement impairment after stroke," *Archives of Physical Medicine and Rehabilitation*, vol. 94, no. 8, pp. 1527–1533, Aug. 2013, ISSN: 1532-821X. DOI: 10.1016/j.apmr.2013.03.007.

[75] D. S. Bassett and E. T. Bullmore, "Small-World Brain Networks Revisited," *The Neuroscientist*, vol. 23, no. 5, pp. 499–516, Oct. 2017, ISSN: 1073-8584. DOI: 10.1177/1073858416667720. [Online]. Available: https://doi.org/10.1177/1073858416667720 (visited on 09/15/2022).

[76] C. Gerloff, K. Bushara, A. Sailer, *et al.*, "Multimodal imaging of brain reorganization in motor areas of the contralesional hemisphere of well recovered patients after capsular stroke," *Brain: A Journal of Neurology*, vol. 129, no. Pt 3, pp. 791–808, Mar. 2006, ISSN: 1460-2156. DOI: 10.1093/brain/awh713.

[77] S. Graziadio, L. Tomasevic, G. Assenza, F. Tecchio, and J. Eyre, "The myth of the 'unaffected' side after unilateral stroke: Is reorganisation of the non-infarcted corticospinal system to re-establish balance the price for recovery?" *Experimental Neurology*, vol. 238, no. 2, pp. 168–175, Dec. 2012, ISSN: 0014-4886. DOI: 10.1016/j.expneurol.2012.08.031. [Online]. Available: https://www.ncbi.nlm.nih.gov/pmc/articles/PMC3508413/ (visited on 07/20/2022).

[78] B. Yu, X. Zhang, Y. Cheng, *et al.*, "The Effects of the Biceps Brachii and Brachioradialis on Elbow Flexor Muscle Strength and Spasticity in Stroke Patients," *Neural Plasticity*, vol. 2022, e1295908, Mar. 2022, ISSN: 2090-5904. DOI: 10.1155/2022/1295908. [Online]. Available: https://www.hindawi.com/journals/np/2022/1295908/ (visited on 07/20/2022).

[79] İ. Şengül, A. Aşkın, and A. Tosun, "Effect of muscle selection for botulinum neurotoxin treatment on spasticity in patients with post-stroke elbow flexor muscle over-activity: An observational prospective study," *Somatosensory & Motor Research*, vol. 39, no. 1, pp. 10–17, Mar. 2022, ISSN: 1369-1651. DOI: 10.1080/08990220.2021.1986383.

[80] A. Esquenazi, Z. Ayyoub, M. Verduzco-Gutierrez, P. Maisonobe, J. Otto, and A. T. Patel, "AbobotulinumtoxinA Versus OnabotulinumtoxinA in Adults with Upper Limb Spasticity: A Randomized, Double-Blind, Crossover Study Protocol," *Advances in Therapy*, vol. 38, no. 11, pp. 5623–5633, 2021, ISSN: 0741-238X. DOI: 10.1007/s12325-021-01896-3. [Online]. Available: https://www.ncbi.nlm.nih.gov/pmc/articles/PMC8475311/ (visited on 07/20/2022).

[81] X. Xi, X. Wu, Y.-B. Zhao, J. Wang, W. Kong, and Z. Luo, "Corticomuscular functional network: An exploration of cortico-muscular coupling in hand movements," *Journal of Neural Engineering*, vol. 18, no. 4, p. 046 084, Jun. 2021, ISSN: 1741-2552. DOI: 10.1088/1741-2552/ac0586. [Online]. Available: https://doi.org/10.1088/1741-2552/ac0586 (visited on 07/20/2022).

[82] G. Morone, S. Paolucci, D. Mattia, F. Pichiorri, M. Tramontano, and M. Iosa, "The 3Ts of the new millennium neurorehabilitation gym: Therapy, technology, translationality," *Expert Review of Medical Devices*, vol. 13, no. 9, pp. 785–787, Sep. 2016, ISSN: 1745-2422. DOI: 10.1080/17434440.2016.1218275.

[83] M. Iosa, G. Morone, A. Fusco, *et al.*, "Seven capital devices for the future of stroke rehabilitation," *Stroke Research and Treatment*, vol. 2012, p. 187 965, 2012, ISSN: 2042-0056. DOI: 10.1155/2012/187965.

[84] J. R. Wolpaw, N. Birbaumer, D. J. McFarland, G. Pfurtscheller, and T. M. Vaughan, "Brain–computer interfaces for communication and control," *Clinical neurophysiology*, vol. 113, no. 6, pp. 767–791, 2002, Publisher: Elsevier.

[85] G. Pfurtscheller, C. Neuper, G. Muller, *et al.*, "Graz-BCI: State of the art and clinical applications," *IEEE Transactions on Neural Systems and Rehabilitation Engineering*, vol. 11, no. 2, pp. 1–4, Jun. 2003, Conference Name: IEEE Transactions on Neural Systems and Rehabilitation Engineering, ISSN: 1558-0210. DOI: 10.1109/TNSRE.2003.814454.

[86] D. J. Mcfarland and J. R. Wolpaw, "Chapter 4 - Brain–Computer Interfaces for the Operation of Robotic and Prosthetic Devices," en, in *Advances in Computers*, vol. 79, Elsevier, Jan. 2010, pp. 169–187. DOI: 10.1016/S0065-2458(10)79004-5. [Online]. Available: https://www.sciencedirect.com/science/article/pii/S0065245810790045 (visited on 07/07/2022).

[87] F. Lotte, M. Congedo, A. Lécuyer, F. Lamarche, and B. Arnaldi, "A review of classification algorithms for EEG-based brain-computer interfaces," eng, *Journal of Neural Engineering*, vol. 4, no. 2, R1–R13, Jun. 2007, ISSN: 1741-2560. DOI: 10.1088/1741-2560/4/2/R01.

[88] C.-W. Hsu, C.-C. Chang, and C.-J. Lin, "A Practical Guide to Support Vector Classification," en, p. 16,

[89] L. Breman, J. Friedman, C. J. Stone, and R. A. Olshen, *Classification and Regression Trees - 1st Edition* -, Jan. 1984. [Online]. Available: https://www.routledge.com/Classification-and-Regression-Trees/Breiman-Friedman-Stone-Olshen/p/book/9780412048418 (visited on 01/21/2022).

[90] B. Wang, C. M. Wong, F. Wan, P. U. Mak, P. I. Mak, and M. I. Vai, "Comparison of different classification methods for EEG-based brain computer interfaces: A case study," in *2009 International Conference on Information and Automation*, Jun. 2009, pp. 1416–1421. DOI: 10.1109/ICINFA.2009.5205138.

[91] E. Lóopez-Larraz, N. Birbaumer, and A. Ramos-Murguialday, "A hybrid EEG-EMG BMI improves the detection of movement intention in cortical stroke patients with complete hand paralysis," in *2018 40th Annual International Conference of the IEEE Engineering in Medicine and Biology Society (EMBC)*, ISSN: 1558-4615, Jul. 2018, pp. 2000–2003. DOI: 10.1109/EMBC.2018.8512711.

[92] N. Birbaumer, T. Elbert, B. Rockstroh, and W. Lutzenberger, "Biofeedback of Event-Related Slow Potentials of the Brain," fr, *International Journal of Psychology*, vol. 16, no. 1-4, pp. 389–415, 1981, _eprint: https://onlinelibrary.wiley.com/doi/pdf/10.1080/00207598108247426, ISSN: 1464-066X. DOI: 10.1080/00207598108247426. [Online]. Available: https://onlinelibrary.wiley.com/doi/abs/10.1080/00207598108247426 (visited on 10/29/2022).

[93] J. Pereira, P. Ofner, A. Schwarz, A. I. Sburlea, and G. R. Müller-Putz, "EEG neural correlates of goal-directed movement intention," *NeuroImage*, vol. 149, pp. 129–140, 2017, ISSN: 1053-8119. DOI: https://doi.org/10.1016/j.neuroimage.2017.01.030. [Online]. Available: http://www.sciencedirect.com/science/article/pii/S1053811917300368.

[94] N. Mrachacz-Kersting, J. Ibáñez, and D. Farina, "Towards a mechanistic approach for the development of non-invasive brain-computer interfaces for motor rehabilitation," en, *The Journal of Physiology*, vol. 599, no. 9, pp. 2361–2374, 2021, _eprint: https://onlinelibrary.wiley.com/doi/pdf/10.1113/JP2813 ISSN: 1469-7793. DOI: 10.1113/JP281314. [Online]. Available: https://onlinelibrary.wiley.com/doi/abs/10.1113/JP281314 (visited on 08/01/2022).

[95] O. Bai, V. Rathi, P. Lin, *et al.*, "Prediction of human voluntary movement before it occurs," *Clinical Neurophysiology*, vol. 122, no. 2, pp. 364–372, 2011, ISSN: 1388-2457. DOI: https://doi.org/10.1016/j.clinph.2010.07.010. [Online]. Available: http://www.sciencedirect.com/science/article/pii/S1388245710005699.

[96] N. Mrachacz-Kersting, N. Jiang, A. J. T. Stevenson, *et al.*, "Efficient neuroplasticity induction in chronic stroke patients by an associative brain-computer interface," eng, *Journal of Neurophysiology*, vol. 115, no. 3, pp. 1410–1421, Mar. 2016, ISSN: 1522-1598. DOI: 10.1152/jn.00918.2015.

[97] A. M. Savić, E. R. Lontis, N. Mrachacz-Kersting, and M. B. Popović, "Dynamics of movement-related cortical potentials and sensorimotor oscillations during palmar grasp movements," en, *European Journal of Neuroscience*, vol. 51, no. 9, pp. 1962–1970, 2020, _eprint: https://onlinelibrary.wiley.com/doi/ ISSN: 1460-9568. DOI: https://doi.org/10.1111/ejn.14629. [Online]. Available: https://onlinelibrary.wiley.com/doi/abs/10.1111/ejn.14629 (visited on 03/22/2021).

[98] D. J. McFarland, L. M. McCane, S. V. David, and J. R. Wolpaw, "Spatial filter selection for EEG-based communication," en, *Electroencephalography and Clinical Neurophysiology*, vol. 103, no. 3, pp. 386–394, Sep. 1997, ISSN: 0013-4694. DOI: 10.1016/S0013-4694(97)00022-2. [Online]. Available: https://www.sciencedirect.com/science/article/pii/S0013469497000222 (visited on 07/20/2022).

[99] G. Schalk, D. J. McFarland, T. Hinterberger, N. Birbaumer, and J. R. Wolpaw, "BCI2000: A general-purpose brain-computer interface (BCI) system," *IEEE Transactions on Biomedical Engineering*, vol. 51, no. 6, pp. 1034–1043, Jun. 2004, ISSN: 0018-9294. DOI: 10.1109/TBME.2004.827072.

[100] C. Bibián, E. López-Larraz, N. Irastorza-Landa, N. Birbaumer, and A. Ramos-Murguialday, "Evaluation of filtering techniques to extract movement intention information from low-frequency EEG activity," in *2017 39th Annual International Conference of the IEEE Engineering*

in Medicine and Biology Society (EMBC), ISSN: 1558-4615, Jul. 2017, pp. 2960–2963. DOI: 10.1109/EMBC.2017.8037478.

[101] G. Schalk and J. Mellinger, *A Practical Guide to Brain–Computer Interfacing with BCI2000*, en. London: Springer London, 2010, ISBN: 978-1-84996-091-5 978-1-84996-092-2. DOI: 10.1007/978-1-84996-092-2. [Online]. Available: http://link.springer.com/10.1007/978-1-84996-092-2 (visited on 07/21/2022).

Section II

Development of a hybrid BCI-controlled FES for upper limb rehabilitation after stroke

Introduction

This section is composed by three main parts. In the first part, I reported a study aiming at the definition and adaptation of a processing pipeline including computation and the consequent CMC-based movement detection to be used in real-time settings. In the second part, the design of a hybrid BCI (h-BCI) based on CMC features to control a Functional Electrical Stimulation (FES) and devoted to post-stroke motor rehabilitation for patients with residual or recovered muscular activity is described and preliminary feasibility tests are reported. The third part focuses on the stimulation strategy and described an adaptive approach to modulate the intensity of FES stimulation based on the residual or recovered muscular activity. Thus, the studies reported in this section aim at the development of a technology able to support post-stroke motor rehabilitation following the patient along each step of rehabilitation path with an intervention tailored to his/her motor impairment.

As assessed by the studies of the Section I, CMC features extracted from multiple EEG-EMG pairs can discriminate offline different simple hand movements, such as finger extension and grasping, from rest condition (see Study 1) [1]. Moreover, cortico-muscular patterns change after stroke and are able to characterize patients' impairment (see Study 2) [2], thus CMC could be a valuable hybrid feature to detect in real-time movement attempts and to train the physiological brain control over muscles in a BCI-based intervention.

Before implementing a CMC-based BCI, classification accuracy and speed, which are crucial factors for BCI technology [3]–[7], should be analyzed to assess the feasibility of CMC as BCI feature. To evaluate and optimize the real-time CMC computation and classification, a pseudo-online analysis on 13 healthy and 12 stroke participants during simple hand movements/attempts was performed and the setting parameters that allow the best trade-off between classification accuracy and speed were identified [8]. Such parameters were then used to design the h-BCI.

The second part of this section describes the development of a h-BCI aimed to RE-establish COrtico-Muscular communication after stroke. Such prototype is a BCI-based rehabilitative device in which a complex pattern of cortico-muscular activation is determined online during movement attempts of the

upper limb and used to control FES. Such device was developed with the ultimate aim of being used during post-stroke motor rehabilitation as an add-on to traditional therapies to assist patients with residual or recovered muscular activity in completing movements during rehabilitative exercises. The main hypothesis is that a hybrid control signal for FES in a BCI setting will ensure that volition (Central Nervous System - CNS activity recorded via EEG) and specific muscular recruitment (multiple EMG recordings) are reinforced in the training, re-establishing natural motor control and contrasting the consolidation of pathological phenomena, i.e. co-contraction of antagonists muscles, spasticity, motor overflow, abnormal muscle co-activation, mirror movements [9]–[12], which often accompany motor skill regaining after stroke (maladaptive plasticity).
Thus, in this h-BCI prototype CMC control features were chosen to reinforce and exercise voluntary residual motor functions, so as to avoid the reinforcement of maladaptive changes, i.e. restoring only 'correct' central-to-peripheral communication. For this reason, the device consists of two branches one aimed to detect the movement attempt based on physiological patterns (to encourage) and the other aimed to check that pathological patterns during such attempt (to discourage) do not occur. Only when both conditions are satisfied the BCI closes the loop delivering a stimulation to the patient to support full movement execution.
The system architecture and the technological implementation of each building module are shown in details. To test the feasibility of the h-BCI prototype, the online classification timing and accuracy were evaluated in 3 healthy participants. The ability of the prototype to generalize across different users and its usability were assessed. Moreover, its ability to detect stroke-related pathological movements was evaluated by a pseudo-online analysis on 11 stroke patients during finger extension attempts of the paretic hand.

Finally, to deliver a stimulation customized to the patient needs, a modulation strategy based on the residual or recovered muscles activity detected during the rehabilitative exercise was developed. Customized stimulation strategies were assessed to better improve the sensorimotor functions in stroke patients [13] and allow to adjust the system according to the rehabilitative approach pursued. Voluntary EMG (vEMG) is used to trigger FES in post-stroke rehabilitation [14], [15] or to proportionally control in real-time the stimulation according to the level of activation [16], [17]. Here, vEMG is used to modulate the FES intensity triggered by the BCI. Thus, the BCI detects the volition based on the EEG signals over the sensorimotor area to rehabilitate, and a stimulation is sent to reinforce a close-to-normal brain activity [18]. The intensity of the stimulation is modulated by the myoelectric level of activation right after the BCI detection. The modulation strategy is based on a compensatory approach: if no voluntary activation is detected, the full FES intensity is delivered to the patient, whereas when residual or recovered muscular activity occurs a percentage of FES intensity complementary to the level of activation is sent. Such a hybrid system allows to longitudinal follow the patient along the rehabilitation

process delivering a stimulation tailored on his/her motor impairment. An EEG-based BCI was used for this study in order to test the adaptive algorithm designed for the modulation strategy on an already tested BCI paradigm [19], [20],[21].

4. Study 4

An optimized approach for real-time Cortico-Muscular Coupling computation

4.1 Background and Objectives

CMC values have been already used as inputs of a h-BCI to discriminate online right-vs-left hand grasp movement in both healthy subjects and hemiparetic stroke patients [22]. However, to the best of my knowledge, CMC studies on h-BCI had neither assessed the ability of CMC to detect movement attempts from rest condition nor optimized the online CMC-based movement classification pipeline finding the parameters that allow to obtain both high accuracy and speed.

Hence, the feasibility of real-time extraction of CMC features suitable for movements versus rest classification, and thus to control a h-BCI system was evaluated. Data of 13 healthy (CTRL) and 12 stroke (EXP) participants during executed (CTRL and EXP unaffected arm) and attempted (EXP affected arm) simple hand movements were analyzed simulating a real-time approach (i.e., pseudo-online) to optimize the choice of the parameters in the real-time CMC algorithm that allow the best trade-off between classification performances and classification speed. Indeed, together with a high classification accuracy, also a short time for the BCI to detect a movement should be pursued, in order to lead to significant plasticity induction and functionally relevant improvement in agreement with Hebbian associative learning theory [23], [24]. For this reason, different updating factors of the CMC computation (shifts) during the trial, as well as different number of consecutive movement predictions to accumulate for a final classification decision, were tested in terms of performance and time for detection. Once identified the best parameters to be used in the real-time CMC

approach, classification accuracy and speed obtained in stroke participants were compared between different movements accomplished with affected and unaffected hands, separately.

4.2 Materials and Methods

4.2.1 Participants

This study was performed on the same dataset acquired in Study 2. Thirteen right-handed healthy subjects (9 females/4 males, age 48.5±19.3 yo) and twelve patients (7 females/ 5 males, age 53.8±18 yo, months from event 5.3±3.5, lesion side: 7 left/5 right) with clinically diagnosed stroke were selected for this analysis. Details about the demographical and clinical data of such patients are reported in Table 4.1.

4.2.2 Experimental Design

Data were collected according to the paradigm described in Study 2 paragraph 2.2.2 and summarizes here. EEG and EMG data were simultaneously recorded and sampled respectively at 1kHz and 2kHz. Sixty-one active electrodes arranged according to an extension of 10-20 system (reference on left mastoid and ground on right mastoid) were used to acquire the EEG data from the scalp by means of BrainAmp amplifiers (Brain Products GmbH, Germany[1]), impedances were kept below 5kΩ. Surface EMG data were recorded through Pico EMG sensors (Cometa S.r.l., Italy[2]) from 16 muscles collected in bipolar fashion: extensor digitorum (ED), flexor digitorum superficialis (FD), lateral head of the triceps muscle (TRI), long head of the biceps brachii muscle (BIC), pectoralis major (PEC), lateral deltoid (Lat_DELT), anterior deltoid (Ant_DELT) and upper trapezius (TRAP) of both sides (L: left, R: right). The quality of EEG and EMG signals was visually checked prior to beginning the recordings and continuously monitored afterwards.
During the experiment, all participants were seated in a comfortable chair with adjustable seat height and with their forearms placed on the table. Visual cues were presented on a screen on the desk in front of them via Matlab's Psychtoolbox[3]. The paradigm was administered using a block-design structure where the four runs were randomly ordered across participants. Each run comprised 40 trials equally divided in task (8s duration) and rest (4s duration) condition, presented to the participants according to a pseudo-random sequence which did not allow more than two consecutive task or rest trials and two consecutive rest trials at the beginning of the run to avoid fatigue and lapse in attention, respectively. The inter-trial-interval, during which a fixation cross was displayed in the middle of the screen, was set to 3s. During rest trials participants had

[1] `https://www.brainproducts.com`
[2] `https://www.cometasystems.com`
[3] `http://psychtoolbox.org`

Table 4.1. Demographic and clinical information of stroke participants. FMA-UE = Fugl-Meyer Assessment scale, upper extremity section, ranging from 0 (most affected) to 66 (least affected); MAS = Modified Ashworth Scale; NIHSS = National Institute of Health Stroke Scale.

ID	Age	Gender	Handedness	Months from event	Type	Lesion type	Lesion side	FMA-UE	NIHSS
P1	76	M	right	3	subacute	ischemic	left	51	1
P2	73	M	right	13	chronic	ischemic	left	63	3
P3	59	M	right	5	subacute	hemorrhagic	left	23	4
P4	75	F	right	3	subacute	ischemic	right	62	4
P5	53	F	right	4	subacute	hemorrhagic	left	57	3
P6	21	F	right	3	subacute	hemorrhagic	right	54	2
P7	55	M	left	5	subacute	hemorrhagic	right	52	0
P8	40	F	right	11	chronic	hemorrhagic	right	58	0
P9	24	F	right	8	chronic	ischemic	left	57	2
P10	51	M	right	4	subacute	hemorrhagic	left	26	3
P11	60	M	right	2	subacute	ischemic	left	42	2
P12	59	M	right	3	subacute	ischemic	right	48	4

to stay relaxed for 4s, whereas task trials began with 4s of preparatory period, after which a go stimulus occurred, and the participant had to perform the task for 4s (Figure 4.1). Participants were instructed to perform the task as fast as they could and to hold it at 15% of Maximum Voluntary Contraction (MVC) of the target muscle until the end of the trial (the experimenter guided the participants via online visualization of EMG traces). MVCs were recorded for each muscle at the beginning of the experiment for 5s and computed right after for the target muscles (ED and FD of both sides). Stroke participants attempted the movements with their affected limb to the best of their own residual ability, following the same instructions.

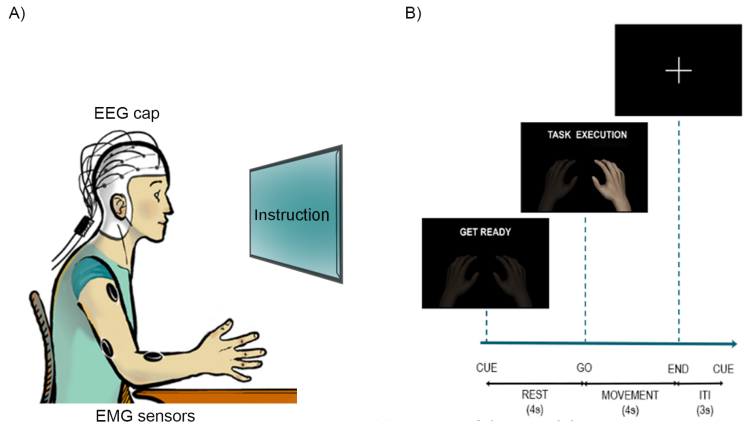

Figure 4.1. A) Schematic of the experimental setup: participants wore an EEG cap over the scalp and EMG sensors over the upper limbs, they watched a screen placed 1m in front of them on which a cue provided information on when to perform/attempt the movement. B) Timeline of the experiment for task trials with instructions provided to the participants on the screen, ITI: inter-trial-interval

4.2.3 Pre-processing

EEG data were band-pass filtered 3—60Hz whereas EMG signals were down-sampled to 1000Hz and band-pass filtered 3—500Hz. A notch filter at 50Hz was applied to remove power-line artifacts on both signals, task trials were segmented in 8s epochs from the cue onset, while rest trials were segmented in 4s epochs from the cue onset. A subset of EEG channels over the sensorimotor area (FC5, FC3, FC1, FCz, FC2, FC4, FC6, C5, C3, C1, Cz, C2, C4, C6, CP5, CP3, CP1, CPz, CP2, CP4, CP6, P5, P3, P1, Pz, P2, P4, P6) was considered for the purposes of this study. Indeed, with the ultimate aim of successful online control, a low number of electrodes is desirable to improve the usability of the system, while the localization of the EEG electrodes over the sensorimotor areas ensures the use of physiologic features for movement detection. The epochs extracted from the trials and related to the subset of channels were then checked for compliance to the instruction and presence of artifacts in the EEG and EMG signals. All the trials labeled as "Rest" in which participants moved, or trials labeled as "Task" where subjects missed the instruction and did not perform the task were identified as non-compliant and removed from the analysis. Regarding the artifacts management, two different criteria for the identification of artifacts were adopted in EEG and EMG signals. The EEG signals exceeding in absolute value the threshold of 100μV were considered as artifactual. If artifacts were detected in more than one channel the trial was rejected; otherwise a spherical interpolation was performed to replace the noisy channel with a weighted average of its neighbors. A semi-automatic approach was used to detect the artifacts in the EMG signals: a statistical criterion based on the comparison between the EMG characteristics [25] of each trial and the

median EMG characteristics of all trials (reference characteristic) was applied separately for task and rest condition. Once the EMG artifacts were detected by the statistical criterion, trials were visually inspected and validated for rejection.

EEG channels were interpolated due to presence of artifacts on average in 1% of trials for the movements performed by healthy participants. No channels were interpolated for the movements performed with the unaffected hand by stroke participants, whereas one EEG channel was interpolated on average in 1% of trials for the movement attempted with the affected hand. One stroke participant was excluded from Ext movements analysis due to the rejection of more than 50% of the trials (n = 11 for Ext movements analysis in stroke participants). After rejection of non-compliant and artefactual trials, the number of trials for healthy participants was on average 18.63 and 18.58 in task and rest condition, respectively. For stroke participants, on average 17.74 task trials and 17.91 rest trials were considered for the following analyses.

Pre-processing of EEG data was computed by means of Vision Analyzer 1.05 software (Brain Products GmbH, Gilching, Germany) while all the other steps described above were performed using custom codes developed in Matlab R2019a (The MathWorks, Inc., Natick, Massachusetts, USA).

4.2.4 EMG onset detection

The EMG data of the target muscle (ED for Ext movements and FD for Grasp movements) have been processed to obtain the EMG onset for each task trial. The continuous raw EMG data were band-pass filtered in the range 30—300Hz and a Teager–Kaiser energy operator was applied to improve Signal to Noise Ratio and minimize erroneous EMG onset detection [26]. Signals were rectified and low pass filtered at 50Hz. Then, EMG data were segmented in the 8s-task trials and the EMG onsets were identified applying the Hodges e Bui algorithm [27] on the EMG envelope of each task trial. Results were validated by visual inspection.

4.2.5 CMC offline analysis

After the EEG/EMG preprocessing, an offline analysis was conducted with the following aims to: i) identify the characteristic frequency of EEG-EMG coupling in beta band (13—30)Hz for each EEG-EMG pair; ii) select the most powerful CMC features in discriminating each movement from rest and iii) assess offline the performances of CMC-based approach in movements detection against rest.

The data used for each participant in the offline analysis referred to a time interval of 1s-length equal to the window [5—6]s in the task trials and [2—3]s in the rest trials. For those two intervals, the cortico-muscular coupling between EEG signal and the rectified EMG signal [28] was computed in the range 0—60Hz as in Study I [1].

CMC characteristic frequency extraction

In this study, only the beta band (13—30)Hz was considered as frequency band of interest, since previous studies identified it as the typical band for CMC [1], [29]. The CMC across trials was computed using 1s-Hann windows with no overlap and the characteristic frequency for each EEG-EMG pair was extracted, as the frequency showing the highest CMC value in the beta band range during task trials (see Study 1 paragraph 1.2.3-Characteristic frequencies). The computation was repeated for each movement and each participant. The single-trial CMC values at the characteristic frequency were thus considered in the further analyses as feature space. Single-trial CMC values were computed using the Welch periodogram with segments of 250ms, 50% of overlap and tapered by means of the Hann window.

Feature selection

Since the number of features used for the classification impacts on the computational cost and the number of physical electrodes required to collect the data, the feature selection approach was used to choose two EEG-EMG pairs to be considered in the analysis. The original feature space extracted as described in the paragraph above was reduced by considering only the EEG-EMG pairs characterized by the EMG channel over the target muscle (ED for Ext movements, FD for Grasp movements) and by the EEG channels placed over the sensorimotor strip of the hemisphere contralateral to the hand involved in the task (ipsilesional hemisphere for the movement attempted with the paretic hand of stroke participants). Feature selection was performed by ranking the remained CMC features according to their discriminant power by Fisher criterion [30] and selecting the two most discriminant ones. This allowed to reduce the computational cost and achieve real-time movement detection.

For each movement and participant, the feature space was reduced to a 2-dimensional feature space, consisting of 40 observations (20 trials x 2 conditions, i.e. task and rest).

Binary classifier training

A 10-iteration cross-validation approach was used for the offline detection of each movement vs rest in both healthy and stroke participants. In each iteration, the 80% of task and rest observations were used as training set, whereas the remaining 20% were used as testing set. A Support Vector Machine (SVM) classifier with a linear kernel was used as classification model on the reduced features space. If the difference between the number of task and rest trials (after rejection of artefactual or non-compliant trials) was equal or higher than three, the two classes were balanced randomly selecting the same number of observations. The offline performances were assessed using the following classification metrics: Area Under the receiver operating characteristic Curve (AUC), accuracy, sensitivity and specificity [31], [32].

4.2.6 CMC pseudo-online analysis

The pseudo-online analysis was conducted using a sliding window approach mimicking the data reading from the temporary buffer of the amplifier used in the online acquisition of biological signals. I considered sliding windows of 1 second duration updated along the trial of a certain number of samples (shift parameter) to be varied in the study. The selected shifts were: 125ms, 250ms and 500ms. For each participant, movement and window in a trial, single-trial CMC values in beta band were computed for the two EEG-EMG pairs selected in the offline analysis (paragraph 4.2.5-Feature selection). The CMC trend along the trial duration was then analyzed for the different shift values in the healthy participants with the aim to identify the best parameters to be used in the future online analyses. The pseudo-online analysis for stroke participants was conducted only for the best shift value identified in the analysis on healthy participants.

Identification of best shift value in data from healthy participants

In order to identify the best shift value to be used in the sliding window approach for CMC computation, the movement onset from CMC trends along trial (in brief CMC onset) was extracted and compared with the one extracted from EMG signal (in brief EMG onset), considered as the temporal reference for the beginning of the movement execution. The CMC onset was identified with a double-threshold criterion: the statistical threshold (95th percentile) was extracted from the distribution built considering all the CMC values of rest trials and the CMC onset was identified as the time point in which CMC values during task trials were above the statistical threshold in a temporal window equal or longer than 500ms. The CMC onset was thus computed for each participant, movement type, shift and trial considering the CMC values of the EEG-EMG pair with the best CMC feature according to Fisher criterion.

For each trial, on the basis of the comparison between the EMG onset and the CMC onset the following cases were identified:

- True Detection (TD) if CMC onset was delayed with respect to the EMG onset
- False Detection (FD) if CMC onset was anticipated with respect to the EMG onset
- No Detection (ND) if no CMC onset was detected in presence of an EMG onset

The occurrence of TD, ND and FD across trials normalized for the total number of trials was computed for each participant, movement type and shift. These three performance parameters were flanked by a fourth one, the Mean Delay (MD) obtained as the temporal difference (in seconds) between the CMC onset

and EMG onset only in TD case.

To identify the best value for shift parameter maximizing both accuracy and speed in CMC-based movement detection in the four movements analyzed, two 2-way repeated measures ANOVA (rmANOVA) were computed considering as within main factors the MOVEMENT (4 levels: ExtL, ExtR, GraspL, GraspR) and the SHIFT (3 levels: 125, 250, 500ms) and as dependent variables the TD and the MD parameters, separately. ND and FD were not included in the statistical analysis due to their low rates obtained in almost all the participants. The statistical significance level for all tests was set to 0.05 and the Duncan's post-hoc test was performed to assess differences among the levels of the within factors. A shift value of 125ms resulted to achieve the highest performances (highest TD and lowest MD - see Results paragraph 4.3.2) and was therefore used for further analyses.

Movement classification in healthy participants

To test the ability of CMC features in discriminating movements from rest condition in real-time, a single-subject pseudo-online validation was firstly performed in healthy participants. The same feature space used in the offline approach (see paragraph 4.2.5) was adopted for the pseudo-online analysis. An adaptation of the Leave-One-Out Cross Validation was used to train the classification model and evaluate the performances in task trials with the pseudo-online approach. For each movement and participant, N different SVM classifiers (where N is the number of task trials) were trained excluding one task trial at a time from the training phase (training set observations = $N_{tot-trial}$ – 1) and tested on the excluded trial divided in 57 consecutive windows of 1s with 125ms of overlap (total number of observations in testing phase equal to 57 for each leave-one-out iteration).

The pseudo-online classification performances were evaluated considering as:

- True Positive (TP) when at least M consecutive sliding windows after the EMG onset of a task trial were predicted as task condition.
- False Positive (FP) when at least M consecutive sliding windows before the EMG onset of a task trial were predicted as task condition.
- False Negative (FN) when no M consecutive windows were predicted as task condition.

Here, the M parameter is the accumulation factor for which three different values (1 – no accumulation, 2 and 3 windows) were tested to identify the best trade-off between classification accuracy and speed. The following metrics were computed according to the number M of windows to be accumulated before a final movement detection:

$$Hit\ rate = \frac{TP}{N} \tag{4.1}$$

$$False\ Positive\ Rate\ (FPR) = \frac{FP}{N} \tag{4.2}$$

$$False\ Negative\ Rate\ (FNR) = \frac{FN}{N} \tag{4.3}$$

$$Mean\ Delay\ (MD) = T_{M_{windows}} - EMG_{onset} \tag{4.4}$$

where $T_{M_{windows}}$ is the time window after which M consecutive task predictions (windows) have been accumulated in TP trials and N is the number of task trials.

To evaluate the differences in the above metrics among the number M of consecutive windows, four 1-way rmANOVA were performed using as within main factor M (3 levels: M=1, M=2, M=3) and as dependent variable the hit rate, the FPR, the FNR and the mean delay, separately. The Duncan's post-hoc analysis was held to assess differences among the different levels of the within factor and the significant level was set to 0.05.

Movement classification in stroke participants

To assess whether the results obtained in healthy participants could be confirmed for movements performed/attempted by stroke patients, the same pseudo-online analysis described in the above paragraph was performed on data from 12 stroke participants for each movement type. In particular, the CMC computation was performed with a sliding window approach considering windows of 1 second duration and a shift of 125ms. Classification performances expressed in terms of hit rate, FPR and MD were firstly evaluated in the stroke participants group and then compared between movements performed with the affected and the unaffected hand by a paired t-test, considering only the 11 stroke participants analyzed during both Ext and Grasp movements. The significance level for all tests was set to 0.05. FNR was evaluated but not included in the comparison due to the low values obtained in all participants and movement types.

4.3 Results

4.3.1 CMC offline analysis

Offline classification performances of the movement versus rest classifier based on two CMC features are shown in Tables 4.2 and 4.3 for healthy and stroke participants respectively. Average AUC across healthy participants were ranging from 0.98 to 1.00, whereas slightly lower performances were achieved in stroke participants with AUC ranging from 0.93 to 0.98.

Table 4.2. Offline task-vs-rest classification performances reported as mean ± standard error across 13 healthy participants. ExtR: finger extension with the right hand; ExtL: finger extension with the left hand; GraspR: grasping with the right hand; GraspL: grasping with the left hand.

Task	AUC	Accuracy	Sensitivity	Specificity
ExtL	0.98±0.01	0.93±0.02	0.90±0.02	0.97±0.01
ExtR	0.99±0.004	0.94±0.02	0.91±0.02	0.97±0.01
GraspL	1.00±0.002	0.97±0.01	0.94±0.01	0.99±0.01
GraspR	0.99±0.004	0.95±0.01	0.91±0.02	0.99±0.01

Table 4.3. Offline task-vs-rest classification performances reported as mean ± standard error across 11 stroke participants for Ext movements and 12 stroke participants for Grasp movements. ExtUH: finger extension with the unaffected hand; ExtAH: finger extension with the affected hand; GraspUH: grasping with the unaffected hand; GraspAH: grasping with the affected hand.

Task	AUC	Accuracy	Sensitivity	Specificity
ExtUH	0.93±0.03	0.88±0.03	0.83±0.05	0.93±0.02
ExtAH	0.98±0.01	0.92±0.03	0.88±0.04	0.96±0.02
GraspUH	0.95±0.03	0.91±0.03	0.84±0.06	0.99±0.01
GraspAH	0.95±0.03	0.90±0.03	0.85±0.05	0.96±0.01

4.3.2 CMC pseudo-online analysis

Identification of best shift value in data from healthy participants

Figure 4.2 shows how the shift value to be used in the sliding window approach for CMC computation affects the shape of CMC trend along the trial and the timing in CMC-based movement onset detection, considering a representative healthy participant during movements performed with the left hand (similar results were obtained for the right-hand movements). Independently of the shift value, it is worthy of note how the CMC trend accurately tracks the muscular activation as revealed by the EMG signal recorded at the target muscle (ED for Ext movement, FD for Grasp movement), superimposed in each graph (Figure 4.2 A and 4.2 B, left). CMC resulted as almost null before the EMG onset while it showed an increase and then a plateau around the holding phase of the movement execution. The higher the shift value (updating factor of each sliding window), the more discontinuous the CMC trend appears, as expected since it is obtained for a reduced number of samples. The qualitative comparison between EMG onset and CMC onset in the trends reported in Figure 4.2 shows how in this representative subject the CMC onset was always delayed with

respect to EMG onset and the delay increased with the increase of shift values in both Ext and Grasp conditions. A similar behavior was observed in the other healthy participants. Overall, pie charts (Figure 4.2 A and 4.2 B, right), reporting the percentages of TD, FD and ND obtained in average across all the healthy participants, show how CMC managed to detect the movement onsets in all movement tasks. Indeed, the averaged percentage of TD across participants (∼88%) considerably overcame the percentages of FD (∼12%) and ND (<1%). FD parameter was the most affected by changes in the shift values, increasing with the increase of the latter (from 9% to 17% in ExtL and from 7% to 15% in GraspL).

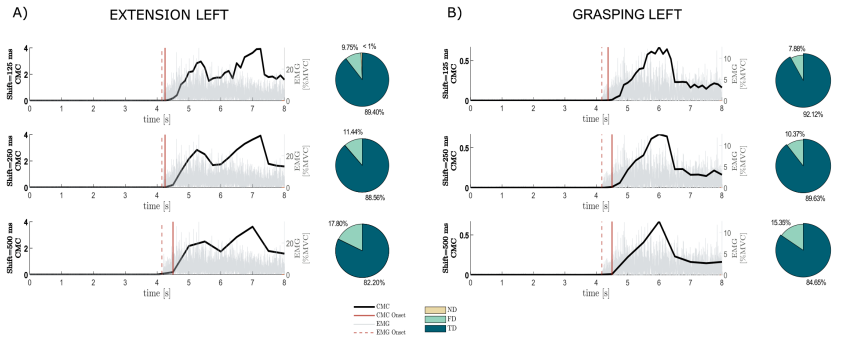

Figure 4.2. Impact of the shift value used in the sliding-window approach on the detection of the movement onset based on CMC (CMC onset). The average CMC and EMG trends across trials, considering the first EEG-EMG pair identified by Fisher criterion and the target muscle respectively, were reported along trial duration for different shift values separately for extension and grasping of the left hand, (A) and (B) right panel respectively, in one representative healthy participant (similar results were obtained for right-hand movements). Dashed vertical line represents movement onset detected from EMG (EMG onset), whereas continuous vertical line stays for detected CMC onset. Each graph is flanked by a pie chart reporting the percentages of No Detection (ND), False Detection (FD) and True Detection (TD) obtained on average across 13 healthy participants for the different shift values in the two motor tasks shown [8].

The 2-way rmANOVA performed on both TD and MD parameters revealed the SHIFT factor as the only significant effect (TD: $F(2,24)=30.99$, $p<0.01$; MD: $F(2,24)=13.13$, $p<0.01$). Duncan's post-hoc test applied on TD highlighted a higher value when using the lowest updating factor (125ms) compared to the others. A significant difference between 250ms and 500ms was also observed. Post-hoc tests applied to MD revealed a significantly higher delay for a shift of 500ms with respect to other shifts tested. No differences were found between shift of 125ms and 250ms for MD.
Figure 4.3 reports the trends of the distributions of TD (panel A) and MD (panel

B) obtained varying the shift values in the sliding window approach for the four movements separately. The lack of significance of the effect MOVEMENT x SHIFT underlines how the shift affected TD and MD parameters independently from the movement type.

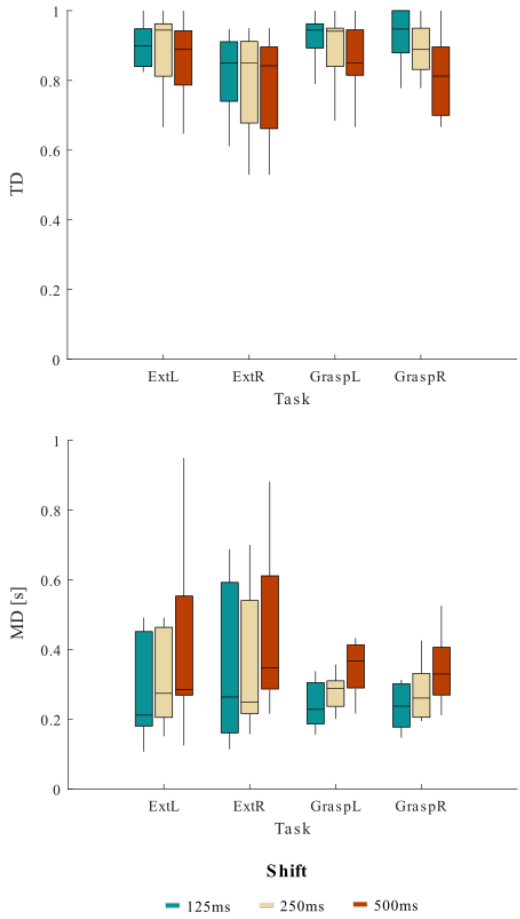

Figure 4.3. Distribution (boxplots) of (A) True Detection (TD) and (B) Mean Delay (MD) at the various shift values across 13 healthy participants, separately for the four motor tasks (ExtL, ExtR, GraspL, GraspR) [8].

Given the results obtained from the statistical analysis, a shift value of 125ms to update the sliding windows used to compute the CMC was chosen

for the pseudo-online movement classification analysis. Using 125ms of shift resulted on average in TD higher than 82.87% and MD lower than 0.42s for the four movements tasks.

Movement classification in healthy participants

Figure 4.4 reports the results of the pseudo-online movement classification performed 1s window at a time every 125ms in each testing trial, for a representative healthy participant (same as Figure 4.2) during extension and grasping of the left hand. It is worth noting how the classifier correctly classified as rest almost all the windows preceding the EMG onset and as movement all the windows succeeding the EMG onset in all the trials. Some misclassifications were found in the movement phase of very few trials where the movement is erroneously classified as rest.

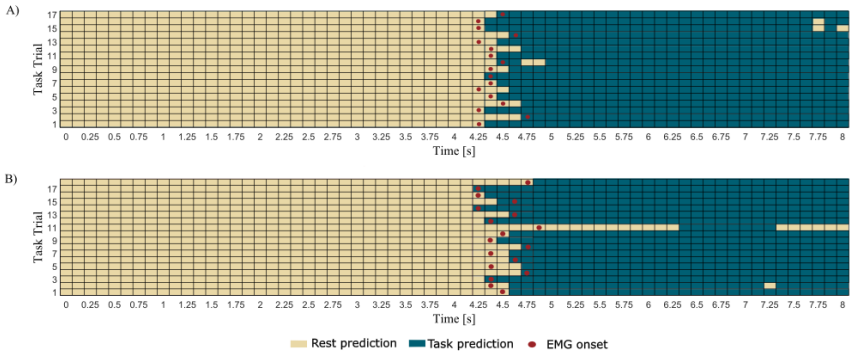

Figure 4.4. Results of the pseudo-online classification (task vs rest) performed for all the 57 windows in which each trial was epoched for a representative healthy participant (same as Figure 4.2) during A) extension and B) grasping of left hand (similar results were obtained for right-hand movements). Rectangles represent the 1s windows processed by the trained classifier one at a time every 125ms. Windows predicted by the classifier as rest condition present light color, whereas windows predicted as task condition present dark color. The red dots indicate the first window including the EMG onset (i.e. which ends 125ms after the EMG onset) [8].

Table 4.4 summarizes the pseudo-online classification performances across the healthy participants obtained for the different number M of consecutive sliding windows tested as accumulation before a final classification decision was taken. The FNR was null in all four movements, with the exception for GraspR where a false negative (FN) occurred for one subject in one trial when M was equal to 2 or 3. For all the movements, it was obtained on average a hit rate above 88%, with a FPR ranging from 0 to 12% and a delay in the movement detection from 320 to 680ms according to the value selected for

the parameter M. Moreover, the results of the rmANOVA showed how the parameter M significantly affected the classification performances (hit rate, FPR and Mean Delay) in both Ext and Grasp conditions, except for hit rate and FPR in Grasp. As expected, for all the movements, the increasing M led to improved classification accuracy (increase of hit rate and decrease of FPR) but also to an increase of the delay in the detection of movement onset. In particular, the post-hoc tests of rmANOVA performed on each classification parameter showed a significant difference between M=1 and M=3 windows and M=1 and M=2 windows. No significant differences were observed in the hit rate and the FPR achieved with M=2 and M=3 windows, whereas such difference resulted to be present for the Mean Delay. Choosing a number M of windows equal to 2 as accumulation before a final movement detection allowed to achieve on average a hit rate higher than 90%, a FPR lower than 10%, and a Mean Delay in the range 470ms and 530ms. Such accumulation factor resulted to be the most promising based on healthy participants' data.

Table 4.4. Pseudo-online classification performances reported as mean ± standard error across 13 healthy participants for each movement task. Performances are shown for the different number M of consecutive sliding windows tested as accumulation before the final movement detection. The fourth column of each parameter reports the p-value of the rmANOVA considering M as within factor. Asterisks (*) indicate significant difference p<0.01, — ANOVA test not applicable.

	Hit Rate				FPR			
Task	**M=1**	**M=2**	**M=3**	**p**	**M=1**	**M=2**	**M=3**	**p**
ExtL	0.89 (±0.04)	0.92 (±0.03)	0.93 (±0.03)	**<0.01***	0.11 (±0.04)	0.08 (±0.03)	0.07 (±0.03)	**<0.01***
ExtR	0.88 (±0.03)	0.90 (±0.03)	0.91 (±0.03)	**<0.01***	0.12 (±0.03)	0.10 (±0.03)	0.09 (±0.03)	**<0.01***
GraspL	0.99 (±0.01)	1.00 (±0.00)	1.00 (±0.00)	—	0.01 (±0.01)	0.00 (±0.00)	0.00 (±0.00)	—
GraspR	0.96 (±0.02)	0.97 (±0.02)	0.97 (±0.02)	0.75	0.04 (±0.02)	0.03 (±0.02)	0.03 (±0.02)	0.14
	FNR				**Mean Delay (s)**			
Task	**M=1**	**M=2**	**M=3**	**p**	**M=1**	**M=2**	**M=3**	**p**
ExtL	0.00 (±0.00)	0.00 (±0.00)	0.00 (±0.00)	—	0.37 (±0.05)	0.53 (±0.06)	0.68 (±0.06)	**<0.01***
ExtR	0.00 (±0.00)	0.00 (±0.00)	0.00 (±0.00)	—	0.34 (±0.04)	0.50 (±0.04)	0.65 (±0.05)	**<0.01***
GraspL	0.00 (±0.00)	0.00 (±0.00)	0.00 (±0.00)	—	0.32 (±0.03)	0.47 (±0.03)	0.61 (±0.03)	**<0.01***
GraspR	0.00 (±0.00)	0.004 (±0.004)	0.004 (±0.004)	—	0.36 (±0.03)	0.50 (±0.03)	0.67 (±0.04)	**<0.01***

Comparing the classification performances obtained with M=2 between the left and the right-hand movements by means of a paired t-test (α=0.05), no significant differences were observed for both Ext (p = 0.56) and Grasp (p=0.12) movement.

Movement classification in stroke participants

Table 4.5 reports the metrics obtained on varying M parameter with the pseudo-online approach in 12 stroke participants for all the movement types. The four 1-way rmANOVAs performed on the accumulation factor M confirmed what obtained in healthy participants. The FPR increased with increasing M and the post-hoc test revealed significant differences between M=1 and M=2 as well as between M=1 and M=3 when the movement was attempted with the paretic hand. A significant difference between the FPR with M=2 and 3 resulted for ExtUH, whereas no significant difference was shown in the FPR for GraspUH. The statistical analysis revealed that in stroke participants the M parameter affected the hit rate only for GraspAH with significant differences between M=1 and M=2 and M=1 and M=3 (no difference was found between the hit rate obtained with M=2 and M=3). As with healthy participants, the higher the M parameter, the greater the Mean Delay. False negatives were more frequent in stroke with respect to healthy participants, in particular for higher M. However, FNR did not exceed 4%.

Table 4.5. Pseudo-online classification performances reported as mean ± standard error across 11 stroke participants for Ext movements and 12 stroke participants for Grasp movements. Performances are obtained considering different number M of consecutive sliding windows tested as accumulation before a final classification decision. The fourth column of each parameter reports the p-value of the rmANOVA considering M as within factor. Asterisks (*) indicate significant difference $p<0.01$, — ANOVA test not applicable.

	Hit Rate				FPR			
Task	**M=1**	**M=2**	**M=3**	**p**	**M=1**	**M=2**	**M=3**	**p**
ExtUH	0.81 (±0.05)	0.82 (±0.05)	0.83 (±0.05)	0.75	0.19 (±0.05)	0.16 (±0.05)	0.13 (±0.04)	**0.015***
ExtAH	0.84 (±0.04)	0.86 (±0.04)	0.87 (±0.04)	0.09	0.15 (±0.04)	0.13 (±0.03)	0.11 (±0.03)	**0.05***
GraspUH	0.92 (±0.04)	0.93 (±0.03)	0.94 (±0.03)	0.25	0.06 (±0.03)	0.05 (±0.02)	0.04 (±0.02)	0.23
GraspAH	0.68 (±0.07)	0.74 (±0.05)	0.79 (±0.05)	**<0.01***	0.32 (±0.07)	0.26 (±0.05)	0.21 (±0.05)	**<0.01***
	FNR				**Mean Delay (s)**			
Task	**M=1**	**M=2**	**M=3**	**p**	**M=1**	**M=2**	**M=3**	**p**
ExtUH	0.00 (±0.00)	0.02 (±0.02)	0.04 (±0.02)	—	0.52 (±0.10)	0.66 (±0.10)	0.88 (±0.13)	**<0.01***
ExtAH	0.01 (±0.01)	0.01 (±0.01)	0.02 (±0.01)	—	0.44 (±0.05)	0.62 (±0.07)	0.77 (±0.07)	**<0.01***
GraspUH	0.01 (±0.01)	0.01 (±0.01)	0.02 (±0.01)	—	0.39 (±0.04)	0.54 (±0.04)	0.70 (±0.05)	**<0.01***
GraspAH	0.00 (±0.00)	0.00 (±0.00)	0.004 (±0.004)	—	0.34 (±0.03)	0.50 (±0.03)	0.68 (±0.05)	**<0.01***

Given the results obtained in both healthy and stroke participants, to avoid false positives while maintaining a good timing, the best accumulation factor resulted to be M=2.

As expected, performances were reduced with respect to those obtained from healthy participants for both movements performed with AH and UH. In Ext condition, for both sides, hit rate was around 84%, the FPR was around 15% while the delay in movement detection was around 580ms. Differences in terms of classification performances between AH and UH were investigated by means of a statistical analysis whose results are reported in Figure 4.5. A significant difference was found between AH and UH in Grasp condition only for hit rate and FPR (Figure 4.5 A and B) highlighting how the detection of the grasping movement performed with the affected hand is significantly more difficult with respect to the same movement performed with the unaffected hand but also to the extension movement with both AH and UH. Indeed, in Grasp condition the differences between AH and UH were bigger with respect to Ext movement, with a hit rate significantly lower in Grasp than in Ext for AH (paired t-test, p=0.046). Whereas the Mean Delay was approximately the same for AH and UH (Figure 4.5C).

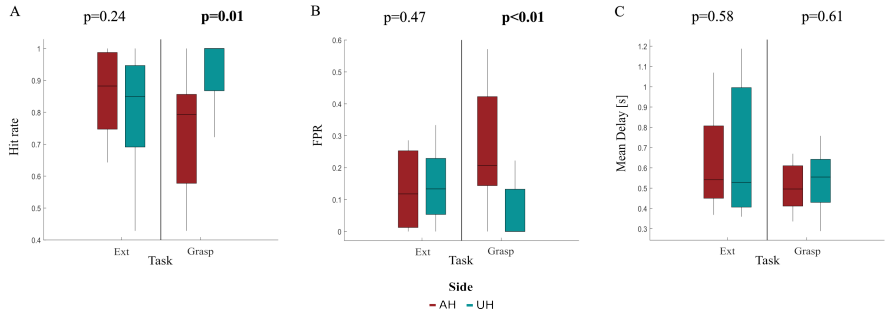

Figure 4.5. Boxplot diagrams reporting the distributions of A) the Hit rate, B) the FPR and C) the Mean Delay in 11 stroke participants as results of the pseudo-online classification using M=2 sliding windows as accumulation before a final classification decision. Performances are reported separately for Ext and Grasp and compared between AH and UH by means of a paired t-test (α=0.05) [8].

4.4 Discussion

In this study, it was shown that the cortico-muscular coupling between brain and muscle activity could discriminate in real-time different hand movements from rest condition in both healthy and stroke participants. The pseudo-online analysis performed on healthy and stroke participants provided information on the parameters representing the best trade-off between classification accuracy and speed when translating CMC computation and its task vs rest classification from offline to online domain. The testing of such parameters on a stroke participants dataset assessed the feasibility of a CMC-based movement detection

in a population of stroke subjects with residual arm activity.

The offline classification performances (Tables 4.2 and 4.3) confirmed the validity of the features extraction and classification approach tested in the Study 1 on healthy subjects, also in stroke patients. The high performances obtained in that study using the entire set of features (CMC values from all possible EEG-EMG pairs), have been confirmed in this work using as features for movement detection CMC values from only few EEG-EMG electrodes, showing its potential applicability in a clinical setting.

The pseudo-online analysis performed on the shift value showed how the updating factor of CMC computation affects the ability of the CMC to detect the movement. Indeed, it affected both the ability to detect the movement onset (True Detection, TD) and the time to detect it (Mean Delay, MD). Moreover, the pseudo-online classification approach showed how the number of predictions to be accumulated before a given final classification decision affected the pseudo-online classification performance. Classification performance increased according to the number of windows accumulated, and the time to detect the movement with respect to the EMG onset also increased according to it.

One of the main challenges faced by BCI technology is to improve speed and accuracy [3]–[7] and achieve the reliability necessary for real-word applications [33]. For this reason, identifying the parameters that allow the best trade-off between classification performances and speed is crucial. Over the past decades, many studies have explored feature extraction and classification approaches to improve the accuracy [34], raise the number of commands [35], increase the information transfer rate and reduce the calibration time [36], [37]. P300-based speller and steady-state visual evoked potential-based BCIs have mainly taken advantages from those methodological improvements [35], [38] in order to avoid patient frustration caused by false and delayed detections [39]. However, also in the context of BCIs for rehabilitation, it is crucial to provide an immediate feedback, contingent with the user's movement intention, in order to re-establish the contingency between cortical activity related to the attempted or imagined movement and the feedback. Indeed, this stimulates the neuroplasticity that leads to motor recovery [40], [41]. In this application, performance improvements were pursued in several ways, e.g. by combining different features such as lateralized readiness potential and event-related desynchronization [4], refining well-established algorithms of feature extraction and classification and combining them in an innovative way [42] or investigating which parameters returned the best performance in terms of both accuracy and timing cost in the ERD/ERS classification [7].

Although great efforts have been devoted to the optimization of EEG-based BCI, the optimization for the real-time CMC computation and classification has not been investigated yet.

Thanks to the results of this study, it was assessed that computing the single-trial CMC every 125ms and accumulating 2 predictions before a final classification decision allows to achieve good performance (hit rate on average equal to 95% and 84%, FPR on average equal to 5% and 15% for healthy and stroke participants, respectively) and timing (mean delay on average equal to 0.5s and 0.58s for healthy and stroke participants, respectively) during two different motor tasks. Meanwhile almost no false negative detections were obtained. The classification accuracy achieved in the present work is higher than that reported in the two available studies using CMC for online control of robotic orthosis in a rehabilitation context [22], [43]. Comparable performances were obtained in [22] when an approach based on statistical correlation is used instead of the classical CMC algorithm. The higher performances obtained in this work could be due to the application of two processing steps helping to manage the variability in CMC spectral and topographical properties among patients: i) computation of CMC characteristic frequency in the two EEG-EMG pairs selected for each patient and movement which takes into account inter-patients differences in CMC frequency peak; ii) application of a feature selection algorithm allowing to select the best EEG-EMG pairs to detect movement, specifically for each patient. No direct comparison can be made between this work and the above-mentioned studies on timing, since they used a different experimental paradigm where the CMC was computed online in a predetermined time interval with respect to the cue and thus the feedback was sent to the patient several seconds after the movement attempt. Hence, this study is the first among those published that analyzed the ability of the CMC in detecting the movement and showed that potentially a CMC-based BCI could send a contingent feedback to the patient right after the attempt.

Moreover, using CMC values as features to discriminate movements from rest condition allows to obtain higher pseudo-online classification performance in stroke patients with respect to previous studies on rehabilitative BCIs based on EEG features only, such as movement related cortical potentials [24] and sensorimotor rhythms in alpha and beta bands [44], detected during movement attempts.
Beside the main purpose of the presented hBCI (i.e. promoting upper limb motor recovery and avoiding the reinforcement of abnormal muscular activity), its superiority in terms of classification performance can guarantee feedback consistency to patients during training sessions, presumably increasing patients' satisfaction and motivation towards the ultimate aim, that is a favorable recovery. It is worthy of note that such classification performances are obtained using only fewer features (EEG and EMG channels) compared to those used in previous EEG-based BCI systems during the attempt of motor tasks [19], [45]. Thus, this approach appears promising in terms of system usability (computational time, comfort) and set up time, meeting the needs of BCI usage in a clinical context.

Regarding the timing achieved in the classification decision with the pa-

rameters selected by this analysis, CMC features were able to provide a fast classification in stroke patients which ensures not only to exploit and train central-to-peripheral communication [43], but also to send ecological feedback to the patient right after the onset of the movement attempt (a feedback that is congruent in timing and content with the exercise setting), favoring an effective motor re-learning. Comparing classification speed with previous works on rehabilitative BCIs during movement attempts, comparable [45] or better ([19], 3.5-5s to deliver feedback) results were obtained with respect to EEG-based approaches.

Furthermore, similar to what reported in Study 1 on healthy subjects, the extension task was easier to detect by means of CMC features also in stroke patients.

Despite the promising results obtained on both healthy and stroke participants by applying the CMC-based approach in movements detection, the performances obtained by means of a pseudo-online approach should be confirmed by online experiments. In fact, the exclusion of both non-compliant and artefactual trials from the analysis before CMC computation might have mildly overestimated the classification performances since they were calculated on data with a higher signal-to-noise ratio. However, I am confident that such overestimation effect is limited since the number of trials rejected were around one/two trials out of the 20 requested per condition. In the online implementation of this approach, non-compliance will be manually checked by the therapist/experimenter who will start a new trial (request of movement attempt) only when the muscle activation level will be below the desired threshold or terminate the trial before the established duration if the patient is not performing the task (i.e., non-compliant trials should virtually never occur).

To the best of my knowledge, this is the first study that tested the ability of CMC features to detect in real-time movement attempts in stroke patients with particular focus on the best parameters to use in the computation to ensure an accurate and fast detection. The results obtained here stated the feasibility of CMC features as inputs of a h-BCI for upper limb motor rehabilitation and grounded the design of a novel non-invasive h-BCI in which the control feature is derived from a combined EEG and EMG connectivity pattern estimated during upper limb movement attempts, described in the next study.
The results obtained in this analysis were published in Frontiers in Human Neuroscience [8].

5. Study 5

Design and implementation of the h-BCI prototype

5.1 Background and Objectives

CMC features can be employed for the real-time detection of different hand movements in both healthy and stroke subjects. The best parameters to use for the online CMC computation were identified (see Study 4) [8] as so as the properties of the CMC pattern corresponding to physiological and pathological movements in stroke patients (see Study 2) [2]. Thus, such features are valuable inputs of a h-BCI able to re-establish impaired cortico-muscular coupling, achieving a good timing and accuracy crucial for patients' motor re-learning and motivation during the rehabilitation training.

Based on the evidence provided, an innovative h-BCI was implemented to support post-stroke upper limb rehabilitation, in which real-time decoding of CMC patterns during paretic hand movement attempts (e.g. finger extension) drives FES to support full movement execution. The device recognizes close-to-normal EEG-EMG coupling, taking into account both the CMC features to reinforce during the h-BCI training, and the ones to discourage to avoid the maladaptive movement abnormalities typical of post-stroke recovery [9]–[12], and initiates FES of the target muscle.

In the next paragraphs the h-BCI design process, paradigm, and the feasibility outcome of the interim analysis are described.

5.2 System Design

The h-BCI prototype was designed to rehabilitate upper-limb function based on brain-muscles communication. User-centred methodologies were used throughout the design phase; usability requirements were updated and refined during

each development and verification phase. Physicians and neurologists provided high-level clinical specifications that were then addressed for the technological implementation.
The h-BCI device has the following hardware components as shown in Figure 5.1:

1. an EEG and an EMG acquisition system used to record simultaneously brain and muscular activity:
   - BrainAmp EEG amplifiers (Brain Products GmbH, Germany[1]) with active electrodes
   - Wave Plus wireless EMG system and Pico EMG sensors (Cometa S.r.l., Italy[2]) capable to acquire the muscular activity of up to 16 muscles in bipolar fashion.
2. a laptop where the prototype's software runs.
3. a FES stimulator (RehaMOVE2 system - Hasomed GmbH, Germany[3]) used to deliver the stimulation to the patient. FIAB[4] fully gelled electrodes are used for neurostimulation.

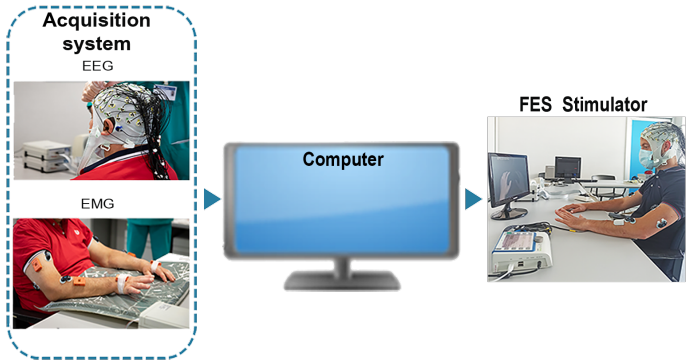

Figure 5.1. The h-BCI components: the acquisition system acquires the EEG and EMG signals through EEG active electrodes and EMG wireless sensors, and sends them to a computer where they are processed in real-time to detect a correct movement and trigger the FES stimulator to deliver the stimulation to the patient.

The h-BCI intervention consists of a screening session used to acquire data and identify the BCI control features, and several BCI training sessions in

[1] https://www.brainproducts.com
[2] https://www.cometasystems.com
[3] https://hasomed.de
[4] https://www.fiab.it/it/category.php?id=188

which patients control the h-BCI device, after a proper calibration. Figure 5.2 shows the steps of the intervention.

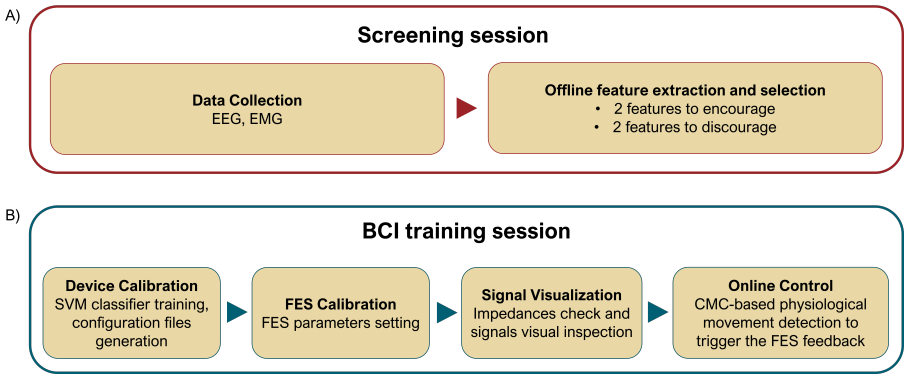

Figure 5.2. The h-BCI intervention - A) Screening session comprises data collection, feature extraction and selection of BCI control features. B) At the first BCI training session the device is calibrated, and during each session FES parameters are set, EEG and EMG signal are visually inspected and the online control of the device during rehabilitative exercises is performed.

Each patient has a dedicated folder named with his/her ID where all the data and information needed for the intervention are saved.

The steps of the h-BCI intervention are made possible by the building modules of the prototype which interact to each other: Acquisition and Feature extraction Modules, Calibration Module, FES Calibration Module, Control and FES Modules. The modularity the h-BCI system allows to have as much as possible the control over the operations performed, and to customize each module according to the rehabilitative needs.

The information collected and extracted in the screening session (Acquisition and Feature extraction Modules,) are managed by the a Graphical User Interface (Configuration GUI) to build the BCI classifier (Calibration Module) and to control in real-time the FES feedback (Control and FES Modules), after setting the FES parameters to use for the stimulation (FES Calibration Module). The h-BCI prototype operates in two domains: offline and in real-time. In the offline domain, each module works in open-loop and generates output files that are asynchronously used as inputs of the next module, whereas during the real-time control a synchronous communication is established between modules and they work in close-loop with the patient.

The core of the h-BCI prototype was developed in OpenViBE v.3.1.0[5] where

[5] `http://openvibe.inria.fr`

patient's EEG and EMG signals can be acquired, processed (offline and online) and the FES feedback can be delivered in real-time to the patient. OpenViBE is an open-source software platform dedicated to design, test and use BCIs in a modular way. In OpenViBE, new software modules can be added according to the users' needs. This is ensured thanks to the box concept, an elementary component in charge of a fraction of the whole processing pipeline, that allows users to develop reusable components, reduces development time, and helps to quickly extend functionalities [46].
Whereas the Feature extraction Module and the Configuration GUI were developed in Matlab 2020a. Detailed description of each module is given in the next paragraphs.

5.2.1 Acquisition Module

During screening session, the same experimental paradigm described in Study 4 is used to collect the data. Thus, EEG signals are recorded at 1kHz from the scalp with 61 active electrodes arranged according to an extension of 10-20 system (reference on left mastoid an ground on right mastoid); surface EMG data are recorded at 2kHz through Pico EMG sensors from 16 muscles of the upper limbs collected in bipolar fashion. Patients are asked to attempt the rehabilitative task with their paretic hand during Task trials (8s duration) and to rest during Rest trials (4s duration). The EEG and EMG data are recorded with the amplifiers' property software Vision Recorder (Brain Products GmbH, Germany) and EMG and Motion Tools (Cometa S.r.l., Italy) respectively, and saved in two different files which will be analyzed to configure the parameters of the BCI training sessions.

5.2.2 Feature extraction Module

Data recorded in the Acquisition Module are used as inputs of the Feature extraction Module. An ad-hoc pipeline was developed to process EEG and EMG data and to extract and select the CMC features to control the BCI. Figure 5.3 shows the block diagram with the inputs, the outputs and the operations performed in the Feature extraction Module.

Feature extraction

EMG signals are downsampled to 1kHz, EEG and EMG data are synchronized and merged in a unique dataset, which is saved in the patient's folder for the h-BCI calibration. EEG signals are band-pass filtered 3—60Hz, whereas EMG signals 3—500Hz with a 6th order Butterworth filter. A notch filter, 10th order IIR filter, at 50Hz is applied to remove power-line artifacts on both signals. Task trials are segmented in 8s epochs from the cue onset, while Rest trials are segmented in 4s epochs from the cue onset.

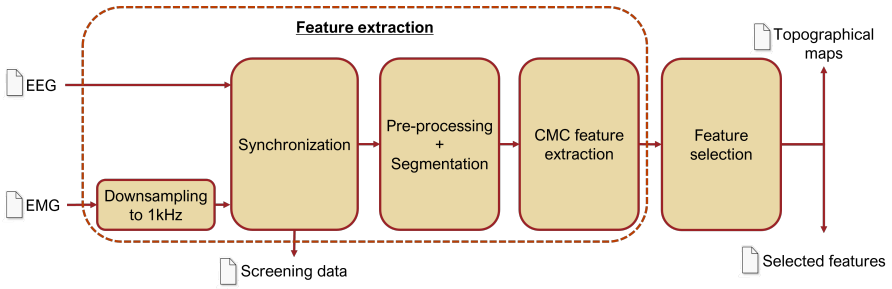

Figure 5.3. Block diagram of the processing steps performed in the Feature extraction Module, with details on the inputs imported and outputs generated.

A 1s-window (time interval [5-6]s for task trials and [2-3]s for rest trials) is extracted from each trial to compute the cortico-muscular coupling between EEG signal and the rectified EMG signal [28] in the range 0-60Hz as in Study 1.
The characteristic frequency for each EEG-EMG pair is extracted and the single-trial CMC values of all the EEG-EMG pairs at the characteristic frequency are considered as features space. The single-trial CMC computation is performed using a Welch periodogram with segments of 250ms, 50% of overlap and tapered by means of the Hann window, as in Study 4 paragraph 4.2.5-CMC characteristic frequency extraction.

Feature selection

Pursuing physiological muscular activation patterns means reinforcing the central communication to target muscles and avoiding pathological muscular activation typical of post-stroke recovery [9]–[12]. CMC has proven to be able to detect both physiological and pathological patterns (Studies 1 and 2). With this aim, a feature selection approach is used to reduce the feature space and choose the h-BCI control features. Two types of features are selected:

Features to encourage The 2 most discriminant and neurophysiologically relevant CMC features are selected to reinforce the natural motor control. The feature space is reduced by considering only the EEG-EMG pairs composed by the EMG channel over the target muscle and by the EEG channels placed over the sensorimotor area (Figure 5.4) of only the ipsilesional hemisphere (neurophysiologically relevant according to the rehabilitation approach). Feature selection is performed by ranking the remaining CMC features according to their discriminant power with Fisher criterion [30] and selecting the 2 most discriminant ones, as in Study 4.
Such features are then used to train the SVM classifier with linear kernel for the real-time discrimination of movement from rest condition.

Features to discourage Dysfunctional activation patterns during the rehabilitative task performed with the paretic side must be discouraged. In particular, co-activation of proximal and contralateral muscles could be possible substrates for compensatory strategies and mirror movements, and as shown in Study 2 they can be detected by CMC patterns. Thus, the following maladaptive changes are detected and monitored during the h-BCI intervention:

1. compensatory proximal muscles activity movements (compensatory movements)

2. abnormal recruitment of healthy side muscles (mirror movements)

through two EEG-EMG pairs, one for each type of dysfunctional pattern, among the EEG signals over the sensorimotor area (Figure 5.4) and the EMG signals of the proximal muscles of the affected limb, and the distal muscles of the unaffected limb, respectively. Such pairs were identified as dysfunctional brain-muscle connections according to a double-threshold statistical criterion.

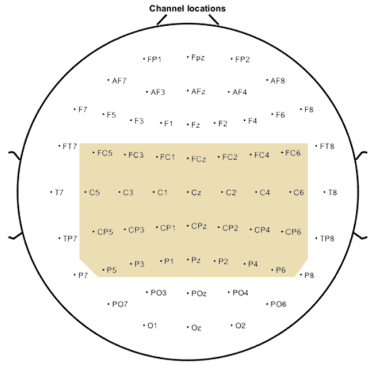

Figure 5.4. 28 out of 61 EEG electrodes over the sensorimotor area considered in the feature selection.

As output of the feature selection, the EEG-EMG pairs selected (the 2 features to encourage and the up to 2 features to discourage) and the corresponding characteristic frequencies are reported in a sheet and saved in the patient's folder. Topographical distributions of such features are generated to allow the neurologist to validate the control features of the h-BCI device.

5.2.3 Configuration GUI

The Configuration GUI was developed to guide with a user-friendly approach the operator/therapist in the calibration and the online use of the h-BCI prototype during the BCI training sessions. This module generates the configuration files to customize each session to the patient.
The Configuration GUI is made by 2 tabs: Patient Tab and Settings Tab. In

the Patient Tab, the patient folder can be selected from a list of all the existing patient IDs saved in the specified database directory, by a drop-down menu or typing the patient ID in search-mode and selecting the desired one. The file with the selected features generated by the Feature extraction Module is uploaded and shown in the Settings Tab. This tab allows the therapist to visualize the selected features to encourage and discourage and the electrodes to place on the patient for the BCI training (up to 4 EEG electrodes and up to 3 EMG sensors). The Configuration GUI generates for each patient the configuration files with the ad-hoc information required for the online control of the device by converting the "Selected features" file in a format readable by the BCI, and sets the session information (i.e. session ID, data directory, saving directory, experimenter, etc).
At the bottom of the Settings Tab, four buttons allow the therapist to calibrate the device and perform the online BCI session. Each button is associated to a step of the BCI training session (Figure 5.2) and opens one of the modules of such a session. Once each module is completed a led associated to the corresponding step of the BCI training session turns green.

5.2.4 Calibration Module

During the first BCI training session, and whenever is needed to re-calibrate the device, the Calibration button of the Configuration GUI is enabled. By pressing it, the Calibration Module is opened and configured according to the information entered in the Configuration GUI (i.e. patient's folder path, session ID, etc.). The module runs in OpenViBE and imports the screening data generated by the Features extraction Module and the configuration files generated by the Configuration GUI. It performs the training of the BCI SVM classifier based on the 2 features to encourage selected for the real-time movement discrimination. The same pipeline described in paragraph 5.2.2-Feature extraction was implemented in OpenViBE to extract the 2 CMC features selected to control the movement detection, and to train the SVM classifier with linear kernel to discriminate task from rest condition. An ad-hoc OpenViBE box (CMC box) was developed in the broader context of Python for OpenViBE (Python version 3.8.1) to compute the CMC with the Welch periodogramm as in the Feature extraction Module (paragraph 5.2.2).
When the calibration ends, the trained classification model is saved in the patient's folder, together with a log file with a summary of the operations performed, the training classification accuracy and the 10-fold cross-validation accuracy performed by OpenViBE classification box to validate the trained model. Each patient will have his/her own SVM model according to the data recorded in the screening session.

5.2.5 FES Calibration Module

FES parameters, such as current amplitude, pulse width and stimulation duration, can be set specifically for each patient at every session according

to standard guidelines to achieve full movement and so as to avoid any kind of discomfort for him/her. By pressing the FES Calibration button in the Configuration GUI , a dedicated interface pops-up and the FES system can be calibrated identifying the best parameters for the stimulation, as well as the best position for the FES electrodes over the target muscle to obtain the desired movement. Such parameters are identified stimulating in open-loop the target muscle. The interface was developed to allow the upload and the edit of existing files or the creation of new ones after the testing. The editable parameters are all those made available by the FES stimulator. The configuration file with the ad-hoc FES parameters is saved in the patient's folder to customize the online session to the user.

5.2.6 Control Module

In all the BCI training sessions, the therapist can check the EEG and EMG traces and start the online session pressing the corresponding button on the Configuration GUI. The Configuration GUI opens the OpenViBE Acquisition Server for the simultaneous real-time acquisition of the EEG and EMG data. A customized driver was developed in collaboration with alfameg S.r.l.[6] to record EMG signals through Wave Plus wireless EMG system.
The Control Module is launched and configured by the Configuration GUI for the online control of the device.

Figure 5.5 provides a zoom of the steps performed in this module and its interaction with the patient. In this module, the EEG and EMG streams recorded from the patient are sent to the Control Module where the data are filtered as in the Feature extraction Module (see paragraph 5.2.2) with a one-way IIR filter design. EMG signals are rectified and both EEG and EMG data are segmented in 1s windows every 125ms. CMC values at the characteristic frequency are extracted for all the selected EEG-EMG pairs by the CMC box. The pre-processed EEG and EMG signals and the temporal evolution of the selected CMC features are displayed to allow the therapist to monitor the session.

[6] `https://www.alfameg.com/`

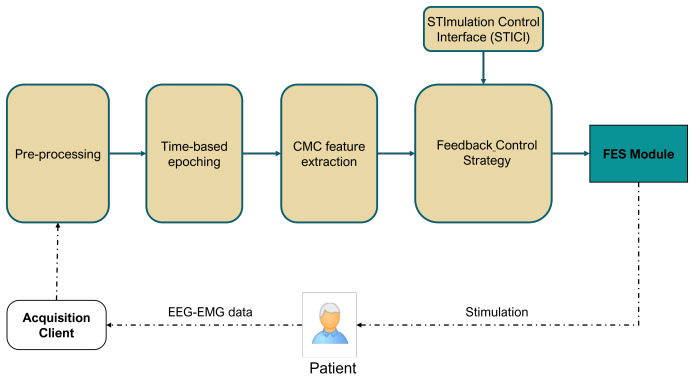

Figure 5.5. Block diagram of the steps performed in the Control Module. The interaction with the FES Module and patient are also shown.

Then, the up to 4 CMC features extracted in CMC feature extraction block are split in two branches:

- the 2 features to encourage are aggregated in a feature vector and sent to the trained SVM classifier which returns the task or rest predictions. This branch detects the brain control over muscles (branch to encourage).
- the up to 2 features to discourage are sent to a box which monitors the dysfunctional patterns (branch to discourage).

The outputs of the two branches are both sent to the Feedback Control Strategy block which represents the core of the Control Module. Such block takes the final decision to trigger the FES, indeed it has 2 possible outputs: 1 - physiological movement detected, 0 - no physiological movement occurred.
The Control Module has embedded a STImulation Control Interface (STICI) developed via Python's PySimpleGUI which temporizes the BCI training session and starts a new trial of the BCI paradigm, (i.e. a new repetition of the rehabilitative exercise, for further details about the timeline see paragraph 5.3).

During each online session, the EEG and EMG signals are saved together with a log file with the outputs of the two branches and all the events occurred during the session. This allows to track the improvement of the patients and evaluate which branch failed to satisfy the physiological condition (branch to encourage, branch to discourage).

5.2.7 FES Module

The FES module closes the loop delivering the stimulation to support the patient in completing the movement when "correct" movements are detected by the BCI, Figure 5.5. A custom OpenViBE box was developed in collaboration with alfameg S.r.l to set the FES parameters according to the output of the

FES Calibration Module and allow a continuous thread between OpenViBE and the stimulator. The configuration files generated by the FES Calibration Module are imported to configure the box. Such box controls the stimulator triggering a standard stimulation pre-defined by RehaMove system.

5.3 The h-BCI paradigm

The h-BCI paradigm was designed as driven by the therapist and consists in several trials/repetitions of the rehabilitative exercise according to the timeline described in Figure 5.6. The STICI (see Figure 5.5), allows the therapist to control the online session. It accepts 3 keyboard commands which corresponds to the following stimuli: "start a new trial", "end bad trial", "end experiment". At the beginning of each trial a beep sound is delivered informing the patient to get ready to attempt the movement, after 3s an acoustic cue "GO" invites the patient to start the task. The stimulation is delivered to the patient when a physiological movement is detected, as described in paragraph 5.2.6.

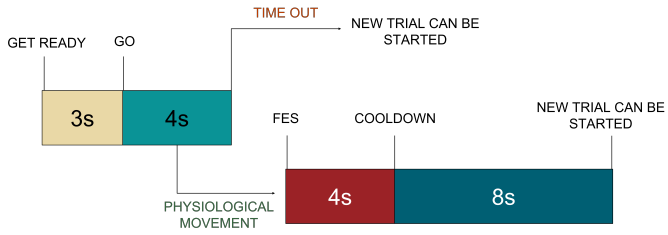

Figure 5.6. Timeline of the experiment during online session.

The target muscle is stimulated for 4s, after which the control interface makes the therapist wait at least 8s before the next trial (duty cycle: 1:2 to preserve muscle fatigue development, i.e. T_{safe}=12s). After 4s from the acoustic cue (T_{trial}), if no physiological movement is detected the trial is ended with a "time out". For safety purpose, the Feedback Control Strategy block can be stopped by the therapist at any moment pressing the "end bad trial" command if problems during the trial occur, such trial will be ended and will be marked as "bad trial".
Letting the session being driven by the therapist allows to avoid as much as possible muscular fatigue, common during FES stimulation, and to perform the BCI training in the safest way possible, taking into account the patient's needs.

5.4 Prototype validation: proof-of-concept study

5.4.1 Online testing on healthy participants

The various components of the h-BCI prototype were tested and resulted to communicate in a reliable and intuitive way. To test the feasibility of the device, 3 right-handed healthy subjects were involved in a proof-of-concept study. The classification speed and accuracy were evaluated and the ability of the prototype to generalize across different users was tested. An evaluation of prototype usability (i.e. preparation time) was performed.
The task performed during the online testing was finger extension, because the rehabilitative exercise chosen for the h-BCI intervention in agreement with the clinicians was finger extension attempt. Indeed, during this movement greater stroke-related CMC alterations was found compared to grasping as resulted by CMC pattern analysis performed in Study 2 on stroke patients, which revealed a more dysfunctional pattern during finger extension attempts performed with the paretic hand.

Data collection and analysis

Participants with no history of neuromuscular disorders and any contraindication to FES (such as pregnancy, proneness to faint, epilepsy, compromised integrity of the stimulated limb, compromised sensation) were enrolled in the proof-of-concept study.
They underwent a screening session and an online BCI session with the h-BCI prototype in two different days, no more than a week apart. During such session, participants performed the movement with their dominant hand (right hand).

After the screening session, the two features to encourage were identified, whereas no dysfunctional pattern were detected, as expected in healthy individuals. For this reason, the branch to discourage was turned off.
During the online session, the 2 selected EEG channels were placed over the scalp (reference on left mastoid and ground on right mastoid), whereas 2 FES electrodes (dimension 40x40mm) were placed over the target muscle (extensor digitorum right, EDR) one next to the other along the fiber direction. The EMG sensor was placed right after the FES electrodes over the ED muscle. FES calibration was performed only with the purpose to evaluate the preparation time of the online session and the placement of the EMG sensor which could affect the CMC. However to perform a study on data not altered by the stimulation, the FES feedback during the online session was replaced by an acoustic feedback. Participants performed 20 trials administrated according to the BCI paradigm described in paragraph 5.3.
The EEG and EMG signals pre-processed in OpenViBE (EEG band-pass filtered 3-60Hz, EMG band-pass filtered 3-500Hz, notch filter applied at 50Hz) were recorded during the online session and analyzed afterwords in Matlab. Signals

were segmented in 20 epochs selecting the time interval [-2, 3]s with respect to the start of the trial. The EMG onset for each trial was computed as in Study 4 paragraph 4.2.4 and the single-trial CMC features used for the movement detection were calculated reproducing the pipeline of the Control Module (see Figure 5.5).
The same metrics evaluated in Study 4 (hit Rate, FPR, FNR and Mean Delay) were computed to assess the performances of the h-BCI prototype.

Results

The EEG channels of EEG-EMG pairs selected as features to encourage for each participant are shown in Table 5.1. They were chosen among all the possible pairs consisting of the EEG channels over sensorimotor area of the hemisphere contralateral to the involved hand (left hemisphere) and the target muscle (extensor digitorum right).

Table 5.1. EEG channels of the CMC features between the scalp and the target muscle (EDR) selected as features to control the BCI, and online classification performances reported as mean ± standard error across 20 cue-based repetitions of the right finger extension (ExtR) in the 3 healthy participants who underwent an online BCI session.

ID	Features to encourage	Hit Rate	FPR	FNR	Mean Delay [s]
H01	FC5, C5	1	0	0	0.48 (±0.03)
H02	FC5, FC3	1	0	0	0.58 (±0.06)
H03	CP3, CP1	1	0	0	0.38 (±0.03)

The preparation time of the h-BCI training session took around 15 minutes, whereas the online BCI session which comprised the preparation time and one run of 20 repetitions lasted overall around 25-30 minutes.

Trends of the two CMC features are reported for each subject in Figure 5.7 together with a marker on the time sample the feedback was delivered for each trial.

H01

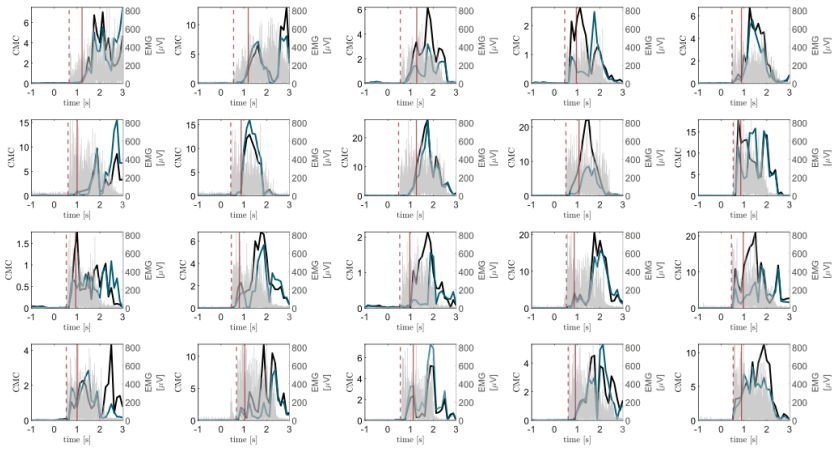

H02

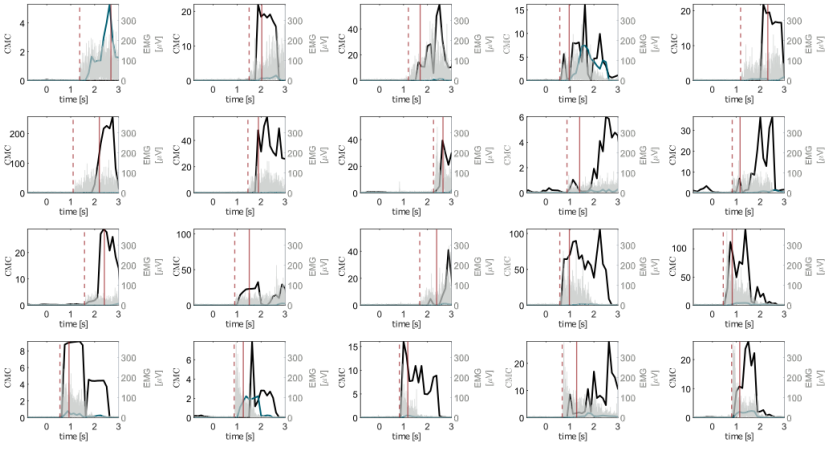

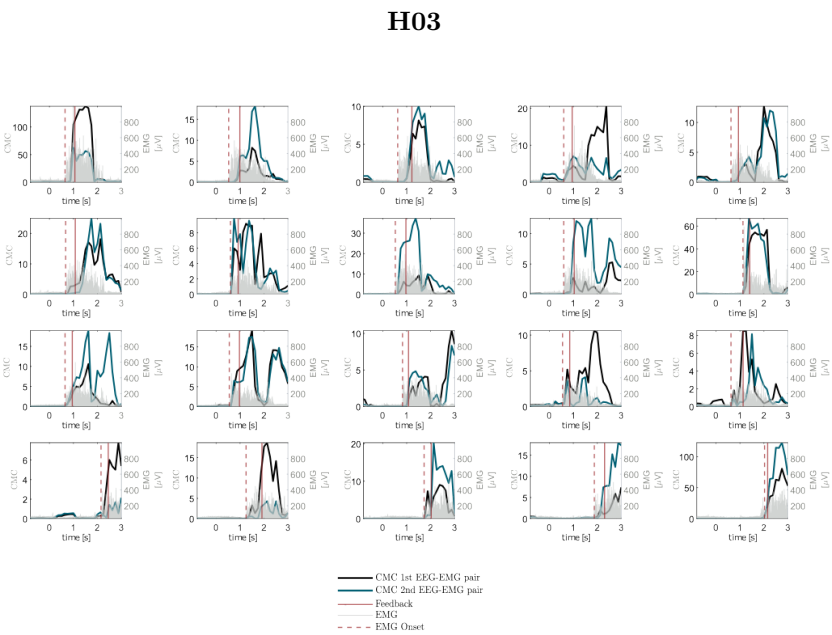

Figure 5.7. Single-trial CMC and EMG trends considering the two EEG-EMG pairs selected by Fisher criterion and the target muscle respectively, recorded online in 3 healthy participants (one panel for each trial). Dashed vertical line represents movement onset detected from EMG (EMG onset), whereas continuous vertical line stays for the time the BCI sent the feedback to the user. The online CMC computation was updated every 125ms and two Task predictions were accumulated (accumulation factor M=2) before a BCI's feedback.

CMC managed to track in real-time the movement execution and the BCI sent always a feedback to the user right after the movement onset. Differences among participants can be attributed to CMC inter-subject variability as well as slightly differences in the EMG electrode placement according to FES electrodes position, which had the priority since they affected the movement induced by the stimulation. Table 5.1 shows the classification performances and the average time to deliver the feedback across trials (Mean Delay).

This testing provided evidence of the ability of the h-BCI prototype to generalize across different users. The results achieved here confirmed what obtained in the pseudo-online analysis performed in Study 4, also in an online paradigm: CMC manages to detect the movement in real-time with high performances in term of classification accuracy and speed. The use of up to 4 channels to control the h-BCI device allows for very short set-up times, whereas the overall experiment time suggests that 2-3 runs could be performed in the h-BCI rehabilitation intervention for a total duration of up to 30 minutes

(preparation time excluded). Moreover, the high performances obtained online in healthy subjects are promising for the real-time use of the h-BCI prototype for post-stroke motor rehabilitation.

5.4.2 Pseudo-online testing on stroke patients

To test the ability of the branch to discourage in detecting pathological movements, such as compensatory proximal muscles activity and abnormal recruitment of healthy side muscles, a pseudo-online study on 11 stroke patients for Ext movement (same as Study 4) was performed. Data related to the finger extension's attempt of the paretic hand were considered here.

Data analysis

The EEG and EMG data acquired as in Study 4 paragraph 4.2.2 were processed with the offline pipeline used to extract and select the CMC features of the h-BCI prototype during the screening session (see paragraph 5.2.2). The double threshold criterion was applied on the CMC values of the reduced feature space, obtained for the selection of the features to discourage, to detect dysfunctional patterns during the movement attempt. Upon detection, a pseudo-online study (mimicking the online pipeline developed in the Control Module) was performed for each participant to evaluate the trends of such CMC features during each trial and thus characterize the temporal evolution of such dysfunctional patterns.
For each task trial the time interval [-4,4]s with respect to the "GO" was considered and the trend of the selected CMC features was computed using 1s-windows and 125ms of shift.

Results

Dysfunctional patterns were detected during the screening session for 5 out of 11 participants.
CMC features selected as to discourage for each participant with his/her related FMA-UE are reported in Table 5.2. Not all stroke participants showed both dysfunctional patterns (i.e. compensatory proximal muscles activity and abnormal recruitment of healthy side muscles), indeed for three of them only the involvement of proximal muscles were revealed.

Figure 5.8 shows the single-trial CMC trends in all task trials for the two features to discourage (one feature for each panel) and their activation thresholds, detected during the screening session, in a representative stroke participant. For each type of dysfunctional pattern analyzed, after the "GO" (t=0s) CMC values of the selected EEG-EMG pair resulted to increase, reach a pick and decrease going under the activation threshold at the end of the trial. Testifying the involvement of the selected dysfunctional connections in the movement.

Table 5.2. EEG-EMG pairs selected as features to discourage for the 5 stroke participants in which dysfunctional patterns were detected. The Fugl-Meyer Assessment scale, upper extremity section (FMA-UE), ranging from 0 (most affected) to 66 (least affected), was reported for each participant. AH = affected hand side, UH = unaffected hand side, movements were attempted with the affected hand.

ID	FMA-UE	Features to discourage
S01	51	CP6-Lat_DELT$_{AH}$, P4-FD$_{UH}$
S02	26	FC6-BIC$_{AH}$
S03	23	FC3-Lat_DELT$_{AH}$, C6-FD$_{UH}$
S04	62	FC1-BIC$_{AH}$
S05	54	FC3-BIC$_{AH}$, CPz-ED$_{UH}$

Results show how the algorithm developed for the selection of the features to discourage (see paragraph 5.2.2) is able to detect dysfunctional patterns, defined according to Study 2 on stroke patients, and follow their evolution during the movement task. Such patterns start right after the movement onset and last until its end.

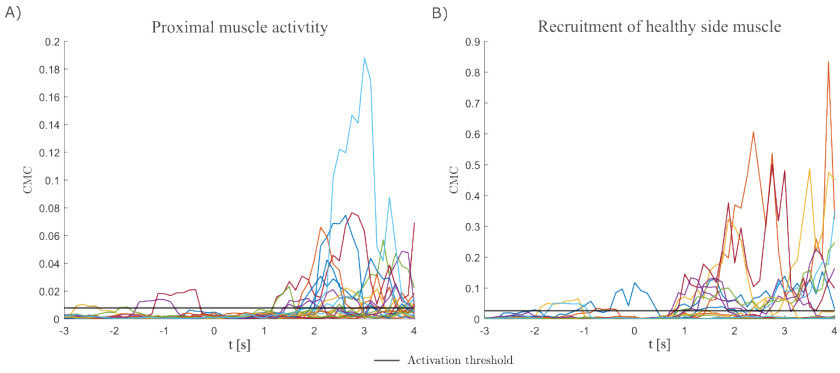

Figure 5.8. Single-trial CMC trends of the CMC features to discourage selected for the two dysfunctional pattern types A) compensatory proximal muscle activity (i.e. compensatory movement) and B) abnormal recruitment of healthy side muscle (i.e. mirror movement) in the 20 task trials for a representative stroke subject (S03). Time was aligned to the "GO", horizontal black line represents the activation threshold.

In the online BCI session, the decision to send a feedback relies on the combination of the branch to discourage and the branch to encourage. This means that a feedback is sent to the patient only when the movement is detected based on the CMC features to encourage and no dysfunctional movement occurs. Assessment of BCI performances in stroke patients during online BCI training sessions is needed to confirm the feasibility of this approach, including an evaluation of usability, satisfaction and workload of patients and professionals in a real-world setting.

5.5 Discussion

The h-BCI prototype was developed with the aim to re-establish cortico-muscular communication after stroke with a BCI-controlled FES intervention. It was design with a modular approach and each module can be adapted according to the rehabilitative needs. Its interface was thought to provide an easy-to-use tool for the therapist to manage the h-BCI intervention.
The preliminary studies on healthy subjects showed the prototype's feasibility and its ability to generalize among different users. The high performances achieved proved the ability of CMC features in detecting movements in real-time and sending a contingent feedback paired with subject's movement intention (branch to encourage), confirming what obtained in Study 4. Whereas, the pseudo-online testing on the branch to discourage showed the prototype's ability to detect dysfunctional activations according to results of Study 2.
Clinical and functional efficacy on upper limb rehabilitation of the h-BCI technology will be assessed in the coming months within a Randomized Controlled Trial (RCT) in chronic stroke patients undergoing rehabilitation (add-on) at Fondazione Santa Lucia, IRCCS, Rome Italy. The study was already designed, authorised by the local ethical committee and registered online at clinicaltrials.gov[7](NCT05511207).

[7]https://clinicaltrials.gov/ct2/show/NCT05511207

6. Study 6

An adaptive EMG-based feedback modulation strategy to use in a BCI context

6.1 Background and Objectives

This study focuses on the stimulation strategy to use to design a rehabilitation training challenging but feasible for the patient and tailored to his/her level of impairment and was conducted during my secondment as visiting PhD student at the Translational Neural Engineering Lab (TNE) - EPFL.
Surface functional electrical stimulation is widely used as a movement rehabilitation technique [47]. Active engagement during the FES-supported rehabilitation training is crucial for its optimal effect [48], [49], indeed administrating the FES in the context of a volitional intent enhances its brain effects ([50], [51]. BCI controlled-FES have led to improvement in motor functions [19], [52]. Moreover, voluntary EMG can be used to trigger FES in post-stroke rehabilitation [14], [15] or to proportionally control in real-time the stimulation according to the level of activation (reinforcement learning) [16], [17]. Active proportional EMG control of FES required to reject the stimulation responses (M-wave) [53] and to adopt comb filtering to reduce the harmonics of stimulation responses. Moreover, to extract the voluntary myoelectric activation, a low stimulation frequency (around 16Hz) [16] or complex adaptive filters [17] are needed to reject the stimulation artifacts. However, low frequency stimulation generates an unstable force far from the natural one [54].

Here, a hybrid system that integrates an EEG-based BCI and an adaptive EMG-based modulation strategy of FES intensity is designed to rehabilitate upper hand functions in post-stroke patients. Such system has the aim to

be the first step for the transition from an «all or nothing» approach to a gradually compensatory feedback targeted on patient's level of impairment. The FES intensity is modulated at each repetition of the rehabilitative exercise based on the residual muscular activity recorded right after the brain-based detection of the movement attempt. The goal is to obtain a modulation strategy which reflects the rehabilitation approach of supporting the patient through the functional recovery, thus a compensatory strategy is developed to deliver during the rehabilitation training a FES intensity complementary to the residual or recovered muscular activity of the patient. A canonical EEG-based BCI [18] was chosen with the aim of validating the adaptive feedback strategy on an already tested BCI paradigm.

6.2 Stimulation strategy

The EEG-based BCI detects the movement attempt and extracts the related muscular level of activation assessed by the EMG signals simultaneously recorded. When a movement attempt is detected by the BCI, the stimulation intensity is delivered to the patient to complete the movement. The stimulation intensity is modulated by the myoelectric level through a compensatory approach: higher the myoelectric level and lower the amount of stimulation used to support the full movement execution (see paragraph 6.4 for further details). To avoid muscles fatigue induced by the stimulation and to make the experimental exercise more dynamic, two deviations of hand extension were chosen as experimental exercise: upward and outward Fdeviations.

FES stimulation patterns can be optimized to produce the desired sensory and motor response without using standard stimulation strategies pre-defined in the FES stimulator [13], [55]. Here, the stimulation strategy was developed to obtain a reliable and safe system customisable according to the patient's needs, modifying some pre-existing ones [13], [55]. Such a strategy was build to stimulate three different muscles of the forearm: abductor pollicis longus (AP), extensor digitorum communis (EDC) and extensor carpi ulnaris (ECU). It allows to stimulate each muscle at a time or two different combinations of muscles: sequential stimulation of AP, EDC and ECU muscles (AP+EDC+ECU strategy) and simultaneous stimulation of AP and EDC muscles (AP+EDC strategy) to provide full extension of the hand. Indeed, fingers and thumb are controlled separately by EDC and AP muscle's fibers respectively, thus to induce the full hand extension they have to be stimulated together.
The stimulation strategy was designed to deliver biphasic rectangular impulses with a controlled amplitude and an adjustable pulse width, the stimulation frequency was set to 40Hz to avoid discomfort for the patient. Moreover for comfort purposes, current amplitude was limited to 20mA for AP, 30mA to EDC and 25mA for ECU muscle. whereas the pulse width range was set from 150μs to 300μs for each muscle.

The stimulation profile was made adjustable according to rehabilitative exercise and it was different for the calibration and the online session. The calibration session is performed in open-loop to identify the maximal stimulation intensity (I_{max}) and the best FES electrodes location for each muscle and subject to obtain the desired movement. The stimulation intensity is set increasing it to the point where sufficient muscle contraction is produced or the subject feels an unpleasant sensation.
For the calibration session, a slow profile was developed, shown in Figure 6.1: 10s duration with a smooth ramp of 4.65s and a steep descent starting at 6.725s (Figure 6.1 A). For the AP+EDC+ECU strategy, after the stimulation of the first muscle, the stimulation of the next one starts right before the descent phase of the previous one (at 6.375s), for a total duration of 25s, Figure 6.1 B. Whereas for the combined stimulation of AP and EDC muscles (AP+EDC strategy), muscles are stimulated simultaneously and the two stimulation profile are superimposed (Figure 6.1 C). A faster profile, adjusted according to patient's characteristics, can be used during the close-loop control in order to overcome the sensory threshold after a minimum of 100ms.

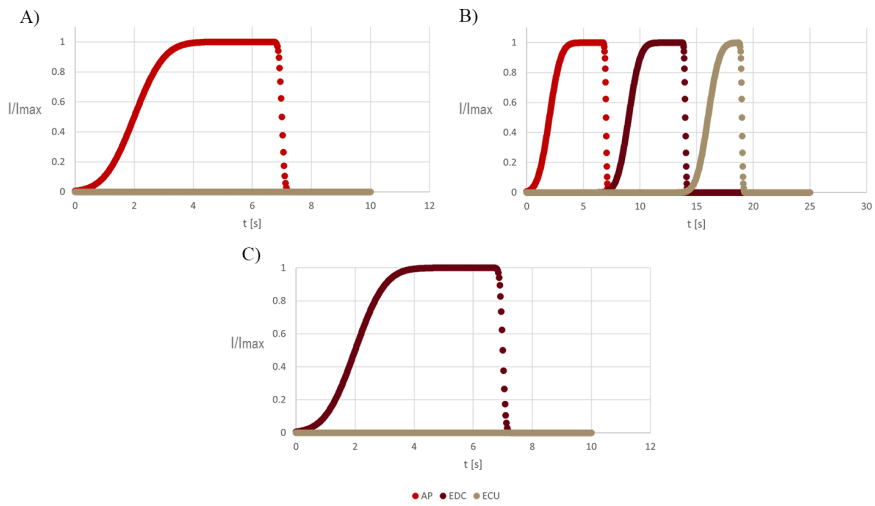

Figure 6.1. Stimulation profiles developed to calibrate the stimulation intensity of A) one single muscle (e.g.AP), B) AP+EDC+ECU combination, C) AP+EDC combination. The intensity is normalized for the tested I_{max}.

6.3 System Design

The hybrid system was designed in a modular, reliable and easy-to-use way. It comprised the following building modules:

- the Acquisition system which records the EEG and EMG data through two gUSBamp amplifiers (g.tec medical engineering GmbH Austria[1]).
- the hybrid BCI which translates user's intention.
- a Control Interface (CI) used to set the experiment and trigger the stimulation.
- the FES Controller which provides the simulation strategy via a Beaglebone Black[2].
- the Stimulation system which delivers the stimulation to the patient via a RehaStim stimulator (Hasomed GmbH, Germany[3]).

The network diagram is shown in Figure 6.2 and explains the communication between the modules.

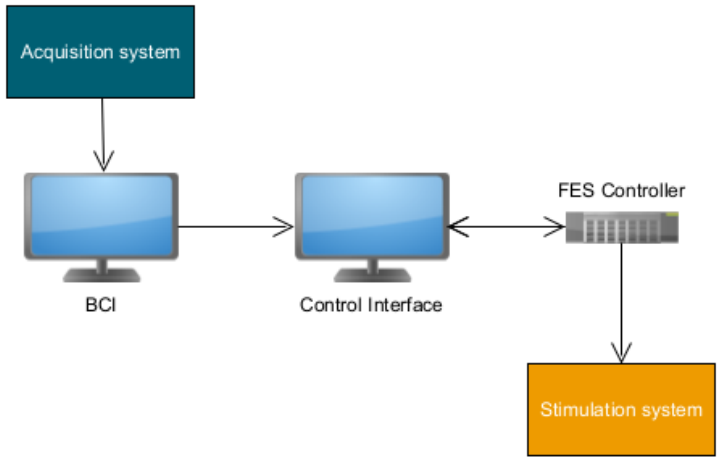

Figure 6.2. Network Diagram of the hybrid system. The BCI processes the signals collected by the Acquisition system and sends a trigger and the EMG parameter used for the modulation strategy to the Control Interface. The Control Interface computes the percentage of FES intensity to deliver and communicates to the FES Controller the stimulation strategy selected by the therapist and the related stimulation intensity. The FES Controller generates the stimulation strategy and loads it to the Stimulation system that delivers the FES to the patient. The FES Controller sends then back a response to the Control Interface about the outcome of the delivery.

To keep the BCI, the CI and FES Controller synchronised, a strict master–slave concept using a custom-made communication protocol based on User

[1] `https://www.gtec.at`
[2] `https://beagleboard.org/black`
[3] `https://hasomed.de`

Datagram Protocol (UDP) was implemented in Python 3.8.1 (socket package) and produces a continuous thread among the modules. Such protocol allows to have, if needed, each module in a different machine and lets them communicate through ethernet, USB or Wi-Fi. This solution allows to reduce the computational cost of each machine in favour of the timing, crucial in BCI applications.

6.3.1 Acquisition system

Two g.USBamp amplifiers allow to record up to 32 channels. EEG signals are recorded trough g.LADYbird active electrodes, whereas for EMG signals collection passive peripheral electrodes are used. Thanks to OpenViBE drivers, the EEG and EMG data are acquired and sent in real-time to the processing boxes.

6.3.2 BCI module

The acquisition system sends the EEG and EMG signals to the BCI, developed in OpenViBE v.3.1.0[4], which uses an EEG-based classifier to detect user's movement intention and computes the EMG parameter for the FES intensity modulation. A customized OpenViBE box was developed in Python 3.8.1 to extract the EMG parameter. The experimental paradigm was designed so that each repetition of the rehabilitative exercise is driven by the therapist pressing a dedicated command from the keyboard. When the key is pressed the BCI starts to accumulate predictions and when the detection rule is satisfied (movement detection), the BCI trigger and the EMG parameter are sent to CI. If patients are not compliant to the instruction or problems occur during the task repetition, a dedicated key can be used to stop the thread between the BCI and the CI, ending the ongoing repetition of the exercise.
An ad-hoc Python box was developed in OpenViBE to send the BCI trigger and the EMG parameter to the CI via UDP.

6.3.3 Control Interface (CI) module

The CI, developed in Python 3.8.1, is the core of the system, it consists of a user-friendly interface which allows the therapist to: i) set the general information about the patient and the rehabilitation session (Figure 6.3 A), ii) calibrate the FES stimulator parameters and testing the optimal current amplitude (I_{max}) for each muscle or combinations of muscles (Figure 6.3 B and C) and iii) send the commands to the FES Controller for the delivery of the stimulation to the user (Figure 6.3D). Local libraries were developed to define the parameters, the tasks identifiers and the message to deliver to the FES Controller. Such message contains the command for starting the stimulation, the ID of the stimulation profile to load (i.e. single muscle stimulation or combined stimulation

[4] `http://openvibe.inria.fr`

of different muscles), the parameters (i.e. current amplitude and percentage of FES intensity) to use for the stimulation.

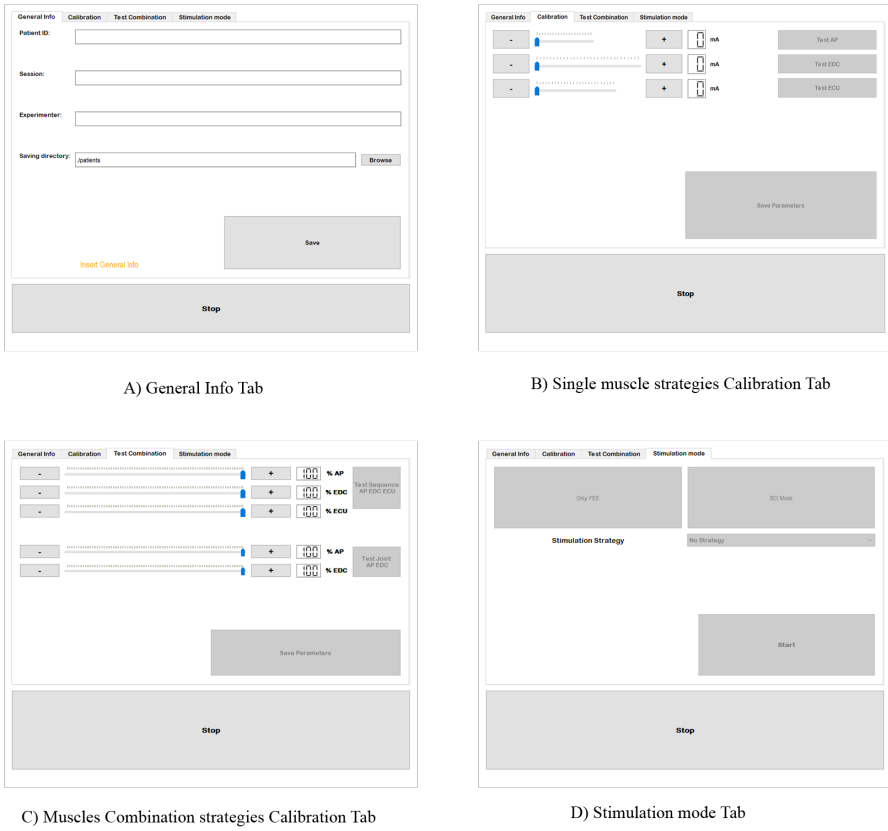

A) General Info Tab

B) Single muscle strategies Calibration Tab

C) Muscles Combination strategies Calibration Tab

D) Stimulation mode Tab

Figure 6.3. Tabs of the Control Interface. A) Calibration of the single muscle strategies B) Calibration of AP+EDC+ECU and AP+EDC combined strategies and C) Stimulation mode.

The FES intensity of each muscle in the AP+EDC+ECU and AP+EDC stimulation strategies is set as a percentage of the I_{max} found during the single muscle stimulation strategy calibration (Figure 6.3C). The CI, through its tab "Stimulation mode" (Figure 6.3D), allows two stimulation modalities: only FES (open-loop) in which the stimulation is driven by the therapist through the dedicated button in the interface; and BCI modality (close-loop) in which the stimulation is driven by the BCI and the FES intensity is modulated by the EMG parameter. The therapist can select the experimental task and thus the muscles to stimulate from a drop-down menu. For the BCI modality, the therapist need to press the dedicated button to open the communication

between the BCI and the CI. The stimulation intensity is modulated as a percentage of I_{max} according to the EMG parameter received from the BCI. For each tab (i.e. calibrations, stimulation mode) a yaml-file with the FES parameters set and a history file with all the actions performed is generated in the patient's folder.
For safety purpose, the CI presents a STOP button that can immediately stop the stimulation even when it is ongoing.

6.3.4 FES Controller module

The FES Controller receives the commands from the CI and loads the stimulation profile on the FES stimulator, it also sends back a response to the CI with the actions performed. FES Controller was developed as the CI in Python 3.8.1. The commands sent to and the responses received from the FES controller were defined and codified in a local library and are saved in a log file to track all the operations and avoid undesired behaviours.

6.3.5 Stimulation system

The stimulator RehaStim is a portable electrical stimulation device that generates impulses on up to eight channels simultaneously. Surface electrodes are used to stimulate target muscles [56]. The stimulation is controlled in ScienceMode through a COM port by the FES Controller. Axelgaard PALS electrodes (Axelgaard Manufactoring Co., Ltd[5] of different dimension and shape are used for the stimulation according to the patient characteristics.

6.4 Adaptive algorithm for a real-time myoelectric modulation of FES intensity

To provide to the patient a stimulation tailored to his/her impairment, the intensity of the stimulation is modulated varying its pulse width according to the residual EMG activity recorded in real-time right after the BCI's movement detection. The compensatory modulation strategy was developed with the aim of delivering a stimulation able to compensate patient's residual muscular activity, thus the developed control-stimulation relation is inversely proportional: if the residual EMG activity does not differ from the activity at rest, then the stimulation intensity is equal to I_{max}, set during the calibration phase to provide the desired movement. Otherwise, the stimulation intensity is computed as a percentage of I_{max} progressively lower until the reference myoelectric level of activation (EMG_{ref}) is reached. Different parameters were evaluated to define the algorithm's adaptive rule, such as the EMG parameter to use to identify the residual muscular activity and the coefficient between the EMG parameter and the pulse width (gain).

[5] `https://www.axelgaard.com/`

6.4.1 Data collection and analysis

Data collection

To rehabilitate different deviations of the hand extension such as upward and outward deviations, the following stimulation strategies are used: combined stimulation of AP and EDC muscles (AP+EDC strategy) and stimulation of only ECU muscle (Only ECU strategy), respectively.
Data from seven healthy participants (3 females/4 males, age 29.1±5.5 yo) were recorded during the execution of upward and outward hand extension deviations with their dominant hand. Participants had no history of neuromuscular disorders and any contraindication to FES (such as pregnancy, proneness to faint, epilepsy, compromised integrity of the stimulated limb, compromised sensation). Three stimulation electrodes (3.2cm, round shape) were placed on the skin over the motor points of the AP, EDC and ECU muscles, whereas a ground electrode (5cm, round shape) were placed over the wrist bones. At the beginning of the experiment, a calibration session was performed to find the electrode position that gave the best fingers and thumb extension (AP+EDC strategy) and lateral deviation (Only ECU strategy) and to set the optimal FES intensity.
EMG signals were acquired at 1200Hz from the EDC and ECU muscles via a g.USBamp amplifier. For each muscle, two surface Ag/AgCl electrodes, 10mm diameter, were placed at 20mm inter-electrode distance right after the stimulation electrodes, in the direction of the muscle fibers. The neutral (ground) electrode was placed over the olecranon. Three repetitions of Maximal Voluntary Contraction (MVC) lasting 5s were recorded for each muscle before starting the experimental task. The paradigm was administrated in a block-design structure in which each run consisted of one deviation. Each run comprised 10 trials of 5s duration, at the beginning of each trial an acoustic beep is sent informing the participants to get ready to perform the movement, after 1s an acoustic "GO" cue invited to start the movement and participants were instructed to hold it for 4s after which a "STOP" stimulus occurred, Figure 6.4.
Stimulation electrodes were placed on participants' forearm to study the compatibility between FES and EMG electrodes placement and to evaluate how to extract the EMG parameter given the EMG signals recorded by such EMG electrodes. No stimulation was delivered during the runs.

Data processing

EMG signals were band-pass filtered 10-500Hz and segmented in 6s epochs in the interval [-1, 5]s with respect to the start of the trial. Epochs were visually inspected and if artifacts were detected, they were rejected.
To calculate the EMG envelope, the root-mean-square (RMS) of the EMG signal on the target muscle (EDC for upward deviation, ECU for outward deviation) was computed on windows of 0.5s length sliding across the whole trial duration and on the three MVC repetitions of the corresponding muscle. For visualization purpose, a baseline correction was performed for each epoch

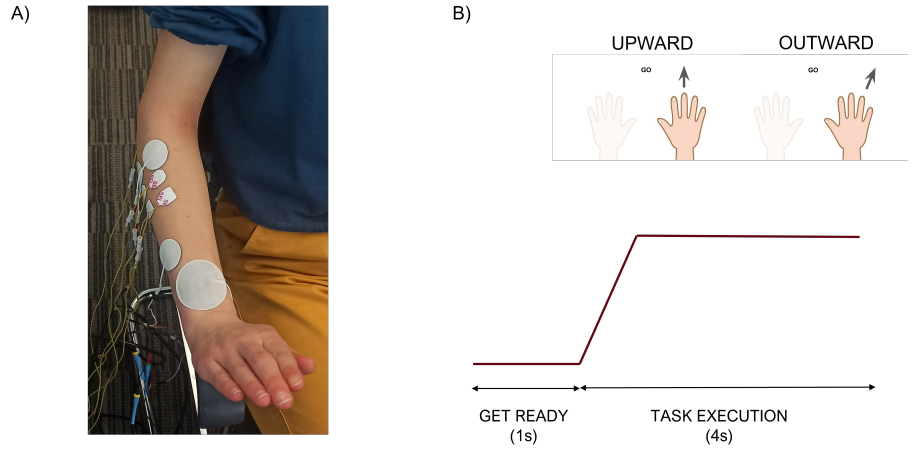

Figure 6.4. A) Position of the FES and EMG electrodes used in the experiment B) Timeline of the trial with representation of the two hand extension deviations

considering the mean value in the time interval [-1, 0]s as baseline, and the EMG envelope was normalized by the the median value among the maximum RMS of the three MVC repetitions (%MVC). The EMG activation levels, expressed as %MVC, were finally averaged across trials.
The EMG onset of each epoch was computed as in Study 4 paragraph 4.2.4.

Compatibility between EMG and FES electrodes placement

To deliver the desired stimulation and support the two hand extension deviations, three active FES electrodes and a ground electrode must be placed over the forearm of the patient. At the same time, to modulate the FES intensity according to the myoelectric level, the voluntary EMG of EDC and ECU muscles must be recorded in bipolar fashion for the upward and outward deviation respectively. Such electrodes must be placed immediately after the stimulation ones, whose position is tied to the muscle motor points to induce the movement, which means that EMG electrodes could be slightly over the muscle belly.
Thus, as first step, the compatibility of the FES and EMG electrodes placement over the forearm of the subject was tested. The mean envelope across epochs were computed and visualized to check if the EMG signals reflected the two movements and if different activations over the two recorded muscles can be revealed depending on the type of movement.

EMG parameter extraction

The EMG parameter used to modulate the percentage of FES intensity delivered to the patient was thought to be extracted in the BCI's accumulation window

needed to have enough evidence for a final classification decision. Thus, the EMG envelope is computed in real-time from the beginning of the session and when the BCI accumulates enough movement predictions, it retroactively looks back to the accumulation window to extract the EMG parameter to send to the Control Interface.
The EMG parameter was extracted as the maximum value of the EMG envelope in the accumulation window. To evaluate the width of the accumulation window needed to extract a EMG parameter which reflects the myoelectric level of activation, three window size were tested: 62.5ms, 125ms and 250ms with respect to the EMG onset. A Friedman's test was applied on the mean EMG parameter across epochs of each subject considering as factor the window width. A Tukey's post hoc test was applied to assess differences between window sizes. Moreover, to test the ability of the EMG parameter to represent the muscular activation level, the EMG values extracted were compared to the maximum EMG value of the envelope through a Wilcoxon signed-ranks test. The significant level was set to 0.05 for all tests. A width of 250ms resulted to be the best window size, and was thus used in following analyses.

Gain definition

The gain of the modulation strategy depends on three parameters: I_{max} (defined in paragraph 6.2), the EMG at rest and EMG_{ref} (i.e. the reference level of muscular activation). The stimulation intensity is computed as a inversely proportional piecewise function between I_{max} at EMG at rest and no intensity at EMG_{ref}. The EMG at rest and EMG_{ref} are obtained performing an EMG recording during the calibration session and were defined as follow: the EMG at rest is defined as the mean value of the EMG envelope computed during rest condition, whereas the EMG_{ref} is defined as the activation level during the non-paretic hand movement in the same window used for the extraction of the EMG parameter, with a certain tolerance range defined according to the difference between the two sides in healthy subjects.
To test the validity of the approach chosen for the extraction of EMG_{ref} and define the tolerance range, the same dataset analysed in Study 2 was analysed here only for the finger extension movement performed with the left and the right hand by the 12 healthy participants (CTRL) and performed/attempted with the unaffected and affected hand in the 12 stroke participants (EXP).
The EMG onset was computed in each trial and the EMG parameter was extracted in the window [0-250]ms with respect to the EMG onset. A Wilcoxon signed-ranks test was applied on the mean EMG parameter across trials to assess the differences across participants between the two sides (left and right side in CTRL group, unaffected and affected side in EXP group). To define the range of tolerance according to which the EMG parameter extracted online is considered equal to EMG_{ref}, the ratio between the mean EMG parameter across trials in left and right side was computed for each healthy participant, and the 75th and 25th percentile of the ratio distribution was used.

6.4.2 Results

Compatibility between EEG and FES electrodes placement

Figure 6.5 shows the mean envelope across epochs during the two movement types for a representative healthy participant recorded with the set up shown in Figure 6.4 A. Similar results were obtained for the other participants.

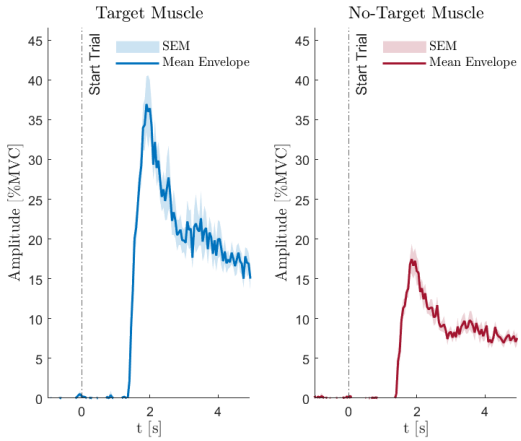

A) Upward deviation

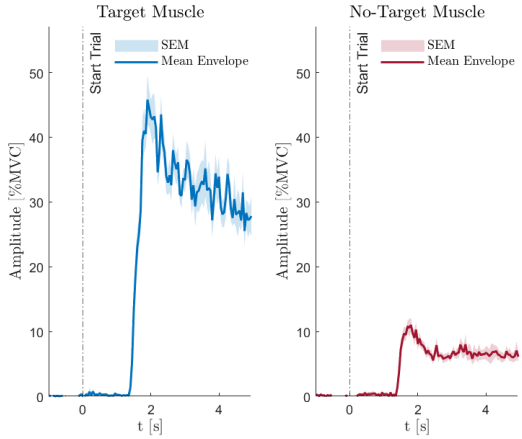

B) Outward deviation

Figure 6.5. EMG envelope (mean ± standard error) of the target and no-target muscles during the two types of movement for a representative participant. A) Upward deviation: EDC target muscle, ECU no-target muscle. B) Outward deviation: ECU target muscle, EDC no-target muscle. EMG values are normalized with respect to the MVC, vertical dashed line represent the start of the trial.

The envelope tracks the movement and the activity of the target muscle overcomes the one of the no-target muscle for each movement type, assessing the discriminability between the two movements according to the EMG level of the target muscle. Thus, the placement of EMG and FES electrodes resulted to be feasible for recording the experimental tasks.

EMG parameter extraction

Figure 6.6 shows the distribution across participants of the mean EMG parameter when considering as window width 62.5ms, 125ms and 250ms, as well as the distribution of the maximum value of the mean EMG envelope during the outward deviation of the hand extension. Similar results were obtained during the upward deviation.

The statistical analysis performed on the EMG parameter on varying the

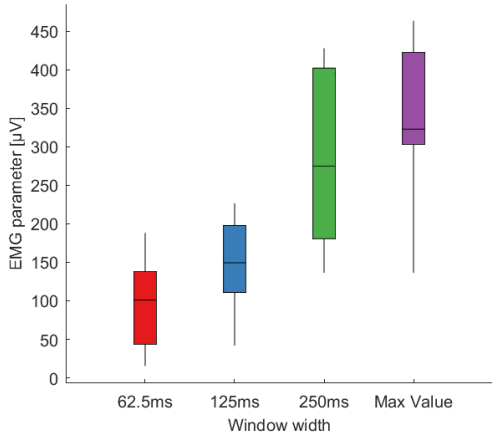

Figure 6.6. Boxplots of the distribution (N = 7 participants) of the EMG parameter extracted in the 3 windows analyzed (window size: 62.5ms, 125ms and 250ms) and the maximum value of the mean EMG envelope (Max Value) during the execution of the outward deviation. Similar results were obtained during the execution of the outward deviation.

window size revealed significant differences in both movement types (Friedman's test, $p<0.01$ in both upward and outward deviation). The post-hoc tests highlighted a significant difference between window size of 62.5ms and 250ms, no differences were found between 125ms and 250ms of window width, which could be due to the high inter-subject variability.

Significant differences were obtained by Wilcoxon signed-ranks test between the the maximum EMG value and the EMG parameter extracted in the window of size 62.5ms for the upward deviation ($p=0.0313$) and in the windows of size

62.5ms and 125ms for the outward deviation (p=0.016 in both windows). No differences were revealed between the maximum EMG value and the EMG parameter extracted in the window [0-250]ms with respect to the EMG onset. Thus, the EMG parameter extracted in such window resulted to represent the best the myoelectric level of activation and it is used to modulate the FES intensity. Consequently the accumulation factor of the BCI was set to the same duration.

Gain definition

For the analysis on EMG_{ref} on the participants of Study 2, the EMG parameter was extracted as the maximum value of EMG envelope in the window [0-250]ms with respect to the EMG onset. The Wilcoxon signed-ranks test revealed no significant differences in the EMG parameter extracted during the movement performed with the left and the right hand in CTRL group (p=0.79), whereas a significant difference was obtained between the EMG parameter extracted during the unaffected and the affected finger extension movement/attempt (p<0.01) in EXP group. Thus, the unaffected side can be used as reference for the target myoelectric activation (EMG_{ref}) with the aim of obtaining during the rehabilitation training the same no significant difference between the two sides as in healthy participants.
Figure 6.7 shows the EMG parameter distribution when the movement was performed by the left and right hand in CTRL group (panel A) and when was performed/attempted by the unaffected and affected hand in EXP group (panel B).

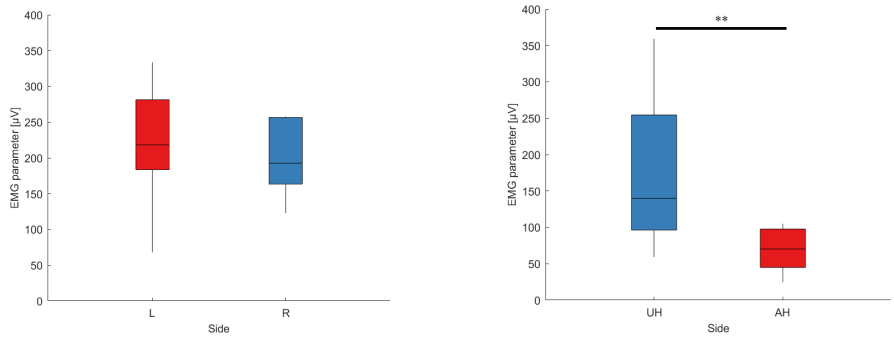

A) CTRL group B) EXP group

Figure 6.7. Boxplots of the distribution (N=12) of the EMG parameter extracted in the window [0-250]ms with respect to the EMG onset during A) finger extension performed with the left and right hand by healthy participants and B) movement/attempt performed with unaffected and the affected hand by the stroke participants. The symbol ** indicates a statistical difference as revealed by Wilcoxon signed-ranks test (p<0.01).

The interquartile range of the ratio between the EMG parameter of the left and the right side in CTRL group resulted to be equal to 64% Thus, such range is used a potential range of tolerance for EMG_{ref} in the adaptive algorithm. In this way, when the EMG parameter extracted after the BCI's movement detection is under the activation threshold (EMG at rest), a FES intensity equal to I_{max} is delivered to the patient and the percentage of stimulation decreases with the increasing of the EMG parameter until when the ratio between the EMG parameter and EMG_{ref} is in the range of tolerance. Analyses on a larger group of participants are needed to confirm such results.

6.5 Discussion and future steps

The developed system manages to apply different stimulation strategies to the patient during a rehabilitation training based on BCI-triggered FES or only FES. In the BCI modality, the FES intensity can be modulated by patient's residual or recovered muscle activity. The modularity of the system design allows to customize each block according to rehabilitative needs. The communication protocol chosen guarantees the reliability and the timing of the processes.
Through the preliminary study performed to build the adaptive algorithm for the myoelectric modulation of FES intensity, the compatibility between the EMG and FES electrodes location was assessed and the EMG parameter to use for extracting the residual muscular activity was defined. The reference muscular activation was identified to build the function of the compensatory strategy used to modulate the FES intensity.

Such system would provide a rehabilitative tool customisable to the patient's rehabilitation stage and potentially valuable for a longitudinal personalized treatment [57]: following the patient from a severe impairment to the functional recovery. Indeed, when a severely impaired patient has no residual activity, the BCI triggers the FES, upon movement detection, and the FES intensity delivered is the maximal one to obtain the full movement. Then when he/she progressively recovers the hand function and has a residual myoelectric activation, the FES intensity provides a muscular recruitment complementary to the natural one detected by the EMG and needed to complete the movement. Higher the EMG parameter and tinier the contraction induced by the stimulation, which even if it goes under the motor recruitment threshold, can still provides a sensory feedback on the patient's skin until the functional movement is completely recovered.
Validation of the hybrid system will be performed to evaluate the feasibility of the approach and refine the modulation strategy through a experimental paradigm designed ad-hoc for the desired rehabilitative exercises (upward and outward deviations of the hand extension). A proof-of-concept study based on a longitudinal trial will be performed on one patient with severe impairment recruited within the inpatients service of Fondazione Santa Lucia, IRCCS,

Rome, Italy.

Conclusion

The studies performed in this section assessed that CMC features are valuable features to discriminate in real-time different hand movements from rest condition in both healthy subjects and individuals with a diagnosed stroke. Thus, such features can be used as inputs for a hybrid BCI control.
This prototype is a non-invasive h-BCI that manages to detect movements in real-time and to send a contingent feedback (i.e., delivery of FES) to the user based on brain-muscles communication. The two branches it consisted of allow to detect physiological movements and, if needed, monitoring for incorrect cortico-muscular patterns of activation related to stroke. Indeed, such a device was designed to encourage only "correct" movements in a post-stroke BCI-based rehabilitative intervention.

Moreover, delivering an ecological feedback which is enriched with sensory inputs via the natural afferent pathways (i.e. via FES) allows to activate all the spare components of the central nervous system involved in the motor control [19], [58]. Adapting such feedback intensity to the muscular activation level would allow to provide a BCI intervention challenging but feasible for the patient, aimed to recover the motor abilities progressively complementing his/her deficit.

In conclusion, the hybrid system developed here exploiting the patients' residual or recovered arm activity has the aim to increase the BCI-based opportunities for upper limb stroke rehabilitation in order to follow patients along recovery and giving him/her a feedback tailored on his/her rehabilitative stage, consolidating the role of BCI in rehabilitation.

References

[1] E. Colamarino, V. de Seta, M. Masciullo, *et al.*, "Corticomuscular and Intermuscular Coupling in Simple Hand Movements to Enable a Hybrid Brain-Computer Interface," eng, *International Journal of Neural Systems*, vol. 31, no. 11, p. 2 150 052, Nov. 2021, ISSN: 1793-6462. DOI: 10.1142/S0129065721500520.

[2] F. Pichiorri, J. Toppi, V. de Seta, *et al.*, "Exploring high-density corticomuscular networks after stroke to enable a hybrid Brain-Computer Interface for hand motor rehabilitation," *Journal of NeuroEngineering and Rehabilitation*, accepted, Jan. 2023.

[3] J. R. Wolpaw, N. Birbaumer, D. J. McFarland, G. Pfurtscheller, and T. M. Vaughan, "Brain–computer interfaces for communication and control," *Clinical neurophysiology*, vol. 113, no. 6, pp. 767–791, 2002, Publisher: Elsevier.

[4] M. Krauledat, G. Dornhege, B. Blankertz, F. Losch, G. Curio, and K.-R. Muller, "Improving speed and accuracy of brain-computer interfaces using readiness potential features," in *The 26th Annual International Conference of the IEEE Engineering in Medicine and Biology Society*, vol. 2, Sep. 2004, pp. 4511–4515. DOI: 10.1109/IEMBS.2004.1404253.

[5] R. Chai, S. H. Ling, G. P. Hunter, Y. Tran, and H. T. Nguyen, "Brain–Computer Interface Classifier for Wheelchair Commands Using Neural Network With Fuzzy Particle Swarm Optimization," *IEEE Journal of Biomedical and Health Informatics*, vol. 18, no. 5, pp. 1614–1624, Sep. 2014, Conference Name: IEEE Journal of Biomedical and Health Informatics, ISSN: 2168-2208. DOI: 10.1109/JBHI.2013.2295006.

[6] D. E. Thompson, L. R. Quitadamo, L. Mainardi, *et al.*, "Performance measurement for brain–computer or brain–machine interfaces: A tutorial," en, *Journal of Neural Engineering*, vol. 11, no. 3, p. 035 001, May 2014, Publisher: IOP Publishing, ISSN: 1741-2552. DOI: 10.1088/1741-2560/11/3/035001. [Online]. Available: https://doi.org/10.1088/1741-2560/11/3/035001 (visited on 08/02/2022).

[7] E. Dagdevir and M. Tokmakci, "Optimization of preprocessing stage in EEG based BCI systems in terms of accuracy and timing cost," en, *Biomedical Signal Processing and Control*, vol. 67, p. 102 548, May 2021, ISSN: 1746-8094. DOI: 10.1016/j.bspc.2021.102548. [Online]. Available: https://www.sciencedirect.com/science/article/pii/S1746809421001452 (visited on 10/05/2022).

[8] V. de Seta, J. Toppi, E. Colamarino, *et al.*, "Cortico-muscular coupling to control a hybrid brain-computer interface for upper limb motor rehabilitation: A pseudo-online study on stroke patients," *Frontiers in Human Neuroscience*, vol. 16, 2022, ISSN: 1662-5161. [Online]. Available: https://www.frontiersin.org/articles/10.3389/fnhum.2022.1016862 (visited on 11/24/2022).

[9] M. F. Levin, R. W. Selles, M. H. Verheul, and O. G. Meijer, "Deficits in the coordination of agonist and antagonist muscles in stroke patients: Implications for normal motor control," eng, *Brain Research*, vol. 853, no. 2, pp. 352–369, Jan. 2000, ISSN: 0006-8993. DOI: 10.1016/s0006-8993(99)02298-2.

[10] L. C. Miller and J. P. A. Dewald, "Involuntary paretic wrist/finger flexion forces and EMG increase with shoulder abduction load in individuals with chronic stroke," *Clinical Neurophysiology: Official Journal of the International Federation of Clinical Neurophysiology*, vol. 123, no. 6, pp. 1216–1225, Jun. 2012, ISSN: 1872-8952. DOI: 10.1016/j.clinph.2012.01.009.

[11] C. C. Silva, A. Silva, A. Sousa, *et al.*, "Co-activation of upper limb muscles during reaching in post-stroke subjects: An analysis of the contralesional and ipsilesional limbs," *Journal of Electromyography and Kinesiology: Official Journal of the International Society of Electrophysiological Kinesiology*, vol. 24, no. 5, pp. 731–738, Oct. 2014, ISSN: 1873-5711. DOI: 10.1016/j.jelekin.2014.04.011.

[12] Y.-T. Chen, S. Li, E. Magat, P. Zhou, and S. Li, "Motor Overflow and Spasticity in Chronic Stroke Share a Common Pathophysiological Process: Analysis of Within-Limb and Between-Limb EMG-EMG Coherence," *Frontiers in Neurology*, vol. 9, p. 795, 2018, ISSN: 1664-2295. DOI: 10.3389/fneur.2018.00795.

[13] A. Crema, M. Bassolino, E. Guanziroli, *et al.*, "Neuromuscular electrical stimulation restores upper limb sensory-motor functions and body representations in chronic stroke survivors," English, *Med*, vol. 3, no. 1, 58–74.e10, Jan. 2022, Publisher: Elsevier, ISSN: 2666-6359, 2666-6340. DOI: 10.1016/j.medj.2021.12.001. [Online]. Available: https://www.cell.com/med/abstract/S2666-6340(21)00381-0 (visited on 01/17/2022).

[14] J. Cauraugh, K. Light, S. Kim, M. Thigpen, and A. Behrman, "Chronic motor dysfunction after stroke: Recovering wrist and finger extension by electromyography-triggered neuromuscular stimulation," English, *Stroke*, vol. 31, no. 6, pp. 1360–1364, 2000, ISSN: 0039-2499. DOI: 10.1161/01.STR.31.6.1360.

[15] E. Ambrosini, S. Ferrante, J. Zajc, *et al.*, "The combined action of a passive exoskeleton and an EMG-controlled neuroprosthesis for upper limb stroke rehabilitation: First results of the RETRAINER project," in *2017 International Conference on Rehabilitation Robotics (ICORR)*, ISSN: 1945-7901, Jul. 2017, pp. 56–61. DOI: 10.1109/ICORR.2017.8009221.

[16] M. Crepaldi, R. Thorsen, J. Jonsdottir, *et al.*, "FITFES: A Wearable Myoelectrically Controlled Functional Electrical Stimulator Designed Using a User-Centered Approach," *IEEE Transactions on Neural Systems and Rehabilitation Engineering*, vol. 29, pp. 2142–2152, 2021, Conference Name: IEEE Transactions on Neural Systems and Rehabilitation Engineering, ISSN: 1558-0210. DOI: 10.1109/TNSRE.2021.3120293.

[17] B. A. C. Osuagwu, E. Whicher, and R. Shirley, "Active proportional electromyogram controlled functional electrical stimulation system," en, *Scientific Reports*, vol. 10, no. 1, p. 21 242, Dec. 2020, Bandiera_abtest: a Cc_license_type: cc_by Cg_type: Nature Research Journals Number: 1 Primary_atype: Research Publisher: Nature Publishing Group Subject_term: Biomedical engineering;Neuromuscular disease Subject_term_id: biomedical-engineering;neuromuscular-disease, ISSN: 2045-2322. DOI: 10.1038/s41598-020-77664-0. [Online]. Available: https://www.nature.com/articles/s41598-020-77664-0 (visited on 01/25/2022).

[18] F. Pichiorri and D. Mattia, "Brain-computer interfaces in neurologic rehabilitation practice," eng, *Handbook of Clinical Neurology*, vol. 168, pp. 101–116, 2020, ISSN: 0072-9752. DOI: 10.1016/B978-0-444-63934-9.00009-3.

[19] A. Biasiucci, R. Leeb, I. Iturrate, *et al.*, "Brain-actuated functional electrical stimulation elicits lasting arm motor recovery after stroke," en, *Nature Communications*, vol. 9, no. 1, p. 2421, Jun. 2018, Number: 1 Publisher: Nature Publishing Group, ISSN: 2041-1723. DOI: 10.1038/s41467-018-04673-z. [Online]. Available: https://www.nature.com/articles/s41467-018-04673-z (visited on 08/01/2022).

[20] F. Pichiorri, G. Morone, M. Petti, *et al.*, "Brain–computer interface boosts motor imagery practice during stroke recovery," en, *Annals of Neurology*, vol. 77, no. 5, pp. 851–865, 2015, _eprint: https://onlinelibrary.wiley.com/doi/pdf/10.1002 ISSN: 1531-8249. DOI: 10.1002/ana.24390. [Online]. Available: https://onlinelibrary.wiley.com/doi/abs/10.1002/ana.24390 (visited on 08/01/2022).

[21] A. Ramos-Murguialday, D. Broetz, M. Rea, *et al.*, "Brain-machine interface in chronic stroke rehabilitation: A controlled study," eng, *Annals of Neurology*, vol. 74, no. 1, pp. 100–108, Jul. 2013, ISSN: 1531-8249. DOI: 10.1002/ana.23879.

[22] A. Chowdhury, H. Raza, Y. K. Meena, A. Dutta, and G. Prasad, "An EEG-EMG correlation-based brain-computer interface for hand orthosis supported neuro-rehabilitation," *Journal of Neuroscience Methods*, vol. 312, pp. 1–11, Jan. 2019, ISSN: 1872-678X. DOI: 10.1016/j.jneumeth.2018.11.010.

[23] D. O. Hebb, *The organization of behavior; a neuropsychological theory* (The organization of behavior; a neuropsychological theory). Oxford, England: Wiley, 1949, Pages: xix, 335.

[24] N. Mrachacz-Kersting, N. Jiang, A. J. T. Stevenson, *et al.*, "Efficient neuroplasticity induction in chronic stroke patients by an associative brain-computer interface," eng, *Journal of Neurophysiology*, vol. 115, no. 3, pp. 1410–1421, Mar. 2016, ISSN: 1522-1598. DOI: 10.1152/jn.00918.2015.

[25] T. Roland, "Motion Artifact Suppression for Insulated EMG to Control Myoelectric Prostheses," *Sensors*, vol. 20, no. 4, p. 1031, Jan. 2020, ISSN: 1424-8220. DOI: 10.3390/s20041031. [Online]. Available: https://www.mdpi.com/1424-8220/20/4/1031 (visited on 07/20/2022).

[26] S. Solnik, P. Rider, K. Steinweg, P. DeVita, and T. Hortobágyi, "Teager–Kaiser energy operator signal conditioning improves EMG onset detection," en, *European Journal of Applied Physiology*, vol. 110, no. 3, pp. 489–498, Oct. 2010, ISSN: 1439-6327. DOI: 10.1007/s00421-010-1521-8. [Online]. Available: https://doi.org/10.1007/s00421-010-1521-8 (visited on 08/02/2022).

[27] P. W. Hodges and B. H. Bui, "A comparison of computer-based methods for the determination of onset of muscle contraction using electromyography," en, *Electroencephalography and Clinical Neurophysiology/Electromyography and Motor Control*, vol. 101, no. 6, pp. 511–519, Dec. 1996, ISSN: 0924-980X. DOI: 10.1016/S0921-884X(96)95190-5. [Online]. Available: https://www.sciencedirect.com/science/article/pii/S0921884X96951905 (visited on 08/02/2022).

[28] V. de Seta, J. Toppi, F. Pichiorri, *et al.*, "Towards a hybrid EEG-EMG feature for the classification of upper limb movements: Comparison of different processing pipelines," in *2021 10th International IEEE/EMBS Conference on Neural Engineering (NER)*, ISSN: 1948-3554, May 2021, pp. 355–358. DOI: 10.1109/NER49283.2021.9441390.

[29] D. Liu, W. Chen, R. Chavarriaga, Z. Pei, and J. d. R. Millán, "Decoding of Self-paced Lower-Limb Movement Intention: A Case Study on the Influence Factors," English, *Frontiers in Human Neuroscience*, vol. 11, 2017, Publisher: Frontiers, ISSN: 1662-5161. DOI: 10.3389/fnhum.2017.

00560. [Online]. Available: https://www.frontiersin.org/articles/10.3389/fnhum.2017.00560/full (visited on 03/19/2021).

[30] T. Lal, M. Schroder, T. Hinterberger, *et al.*, "Support Vector Channel Selection in BCI," en, *IEEE Transactions on Biomedical Engineering*, vol. 51, no. 6, pp. 1003–1010, Jun. 2004, ISSN: 0018-9294. DOI: 10.1109/TBME.2004.827827. [Online]. Available: http://ieeexplore.ieee.org/document/1300795/ (visited on 06/15/2022).

[31] K. Chu, "An introduction to sensitivity, specificity, predictive values and likelihood ratios," en, *Emergency Medicine*, vol. 11, no. 3, pp. 175–181, 1999, _eprint: https://onlinelibrary.wiley.com/doi/pdf/10.1046/j.1442-2026.1999.00041.x, ISSN: 1442-2026. DOI: 10.1046/j.1442-2026.1999.00041.x. [Online]. Available: https://onlinelibrary.wiley.com/doi/abs/10.1046/j.1442-2026.1999.00041.x (visited on 06/15/2022).

[32] T. Fawcett, "An introduction to ROC analysis," en, *Pattern Recognition Letters*, ROC Analysis in Pattern Recognition, vol. 27, no. 8, pp. 861–874, Jun. 2006, ISSN: 0167-8655. DOI: 10.1016/j.patrec.2005.10.010. [Online]. Available: https://www.sciencedirect.com/science/article/pii/S016786550500303X (visited on 08/02/2022).

[33] V. M. McClelland, Z. Cvetkovic, and K. R. Mills, "Rectification of the EMG is an unnecessary and inappropriate step in the calculation of Corticomuscular coherence," en, *Journal of Neuroscience Methods*, vol. 205, no. 1, pp. 190–201, Mar. 2012, ISSN: 0165-0270. DOI: 10.1016/j.jneumeth.2011.11.001. [Online]. Available: http://www.sciencedirect.com/science/article/pii/S0165027011006571 (visited on 11/18/2020).

[34] L. Bianchi, C. Liti, G. Liuzzi, V. Piccialli, and C. Salvatore, "Improving P300 Speller performance by means of optimization and machine learning," en, *Annals of Operations Research*, vol. 312, no. 2, pp. 1221–1259, May 2022, ISSN: 1572-9338. DOI: 10.1007/s10479-020-03921-0. [Online]. Available: https://doi.org/10.1007/s10479-020-03921-0 (visited on 10/05/2022).

[35] M. Xu, J. Han, Y. Wang, T.-P. Jung, and D. Ming, "Implementing Over 100 Command Codes for a High-Speed Hybrid Brain-Computer Interface Using Concurrent P300 and SSVEP Features," *IEEE Transactions on Biomedical Engineering*, vol. 67, no. 11, pp. 3073–3082, Nov. 2020, Conference Name: IEEE Transactions on Biomedical Engineering, ISSN: 1558-2531. DOI: 10.1109/TBME.2020.2975614.

[36] C. M. Wong, Z. Wang, B. Wang, *et al.*, "Inter- and Intra-Subject Transfer Reduces Calibration Effort for High-Speed SSVEP-Based BCIs," eng, *IEEE transactions on neural systems and rehabilitation engineering: a publication of the IEEE Engineering in Medicine and Biology Society*, vol. 28, no. 10, pp. 2123–2135, Oct. 2020, ISSN: 1558-0210. DOI: 10.1109/TNSRE.2020.3019276.

[37] L. Yao, N. Jiang, N. Mrachacz-Kersting, X. Zhu, D. Farina, and Y. Wang, "Reducing the Calibration Time in Somatosensory BCI by Using Tactile ERD," eng, *IEEE transactions on neural systems and rehabilitation engineering: a publication of the IEEE Engineering in Medicine and Biology Society*, vol. 30, pp. 1870–1876, 2022, ISSN: 1558-0210. DOI: 10.1109/TNSRE.2022.3184402.

[38] M. Nakanishi, Y. Wang, X. Chen, Y.-T. Wang, X. Gao, and T.-P. Jung, "Enhancing Detection of SSVEPs for a High-Speed Brain Speller Using Task-Related Component Analysis," *IEEE Transactions on Biomedical Engineering*, vol. 65, no. 1, pp. 104–112, Jan. 2018, Conference Name: IEEE Transactions on Biomedical Engineering, ISSN: 1558-2531. DOI: 10.1109/TBME.2017.2694818.

[39] A. Eliseyev, I. J. Gonzales, A. Le, *et al.*, "Development of a brain-computer interface for patients in the critical care setting," en, *PLOS ONE*, vol. 16, no. 1, e0245540, 2021, Publisher: Public Library of Science, ISSN: 1932-6203. DOI: 10.1371/journal.pone.0245540. [Online]. Available: https://journals.plos.org/plosone/article?id=10.1371/journal.pone.0245540 (visited on 10/05/2022).

[40] R. Mane, T. Chouhan, and C. Guan, "BCI for stroke rehabilitation: Motor and beyond," eng, *Journal of Neural Engineering*, vol. 17, no. 4, p. 041 001, Aug. 2020, ISSN: 1741-2552. DOI: 10.1088/1741-2552/aba162.

[41] A. B. Remsik, P. L. E. van Kan, S. Gloe, *et al.*, "BCI-FES With Multimodal Feedback for Motor Recovery Poststroke," *Frontiers in Human Neuroscience*, vol. 16, 2022, ISSN: 1662-5161. [Online]. Available: https://www.frontiersin.org/articles/10.3389/fnhum.2022.725715 (visited on 10/05/2022).

[42] D. Lee, S.-H. Park, and S.-G. Lee, "Improving the Accuracy and Training Speed of Motor Imagery Brain-Computer Interfaces Using Wavelet-Based Combined Feature Vectors and Gaussian Mixture Model-Supervectors," eng, *Sensors (Basel, Switzerland)*, vol. 17, no. 10, E2282, Oct. 2017, ISSN: 1424-8220. DOI: 10.3390/s17102282.

[43] Z. Guo, Q. Qian, K. Wong, *et al.*, "Altered Corticomuscular Coherence (CMCoh) Pattern in the Upper Limb During Finger Movements After Stroke," *Frontiers in Neurology*, vol. 11, 2020, ISSN: 1664-2295. [Online]. Available: https://www.frontiersin.org/articles/10.3389/fneur.2020.00410 (visited on 07/20/2022).

[44] E. Lóopez-Larraz, N. Birbaumer, and A. Ramos-Murguialday, "A hybrid EEG-EMG BMI improves the detection of movement intention in cortical stroke patients with complete hand paralysis," in *2018 40th Annual International Conference of the IEEE Engineering in Medicine and Biology Society (EMBC)*, ISSN: 1558-4615, Jul. 2018, pp. 2000–2003. DOI: 10.1109/EMBC.2018.8512711.

[45] N. Mrachacz-Kersting and S. Aliakbaryhosseinabadi, "Comparison of the Efficacy of a Real-Time and Offline Associative Brain-Computer-Interface," *Frontiers in Neuroscience*, vol. 12, 2018, ISSN: 1662-453X. [Online]. Available: https://www.frontiersin.org/article/10.3389/fnins.2018.00455 (visited on 06/11/2022).

[46] Y. Renard, F. Lotte, G. Gibert, *et al.*, "OpenViBE: An Open-Source Software Platform to Design, Test, and Use Brain–Computer Interfaces in Real and Virtual Environments," en, *Presence: Teleoperators and Virtual Environments*, vol. 19, no. 1, pp. 35–53, Feb. 2010, ISSN: 1054-7460. DOI: 10.1162/pres.19.1.35. [Online]. Available: https://direct.mit.edu/pvar/article/19/1/35-53/18759 (visited on 08/31/2022).

[47] M. B. Popovic, D. B. Popovic, L. Schwirtlich, and T. Sinkjaer, "Functional Electrical Therapy (FET): Clinical Trial in Chronic Hemiplegic Subjects," eng, *Neuromodulation: Journal of the International Neuromodulation Society*, vol. 7, no. 2, pp. 133–140, Apr. 2004, ISSN: 1094-7159. DOI: 10.1111/j.1094-7159.2004.04017.x.

[48] D. N. Rushton, "Functional electrical stimulation and rehabilitation–an hypothesis," eng, *Medical Engineering & Physics*, vol. 25, no. 1, pp. 75–78, Jan. 2003, ISSN: 1350-4533. DOI: 10.1016/s1350-4533(02)00040-1.

[49] M. Lotze, C. Braun, N. Birbaumer, S. Anders, and L. G. Cohen, "Motor learning elicited by voluntary drive," *Brain*, vol. 126, no. 4, pp. 866–872, Apr. 2003, ISSN: 0006-8950. DOI: 10.1093/brain/awg079. [Online]. Available: https://doi.org/10.1093/brain/awg079 (visited on 10/25/2022).

[50] M. Gandolla, S. Ferrante, F. Molteni, *et al.*, "Re-thinking the role of motor cortex: Context-sensitive motor outputs?" en, *NeuroImage*, vol. 91, pp. 366–374, May 2014, ISSN: 1053-8119. DOI: 10.1016/j.neuroimage.2014.01.011. [Online]. Available: https://www.sciencedirect.com/science/article/pii/S1053811914000226 (visited on 10/25/2022).

[51] A. M. Sinha, V. A. Nair, and V. Prabhakaran, "Brain-Computer Interface Training With Functional Electrical Stimulation: Facilitating Changes in Interhemispheric Functional Connectivity and Motor Outcomes Post-stroke," *Frontiers in Neuroscience*, vol. 15, 2021, ISSN: 1662-453X. [Online]. Available: https://www.frontiersin.org/article/10.3389/fnins.2021.670953 (visited on 01/17/2022).

[52] F. Cincotti, F. Pichiorri, P. Aricò, *et al.*, "EEG-based Brain-Computer Interface to support post-stroke motor rehabilitation of the upper limb," *Conference proceedings : ... Annual International Conference of the IEEE Engineering in Medicine and Biology Society. IEEE Engineering in Medicine and Biology Society. Conference*, vol. 2012, pp. 4112–5, Aug. 2012. DOI: 10.1109/EMBC.2012.6346871.

[53] R. Merletti and D. Farina, "Surface Electromyography: Physiology, Engineering, and Applications," en, p. 593, 2016.

[54] B. M. Doucet, A. Lam, and L. Griffin, "Neuromuscular Electrical Stimulation for Skeletal Muscle Function," *The Yale Journal of Biology and Medicine*, vol. 85, no. 2, pp. 201–215, Jun. 2012, ISSN: 0044-0086. [Online]. Available: https://www.ncbi.nlm.nih.gov/pmc/articles/PMC3375668/ (visited on 10/25/2022).

[55] A. Crema, I. Furfaro, F. Raschellà, *et al.*, "Reactive Exercises with Interactive Objects: Interim Analysis of a Randomized Trial on Task-Driven NMES Grasp Rehabilitation for Subacute and Early Chronic Stroke Patients," en, *Sensors*, vol. 21, no. 20, p. 6739, Jan. 2021, Number: 20 Publisher: Multidisciplinary Digital Publishing Institute. DOI: 10.3390/s21206739. [Online]. Available: https://www.mdpi.com/1424-8220/21/20/6739 (visited on 11/24/2021).

[56] A. Schicketmueller, G. Rose, and M. Hofmann, "Feasibility of a Sensor-Based Gait Event Detection Algorithm for Triggering Functional Electrical Stimulation during Robot-Assisted Gait Training," en, *Sensors*, vol. 19, no. 21, p. 4804, Jan. 2019, Number: 21 Publisher: Multidisciplinary Digital Publishing Institute, ISSN: 1424-8220. DOI: 10.3390/s19214804. [Online]. Available: https://www.mdpi.com/1424-8220/19/21/4804 (visited on 10/23/2022).

[57] M. Coscia, M. J. Wessel, U. Chaudary, *et al.*, "Neurotechnology-aided interventions for upper limb motor rehabilitation in severe chronic stroke," eng, *Brain: A Journal of Neurology*, vol. 142, no. 8, pp. 2182–2197, Aug. 2019, ISSN: 1460-2156. DOI: 10.1093/brain/awz181.

[58] M. Sur and J. L. R. Rubenstein, "Patterning and plasticity of the cerebral cortex," eng, *Science (New York, N.Y.)*, vol. 310, no. 5749, pp. 805–810, Nov. 2005, ISSN: 1095-9203. DOI: 10.1126/science.1112070.

General Conclusion

Because of the multifaceted nature of stroke, a BCI system for motor rehabilitation should allow to train both brain and peripheral activity, reinforcing the volition that is brain control over muscular activation together with physiological muscular activation patterns. For this reason, my three years of PhD were dedicated to the study and the development of a rehabilitative technology aimed to strengthen the communication between brain and muscles.

I went beyond the state of the art by extending the concept of CMC itself to a complex pattern of synchronization between brain and muscular activations thanks to a multivariate approach for connectivity estimation. The properties of the widespread cortico-muscular patterns proved to be a valuable tool for the identification of physiological and pathological (stroke-related) characteristics during motor tasks. Moreover, the ability of cortico-muscular coupling to detect movement in real-time was assessed. Such feature resulted to be able to detect movements with high performance and a timing that allows the temporal association between the cortical activation and the peripheral stimulation (i.e. FES). Thus, a BCI-controlled FES system based on CMC features was designed with the aim to encourage physiological movements and discourage pathological ones, guiding the patient in the upper limb functions recovery.
The developed system will be validated in the coming months by assessing its clinical and functional efficacy on upper limb rehabilitation within a Randomized Controlled Trial (RCT) in chronic stroke patients undergoing standard rehabilitation according to the NCT05511207 clinical trial registered online at clinicaltrial.gov[6]. The h-BCI intervention will be compared with physiotherapy intervention focus on the upper limb in which FES is activated externally by the physiotherapist. Greater clinical improvement is expected in the experimental group as measured by functional scales (e.g. FMA) accompanied by a reduction in spasticity.

This BCI-based protocol will allow to exploit the patient's residual or recovered motor abilities, delivering a feedback that is not only functionally meaningful (e.g. via virtual reality or passive movement of the paretic limb by a robot), but also tailored to reorganize the targeted neural circuits by provid-

[6] `https://clinicaltrials.gov/ct2/show/NCT05511207`

ing rich sensory inputs via the pathways natural afferent. Such system takes into account not only both the cerebral and muscular activity involved in the movement, but their interconnection, giving a global vision of the physiological patterns involved in the movement that has to be recovered.

In conclusion, the hybrid BCI technology developed during my PhD has the aim to do a step closer to increase the currently available BCI-based opportunities for upper limb stroke rehabilitation in order to follow patients along the process of regaining motor abilities. Indeed, such CMC-based BCI would allow to fill the gap between the early stage of rehabilitation when severely disabled patients (i.e., plegic) can only imagine the movements during a BCI-based training intervention [1], [2] and the progressive functional recovery. This would allow to follow patients along each stage of their rehabilitation path with a strategy tailored to their level of impairment and hence maximizing the time and amount of functional recovery with potentially high impact on the stroke survivors' quality of life (personalized medicine).

References

[1] F. Pichiorri, G. Morone, M. Petti, *et al.*, "Brain-computer interface boosts motor imagery practice during stroke recovery," eng, *Annals of Neurology*, vol. 77, no. 5, pp. 851–865, May 2015, ISSN: 1531-8249. DOI: 10.1002/ana.24390.

[2] A. Ramos-Murguialday and N. Birbaumer, "Brain oscillatory signatures of motor tasks," *Journal of Neurophysiology*, vol. 113, no. 10, pp. 3663–3682, Jun. 2015, Publisher: American Physiological Society, ISSN: 0022-3077. DOI: 10.1152/jn.00467.2013. [Online]. Available: https://journals.physiology.org/doi/full/10.1152/jn.00467.2013 (visited on 10/27/2022).

List of Publications

International Journal Papers

1. F. Pichiorri*, J. Toppi*, **V. de Seta**, E. Colamarino, M. Masciullo, F. Tamburella, M. Lorusso, F. Cincotti, D. Mattia, "Exploring high-density corticomuscular networks after stroke to enable a hybrid Brain-Computer Interface for hand motor rehabilitation", Journal of NeuroEngineering and Rehabilitation, * equal contributions, Jan. 2023.

2. **V. de Seta**, J. Toppi, E. Colamarino, R. Molle, F. Castellani, F. Cincotti, D. Mattia, F. Pichiorri, "Cortico-Muscular Coupling to control a hybrid Brain-Computer Interface for upper limb motor rehabilitation: a pseudo-online study on stroke patients", Frontiers in Human Neuroscience, Nov. 2022.

3. E. Colamarino, **V. de Seta**, M. Masciullo, D. Mattia, F. Cincotti, F. Pichiorri, J. Toppi, "Corticomuscular and intermuscular coupling in simple hand movements to enable a hybrid Brain-Computer Interface", International Journal of Neural Systems, Sept. 2021.

4. A. Ranieri, F. Pichiorri, E. Colamarino, **V. de Seta**, D. Mattia, J. Toppi, "Parallel factorization to implement group analysis in brain networks estimation", accepted for publication to Sensors, Jan. 2023.

5. F. Pichiorri, J. Toppi, M. Masciullo, E. Colamarino, **V. de Seta**, F. Tamburella, M. Lorusso, G. Morone, F. Cincotti, D. Mattia, "Randomized Controlled Trial to validate the efficacy of a novel Hybrid Brain-Computer Interface driven Functional Electrical Stimulation of upper limb in moderately impaired stroke survivors: the RECOMmENceR project", BMC Neurology, under preparation

Papers in International Conferences indexed on medline

1. E. Mongiardini, E. Colamarino, J. Toppi, **V. de Seta**, F. Pichiorri, D. Mattia, F. Cincotti, "Low Frequency Brain Oscillations for Brain-Computer Interface Applications: From the Sources to the Scalp Domain", presented at 2022 IEEE International Conferences MetroXRAINE, 26-28 Oct. 2022, Rome.

2. **V. de Seta**, E. Colamarino, F. Cincotti, D. Mattia, E. Mongiardini, F. Pichiorri, J. Toppi, "Cortico-Muscular Coupling Allows to Discriminate Different Types of Hand Movements", in 2022 44th Annual International Conference of IEEE Engineering in Medicine and Biology Society (EMBC), 11-15 July 2022, Glasgow.

3. E. Colamarino, **V. de Seta**, J. Toppi, F. Pichiorri, I. Conforti, I. Mileti, E. Palermo, D. Mattia, F. Cincotti, "Distinctive physiological muscle synergy patterns define the Box and Block Task execution as revealed by electromyographic features", in 2022 44th Annual International Conference of IEEE Engineering in Medicine and Biology Society (EMBC), 11-15 July 2022, Glasgow (oral presentation).

4. E. Mongiardini, E. Colamarino, J. Toppi, **V. de Seta**, F. Pichiorri, D. Mattia, F. Cincotti, "Low Frequency Brain Oscillations during the execution and imagination of simple hand movements for Brain-Computer Interface applications", in 2022 44th Annual International Conference of IEEE Engineering in Medicine and Biology Society (EMBC), 11-15 July 2022, Glasgow (oral presentation).

5. **V. de Seta**, J. Toppi, F. Pichiorri, M. Masciullo, E. Colamarino, D. Mattia, F. Cincotti, "Towards a hybrid EEG-EMG feature for the classification of upper limb movements: comparison of different processing pipelines", in 2021 10th International IEEE/EMBS Conference on Neural Engineering (NER), 4-6 May 2021, Virtual.

6. E. Colamarino, F. Pichiorri, J. Toppi, **V. de Seta**, M. Masciullo, D. Mattia, F. Cincotti, "Inter-muscular coherence features to classify upper limb simple tasks", in 2021 10th International IEEE/EMBS Conference on Neural Engineering (NER), 4-6 May 2021, Virtual.

Abstract in International and National Conferences

1. E. Colamarino, **V. de Seta**, J. Toppi, F. Pichiorri, G. Morone, I. Conforti, I. Mileti, E. Palermo, D. Mattia, F. Cincotti, "Muscle synergy patterns in the Box and Block Task execution", XXII Congresso SIAMOC, 05-08 Oct. 2022, Bari.

2. **V. de Seta**, J. Toppi, E. Colamarino, F. Cincotti, D. Mattia, F. Pichiorri, "Hybrid Brain-Computer Interface aimed to Re-establish Cortico-Muscular communication after stroke", Summer School on Neurorehabilitation 2022, 12-17 June 2022, Baiona.

3. **V. de Seta**, E. Colamarino, F. Pichiorri, J. Toppi, M. Masciullo, F. Cincotti, D. Mattia, "Hand movements classification for a hybrid rehabilitative BCI: study on corticomuscular and intermuscular coherence", 8th International BCI Meeting, 7-9 June 2021 Virtual.

4. F. Pichiorri, **V. de Seta**, E. Colamarino, J. Toppi, F. Cincotti, D. Mattia, "Movement-Related Cortical Potential during post-stroke motor recovery: preliminary study for a novel hybrid BCI paradigm", 8th International BCI Meeting, 7-9 June 2021 Virtual.

5. **V. de Seta**, E. Colamarino, F. Pichiorri, M. Masciullo, F. Cincotti, D. Mattia, J. Toppi, "Towards A Novel Hybrid Brain-Computer Interface for Motor Rehabilitation: Study on Cortico-Muscular Coherence Patterns for Movement Classification", Nature Conferences - Technologies for Neuroengineering, 26-28 May 2021 Virtual, (selected for oral presentation).

6. **V. de Seta**, E. Colamarino, F. Pichiorri, J. Toppi, F. Cincotti, D. Mattia, "Movement-Related Cortical Potential changes following functional motor recovery in subacute stroke patients", FENS 2020 Virtual Forum, 11-15 July 2020.

Ringraziamenti

Il mio grazie più speciale va alla Professoressa Jlenia Toppi per avermi guidata e accompagnata in questo viaggio senza mai avermi fatto sentire sola. Ha creduto in me e ha saputo riconoscere fin da subito il mio valore. La ricercatrice che sono oggi lo devo prevalentemente a lei e ai suoi insegnamenti. Discutere con lei di scienza, che sia per lavoro o non, è sempre stimolante e appassionante. La ringrazio per le opportunità che mi ha dato, che spero di aver saputo cogliere nel modo migliore.
Il mio secondo grazie va al Professor Febo Cincotti per avermi dato l'opportunità di lavorare alla Fondazione Santa Lucia e avermi permesso di fare un'esperienza di ricerca all'estero durante questi 3 anni. Gli scambi critici con lui mi hanno permesso di maturare molto professionalmente e personalmente.
Vorrei inoltre ringraziare la Dott.ssa Donatella Mattia per essere un capo lab presente e disponibile e avermi dato la possibilità di lavorare in un laboratorio formato da persone con diversi background che lavorano sinergicamente insieme. La sua esperienza e competenza sono state preziose in questi anni.
Ringrazio la Dott.ssa Floriana Pichiorri, PI del progetto che ha caratterizzato questi 3 anni, per avermi dato il punto di vista clinico della mia ricerca, avermi supportato, stimolato con il suo spirito critico ed essere stata sempre diretta. La sua preparazione ed arguzia sono state fondamentali per i traguardi raggiunti, p.s. "Il PI ha sempre ragione".

Ringrazio i ragazzi coinvolti nel progetto: in primis l'Ing. Emma Colamarino, sempre disponibile a darmi una mano, Giorgio Tartaglia per essere i miei occhi e le mie braccia quando non sono in lab e per il suo costante supporto nelle sperimentazioni, e i ragazzi più giovani come Filippo con il quale è stato un piacere lavorare grazie al suo entusiasmo, la sua gentilezza e capacità, e Rita per la sua costante presenza e disponibilità. Grazie a tutti i componenti del lab, senior e junior per renderlo un luogo vivace e stimolante.
Un ringraziamento speciale a tutti coloro che si sono sottoposti al testing iniziale del prototipo, per la loro pazienza, e a tutti i pazienti per avermi constantemente ricordato perché stavo facendo tutto questo.

Then, I would like to thank Prof. Silvestro Micera for the opportunity he gave me and my TNE family for welcoming me from day one and reviving my PhD student life after two years of pandemic. Thanks for the great memories

made of science, laugh and drama.

Infine, un grazie che non sarà mai abbastanza ad Alessandro per essere sempre stato il mio sostenitore numero uno, per essermi stato accanto nei momenti più difficili di questo percorso ed avermi guardato con occhi fieri nei momenti più belli. Grazie alla mia famiglia per il costante affetto e sostegno in tutte le mie scelte, e per i valori che mi ha insegnato. Grazie a mia nonna per credere e chiedere costantemente della mia ricerca.

Grazie a tutte le persone che ho incontrato durante questo percorso, ognuno ha contribuito a modo suo ad arricchire il mio bagaglio personale e professionale.

Valeria de Seta
PhD student in Bioengineering

deseta@diag.uniroma1.it
research gate | google scholar

EDUCATION AND TRAINING

11/19 – date	Sapienza University of Rome, PhD in Bioengineering at Neuroelectric Imaging and BCI Lab of Fondazione Santa Lucia IRCCS –Defense date: 25/01/23
10/21 - 06/22	École Polytechnique Fédérale de Lausanne, Visiting PhD student at Translational Neural Engineering Lab
12/18 - 10/19	Fondazione Santa Lucia IRCCS, Internship at Neuroelectric Imaging and BCI Lab
03/17 - 07/19	Sapienza University of Rome, M. S. in Biomedical Engineering - Final grade: 110/110 cum laude – GPA: 29.71/30
03/18 - 09/18	Technical University of Munich, Exchange semester
01/17- 03/17	Intern in consultancy at Looking for Value (L4V) and Day One Ltd – Strategy consultancy with the aim to support medical start-ups and SMEs during their growth
09/13 - 12/16	Sapienza University of Rome, B. S. in Clinical Engineering - Final grade: 110/110 cum laude

RESEARCH PROJECTS

12/19- date	Investigator for the project "RECOMmENceR: RE-establishing COrtico Muscolar COMunication to ENhance Recovery. Clinical validation of BCI-controlled Functional Electrical Stimulation for upper limb rehabilitation after stroke" (GR-2018-12365874), funded by the Italian Ministry of Health.
12/20-date	Investigator for the project "MOVE: MultimOdal framework for the eValuation of upper-limb motor impairment and its rEcovery in stroke patients" (RM120172B8899B8C) funded by Sapienza University of Rome.
11/21-11/22	Principal Investigator for the project Avvio alla Ricerca (AR12117A8B2FF0F7) titled "Towards a novel hybrid Brain-Computer Interface for post-stroke motor rehabilitation based on brain-muscles patterns", grant received from Sapienza University of Rome.
10/20-10/22	Principal Investigator for the project Avvio alla Ricerca (AR120172B8B5B405) titled "Characterization of Cortico-Muscular Coherence during the execution of simple motor tasks aimed at the development of a hybrid feature for the classification of upper limb movements", grant

		received from Sapienza University of Rome
	12/21 - 06/22	Principal Investigator for the Exchange PhD project "Development of an integrated platform exploiting cortico-muscular activation and functional electrical stimulation for the neurorehabilitation of post-stroke patients", founded by the National Centre of Competence in Research (NCCR) Robotics and carried out at TNE lab – EPFL.
FELLOWSHI AND AWARDS	10/20 – date	**IEEE EMBS** Fellow
	08/20 – date	**Gruppo Nazionale di Bioingegneria** (GNB) Fellow
	01/20 – date	**BCI Society** Fellow
	08/22	**STI Teaching Assistant Award** of the School of Engineering of EPFL for the course "Fundamentals of Neuroengineering".
	09/20	**Second place at the GNB Datathon Challenge** - XXXIX Annual Bioengineering School "AI-enabled health care: from decision support to autonomous robots".
	08/20	**Best team project using Backyard Brains IEEE Brain Virtual Summer School.**
	04/20 - 05/20	**Winner of the UBORA 2020 International Design Competition**, Open-source medical technologies for integral management of COVID-19 pandemic and infectious disease outbreaks. (Team Project: LearnFromCovid19).
	02/20	**License for Professional Practice in Civil and Industrial Engineering**.
	01/20	"Fondo Mario Negri" Prize for excellent Master thesis-Fondo Mario Negri
	01/20	Award for the best Master thesis on disability a.y. 2018/2019-Sapienza University
ACADEMIC ACTIVITY	<u>Seminar and Teaching Assistant</u>	
	09/22 - date	"Models of biological systems" Course (Biomedical Engineering, ING-INF/06, 9ECTS), A.Y. 2022/23.
	02/22 - 06/22	"Fundamentals of Neuroengineering" Course (Biomedical Engineering, BIOENG-448, 4ECTS), A.Y. 2021/22
	05/22	"Deterministic and stochastic signals and biomedical data processing I" Course (Biomedical Engineering, ING-INF/06, 6ECTS), A.Y. 2021/22.
	<u>Co-supervisor to Master theses in Biomedical Engineering</u>	
	07/22 - date	"Analysis of brain and cortico-muscular features as input of a Brain-Computer Interface to discriminate simple hand movements".

09/21 - 03/22 “Characterization of brain and cortico-muscular features to discriminate different simple hand movements”.

07/21- 01/22 “Characterization of physiological and pathological brain-muscles patterns in healthy subjects and stroke patients during simple upper limb movements”.

04/21- 10/21 "Development of an algorithm for the real-time estimation of cortico-muscular coherence to use in a Brain-Computer Interface for post-stroke motor rehabilitation"."

02/20 – 05/21 “Development and characterization of hybrid cortico-muscular features for classification of simple upper limb movements".

Co-supervisor to Semester Projects

03/22 – 06/22 “EMG-based modulation of Functional Electrical Stimulation for a Brain-Computer Interface-based rehabilitative intervention” (EPFL).

12/21 – 05/22 “Development of a Graphical User Interface to manage Brain-Computer Interface scenarios developed in OpenViBE”.

Co-supervisor to Bachelor thesis in Clinical Engineering

06/21 – 10/21 “Implementation in OpenViBE of a Brain-Computer Interface based on cortico-muscular features for post-stroke upper limb motor rehabilitation".

EDITORIAL ACTIVITY

Reviewer for IEEE Journal of Biomedical and Health Informatics (JBHI, IF = 7.021)

Reviewer for IEEE Conference Proceedings

Reviewer for IEEE Transactions on Neural Systems & Rehabilitation Engineering (TNSR, IF = 4.528)

OTHER EXPERIENCES

Treasurer of the Social Campus Biotech Association (SCBA), Geneva (Oct. 2021 – Jun 2022) - SCBA aims at organising social events at the campus scale while fostering fruitful collaborations and the exchange of ideas inside the community made by EPFL and UNIGE researchers.

IT SKILLS

MATLAB, Python, BrainVision Software, BCI2000, OpenViBE, LabVIEW (CLAD Certificate), LateX

TECHINICAL SKILLS

EEG recordings, EMG recordings, IMU recordings, FES stimulation

Re-establishing Cortico-Muscular Communication to enhance recovery: development of a hybrid Brain-Computer Interface for post-stroke motor rehabilitation

Stroke is a leading cause of adult serious and long-term disability. Notably, improving upper limb functioning is the primary therapeutic goal in stroke rehabilitation to maximize patients' functional recovery and reduce long-term disability. Nowadays, Brain-Computer Interfaces (BCIs) can be used as add-on to traditional therapies to activate rehabilitative devices directly decoding the brain activity of the user noninvasively, e.g. by means of electroencephalogram (EEG). However, the consequences of a stroke involve regions apart from the focal lesions due to disruption of connections along neural pathways. Therefore, a BCI system for motor rehabilitation should allow to train both brain and peripheral activity, reinforcing the volition that is brain control over muscular activation together with physiological muscular activation patterns.

In this PhD thesis, Cortico-Muscular Coupling (CMC), which measures the synchronization between central and peripheral activation (recorded respectively through EEG and electromyogram – EMG), was studied as feature to detect movement attempts and to reinforce the physiological brain control of muscles activity.

The widespread functional brain-muscle connectivity (derived from multiple EEG-EMG pairs) was characterized and compared in healthy subjects and stroke patients by means of indices derived ad-hoc from graph theory. CMC resulted to contain information about the movement type performed as well as the general clinical status of stroke patients in terms of their hand functionality, showing a high potential to be used as input of hybrid BCI (h-BCI) systems.

Thus, a processing pipeline for the translation of CMC computation and the consequent CMC-based movement detection from offline to real-time was defined and optimized. A novel h-BCI prototype aimed to Re-establish Cortico-Muscular communication was developed and its feasibility was validated. Moreover, a study on the strategy of the feedback delivery (i.e. Functional Electrical Stimulation - FES) was performed with the ultimate aim of tailoring the stimulation to patients' impairment.

Such rehabilitative prototype recognizes close-to-normal EEG-EMG coupling during hand movement attempts, taking into account both the CMC features to reinforce during the h-BCI training, and the ones to discourage to avoid the maladaptive movement abnormalities typical of post-stroke recovery. Upon movement detection, it triggers the delivery of FES to the target muscle to support full movement execution. Such system resulted to be reliable and easy-to-use with high accuracy and timing.

The developed hybrid device would allow to follow patients along recovery with a strategy tailored on their rehabilitative stage and hence maximizing the time and amount of functional recovery with potentially high impact on the stroke survivors' quality of life (personalized medicine).